Modulating ADAM-10 activity and expression in cervical and oesophageal cancer cells

Mateen Wagiet

Dissertation presented in fulfillment of the requirements for the degree of Master of Science (M.Sc.) (Medicine) in Medical Biochemistry

In the

Faculty of Health Sciences
University of Cape Town

Supervisor: A/Prof. Virna D. Leaner

Co-supervisor: A/Prof Denver T. Hendricks

July 2016

Declaration

I, **Mateen Wagiet,** hereby declare that the work on which this dissertation/thesis is based is my original work (except where acknowledgements indicate otherwise) and that neither the whole work nor any part of it has been, is being, or is to be submitted for another degree in this or any other university.

I empower the university to reproduce for the purpose of research either the whole or any portion of the contents in any manner whatsoever.

Signature: …Signed by candidate.

Date: **16 August 2016**

Acknowledgements

I would sincerely like to thank you to my supervisor A/Prof Virna Leaner, for her invaluable support and guidance during this project. I am truly grateful for the excellent grounding that she has given me in basic cancer biology research. Secondly, I would like to thank A/Prof Denver Hendricks for his unfailing advice, support, and constant encouragement during this study. To our laboratory manager, Mrs Hajira Guzgay, thank you for your support and the way in which the laboratory was run. To our Laboratory Technician, Mr Robert Samuels, thank you for your unwavering support, kindness, and the early morning experiment encouragement.

I would like to thank past and present members of the cancer lab, particularly Ursula Edzidzi-Andong, Cherise Dunn, Aderonke Ajayi-Smith, Sian De Silva, Waldo Lexow, Dr Pauline van De Watt, Dr Nina Holderness-Parker and Dr Kate Hadley, for their equally valuable support and critical input, especially during lab data meetings, on this project. Thank you to my best friend Erin Strydom, for her advise and guidance through many laboratory techniques, as well as for her continued support, unfailing encouragement and friendship.

I would also like to thank Dr Dirk Lang and Susan Cooper of the confocal microscopy unit at UCT. Additionally, I would like to thank Dr Kobus Slabbert of iThemba Labs, Department of Science and Technology (DST). I would like to acknowledge and thank the National Research Foundation (NRF) of South Africa, NTHEMBI initiative of the Nuclear Energy Corporation of South Africa (NECSA) as well as the University of Cape Town (UCT) for providing funding for the project.

Lastly, thank you to my parents for their unfailing guidance, continued support and unconditional love.

Table of Contents

Figures and Tables Index:

Abbreviations

ACT	Activation
ADAM	A Disintegrin And Metalloproteinase
ADC	Adenocarcinoma
APP	Amyloid precursor protein
BCA	Bicinchoninic Acid Assay
Bp	Base Pairs
°C	Celcius
cDNA	Complementary Deoxyribonucleic acid
CX_3CL1	Chemokine (C-X3-C motif) ligand 1 (fractalkine)
DAPI	4',6-diamidino-2-phenylindole dihydrochloride
DMEM	Dulbecco's modified Eagle's Medium
DMSO	Dimethyl Sulphoxide
DNA	Deoxyribonucleic acid
EC_{50}	Half maximal effective concentration
EGF	Epidermal growth factor
EMT	Epithelial Mesenchymal Transition
ERK	Extracellular signal-regulated kinases
FCS	Foetal calf serum
FRET	Fluorescence Resonance Energy Transfer
H_2O	Water
HeLa	Immortal cervical cancer cell line derived from the patient Henrietta Lacks in 1951
HPV	Human papilloma virus

Hr	Hour
IC_{50}	Half maximal inhibitory concentration
IgG	Immunoglobulin G
Kb	Kilobases
kDa	Kilodaltons
M	Molar
mM	Millimolar
mg	Milligram
mL	Millilitre
MET	Mesenchymal –epithelial transition
M:I	Mortality incidence ratio
mRNA	messenger ribonucleic acid
MTT	3’-(4’,5’-Dimethylthiazol-2’-yl)-2’,5’-diphenyltetrazolium bromide
NaF	Sodium Fluoride
Na_2VO_4	Sodium orthovanadate
NCD	Non-communicable disease
NECSA	Nuclear Energy Corporation of South Africa
NRF	National Research Foundation of South Africa
OSCC	Oesophageal squamous cell carcinoma
OD	Optical Density
p	Probability value
PAGE	Polyacrylamide gel electrophoresis
PARP	Poly (ADP-ribose) polymerase
PBS	Phosphate-buffered saline
P/S	Penicillin / Streptomycin
RIPA	Radio-immunoprecipitation assay buffer
RNA	Ribonucleic Acid
RPM	Revolutions per minute

RT	Room temperature
SD	Standard deviation
SDS	Sodium dodecyl sulfate
SEM	Standard Error of the Mean
shRNA	Short hairpin RNA
siRNA	Small interference RNA
TBS-T	Tris-Buffered Saline and Tween 20
TNF-α	Tumour Necrosis Factor Alpha
µg/ µL	Micro-gram per micro-litre
µL	Micro-litre
µM	Micromole
UCT	University of Cape Town
V	Volts
VEGF	Vascular endothelial growth factor
WHO	World Health Organization

Abstract

The ADAMs (**A** **D**isintegrin **A**nd **M**etalloproteinase) is a family of trans-membrane and secreted proteins essential in cellular fate determination, wound healing, cell migration, proliferation and angiogenesis. Previous studies have linked a range of ADAMs, which include ADAM10 to cancer development and progression. Research in our laboratory found endogenous ADAM10 levels to be higher in both oesophageal and cervical cancer cell lines. Reports in the literature have highlighted a correlation between high levels of ADAM10 expression with that of cancer cell biology; hence ADAM10 shows promise as an anti-cancer target.

The aim of this study was to modulate ADAM10 activity in oesophageal and cervical cancer cell lines using the small molecule inhibitor GI254023X as well as previously undescribed two molecules generated en route to synthesizing GI254023X, namely SN-254 and SN-311. A CX_3CL1 ELISA functional assay as an indicator of ADAM10 activity showed a decrease in CX_3CL1 cleavage after treatment with GI254023X, SN-311 and SN-254 suggesting that all three compounds substantially inhibited ADAM10 activity. The effects of these compounds on the cell biology of WHCO5 oesophageal and HeLa cervical cancer cells were monitored. Our data shows that GI254023X, SN-254 and SN-311 inhibit oesophageal and cervical cancer cell proliferation, and cause

cell death via apoptosis as observed by PARP cleavage, and elevated Caspase 3/7 activity. Drug treatment also resulted in an increase in cellular adhesion as well as a significant decrease in the invasion and migration of WHC05 and HeLa cells. The effect of ADAM10 inhibition on typical markers of the epithelial to mesenchymal transition state was also examined. An increase in epithelial cell markers (E-Cadherin, B-Catenin) and a decrease in mesenchymal marker expression (Vimentin) post treatment with the compounds tested strongly suggested that ADAM10 plays a role in mesenchymal cell transition. These results suggest that ADAM10 activity is necessary for the biological phenotypes that associate with cervical and oesophageal cancer cells and that targeting ADAM10 with inhibitors have potential as anticancer therapies.

Chapter 1:
Introduction

1.1 Preamble

The ADAMs (A Disintegrin And Metalloproteinase) is a family of transmembrane bound and secreted proteins of approximately 750 amino acids in length, with documented functions in cell adhesion and ectodomain shedding of a variety of cell surface receptors and signaling molecules (Duffy *et al.,* 2009). The ADAM proteins are essential in cellular fate determination, wound healing, cell migration, proliferation and angiogenesis (Fu, *et al.,* 2014; Edwards, *et al.,* 2008; Rocks, *et al.,* 2008).

Previous work conducted in our laboratory aimed at identifying differentially expressed genes that associate with cancer development using microarray analysis, identified ADAM10, a membrane metalloproteinase as having elevated expression in cervical cancer cells (Van der Watt, *et al.,* 2009). Determining the endogenous expression levels of ADAM10 in oesophageal and cervical cancer, found an up-regulation of expression in both oesophageal and cervical cancer cells (Williams MSc dissertation, 2013). ADAM10 has thus become a protein of interest with potential to serve as a potential cancer biomarker. Evidence in the literature has highlighted a correlation between high levels of ADAM10 expression with many markers of

of cancer cell biology; hence, the inhibition of ADAM10 has appeal as a potential chemotherapeutic target (Duffy, *et al.,* 2011; Edwards, 2008).

The inhibition of ADAM10 using short hairpin RNA plasmid (shRNA) and a small interference RNA (siRNA) has significant effects on cancer cell biology including changes in cell morphology and actin organization when ADAM10 is inhibited (Williams, MSc Dissertation, 2013). Furthermore, the inhibition of ADAM10 had caused a significant increase in cell adhesion accompanied by decreased migration and invasion. The changes in actin organisation, cell adhesion, motility and invasion because of ADAM10 inhibition were properties all indicative of Mesenchymal-epithelial transition. In this study we aimed to investigate the potential of ADAM10 as a cancer biomarker and inhibit its activity using a known small molecule inhibitor GI254023X and two previously undescribed molecules. Modulating ADAM10, expression and activity will be monitored in two cancer types prevalent in Southern Africa, oesophageal and cervical cancer.

1.2 Global burden of cancer

The earliest recorded description of cancer was chronicled in the Edwin Smith Papyrus, written approximately 3000BC (Hadju, 2011). Despite the multitude of documented texts accumulated over the millennia, our vast and ever growing knowledge of this disease has not yet led to its' complete eradication (Hadju, 2011). The global burden of cancer includes 14.1 million newly diagnosed cases per year; of which a greater proportion of these reported diagnoses (approximately 56%) occur within the economically developing

world including sub-Saharan Africa (Ferlay, *et al*., 2015; Varmus and Kumar, 2013).

Highlighting the urgency to alleviate the adverse effects of this non-communicable disease (NCD), in 2012, a group of leading cancer researchers and policy makers from fifteen economically diverse countries described cancer as a group of diseases poised as a major liability to human life (Varmus and Kumar, 2013). This multi-national gathering discussed opportunities for global targets to reduce incidence and mortality of cancer, strategies to improve cancer health care, as well as to increase and develop a comprehensive understanding of the disease pathophysiology.

A report discussing the incidence and mortality worldwide of cancer presented in a GLOBOCAN 2012 document, noted that approximately 8.2 million cases of cancer-related deaths occurred, which constitutes 13% of all reported deaths worldwide. Furthermore, 64% of the approximate 8.2 million cases were recorded within the economically developing world (Ferlay, *et al.,* 2015; Jemal, *et al*., 2011; Ferlay, *et al.,* 2010). GLOBOCAN 2012 further predicts that cancer-associated deaths globally, are projected to increase to account for 51% of all recorded deaths (up from 13%) within the time period of 2008 to 2030 (± 11.5 million deaths) (Ferlay, *et al.,* 2010).

As a vast majority of recorded cancer-related deaths are reported to occur within the developing world, it poses a major public health risk, which is further aggravated by poor health care access resulting in late stage

diagnosis and limited access to sufficient treatment (Jemal, *et al*., 2011). A further challenge facing economically developing nations is the reality that many new cancer therapies are largely inaccessible due to high costs incurred in drug development (Hanahan, 2014). Therefore, research into innovative and cost efficient diagnostic tools and therapeutic strategies continue.

1.3 Cervical and oesophageal cancer

1.3.1 Cancer of the cervix uteri

An estimated 528 000 new cases of cervical cancer is diagnosed globally per annum, with a mortality of 266 000 in 2012 (GLOBOCAN, 2012). According to Arbyn and colleagues (2011), Africa has been classified as the region with the highest burden of cervical cancer; with 80 000 women diagnosed per annum, and 60 000 dying, in a population of 270 million women (aged 15 years and older). An estimated 7 735 women are diagnosed with cervical cancer every year in South Africa, representing 19.3% of all cancers in women (Bruni, *et al.,* 2014; GLOBOCAN, 2012; Tathiah, *et al.,* 2013; Vaccarella, *et al.,* 2013). Furthermore, the WHO identified the Southern Africa region to have recorded the third highest incidence (31.5 per 100 000) and mortality rate (17.9 per 100 000) for cervical cancer worldwide (See figure 1.1; published by: Torre, *et al.,* 2015).

Most cervical cancer cases (>90%) are caused by the Human Papilloma Virus (HPV) (WHO, 2012). Of the identified 150 different HPV categories, an

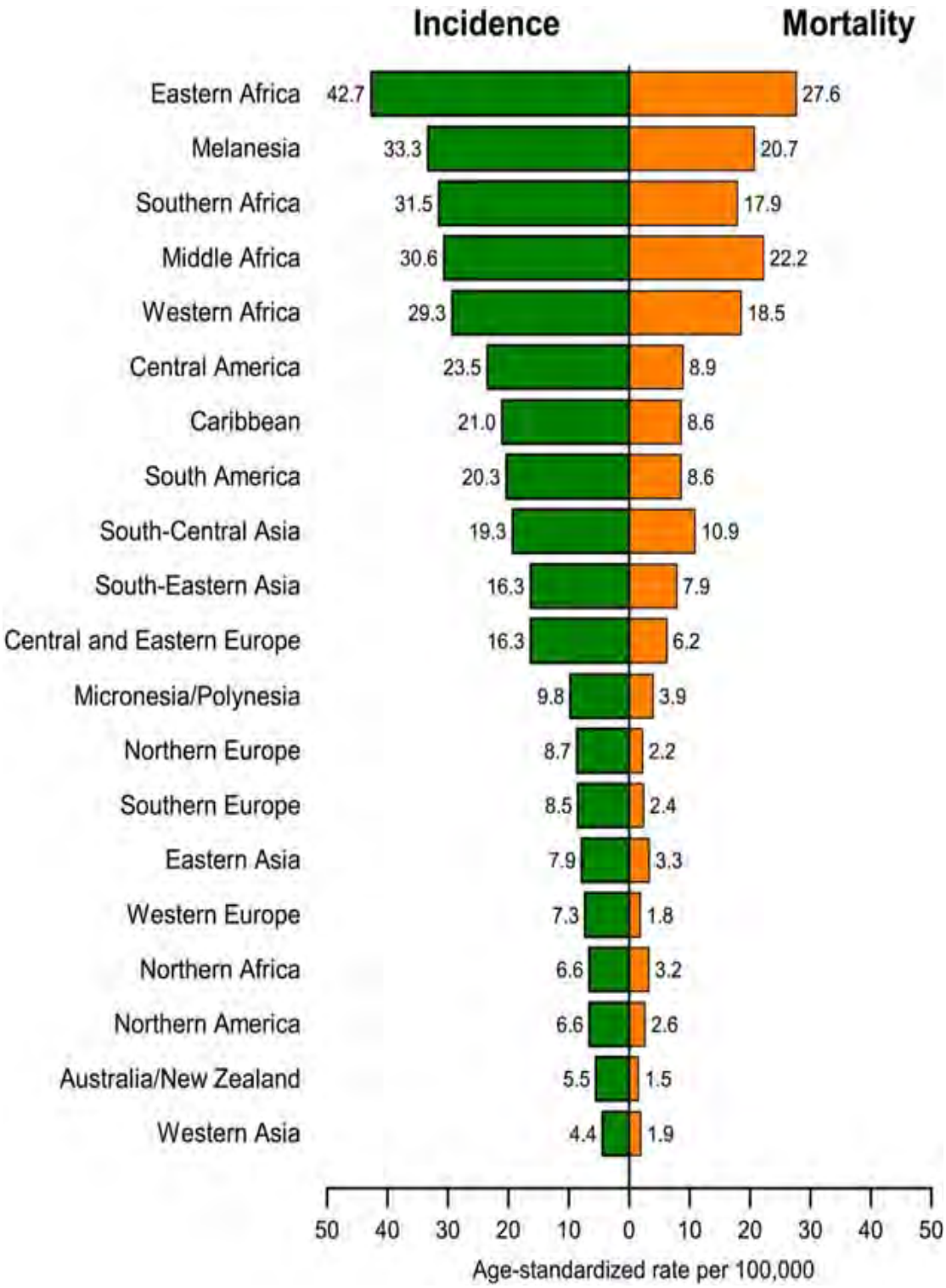

Figure 1.1: Incidence and mortality rate of cervical cancer worldwide, WHO. This data spread depicts the incidence and mortality rates of cervical cancer in women worldwide. The graph shows Eastern Africa, Melanesia and Southern Africa demonstrating the highest mortality and incidence rates (Torre, *et al.,* 2015).

estimated 40 have been identified as causative agents of infections around the ano-genital tract, resulting in genital warts, and pre-invasive and invasive lesions (Denny, 2009). Obstinate infection caused by the high-risk types (HPV-16, HPV-18) have been associated with 70% of cervical cancers worldwide, and types (HPV-6, HPV-11) are linked to 90% of genital warts (Denny, 2009; WHO, 2012). Currently, there exists two vaccines, Gardasil (Merck and Company, Whitehouse Station, NJ) and Cervarix (GlaxoSmithKline, Brentford, UK) available to the public (Torre, *et al.,* 2015). A major barrier experienced within the economically developing world is access to these vaccines due to their high costs (Torre, *et al.,* 2015). Overcoming this challenge, GAVI, world renowned Vaccine Alliance, negotiated lower prices to facilitate access and role-out of these HPV vaccines in economically developing countries (GAVI, 2013; Torre, *et al.,* 2015).

Papanicolaou (Pap) smears are routinely used to assess cytological abnormalities from cervical swabs. This histological based Pap test, while proven to be highly effective in reducing the incidence and mortality of the disease, detects morphological changes and thus often has a high rate of false positive and false negative results due to inadequate specificity or sensitivity of the test (Nanda, *et al*., 2000). Liao and colleagues (1994) have highlighted a need for the identification of diagnostic biomarkers to supplement cytological tests to help address some of these problems.

1.3.2 Cancer of the oesophagus

Described as the 8th most common cancer worldwide, 455 800 new cases of oesophageal cancer was diagnosed in 2012, with an estimated 400 200 cancer-related deaths, rendering it the sixth most common cause of death from cancer within that year under review (Arnold, *et al*., 2015; Torre, *et al.,* 2015). An estimated 80% of cases reported worldwide originated from low to middle income regions (Arnold, *et al*., 2015; Ferlay *et al*., 2015). Oesophageal cancer has an incidence rate in 2012 threefold greater in males than females (Torre, *et al.,* 2015). This form of cancer is known to have a very poor survival rate (M:I ratio is 0.88) (Arnold, *et al*., 2015; Ferlay, *et al*., 2015). The mortality rate within the Southern African region amongst men was 12.8 per 100,000, whilst in women the rate was 6.2 per 100,000 (Ferlay, *et al*., 2015).

Malignant tumours of the oesophagus can be classified into two main histological subtypes, namely (i) adenocarcinoma (ADC), which developes from cells in the oesophago-gastric junction region or columnar epithelial cells in the lower oesophagus, and (ii) oesophageal squamous cell carcinoma (OSCC), which originates from within the stratified squamous epithelial layer in the upper two thirds of the oesophagus (Gatenby and Preston, 2014).

Major risk factors contributing to the development of oesophageal adenocarcinoma include Barrett's oesophagus and chronic gastro-oesophageal reflux, with notable documented associations with hiatus hernia, obesity and smoking (Gatenby and Preston, 2014).

Despite steadfast advances made in diagnostic and treatment regiments for oesophageal cancer globally, it remains the eighth most common cancer worldwide (Arnold, *et al.,* 2015; Ferlay, *et al.,* 2013). This ever-growing global burden poses an even greater, more devastating effect on the health and economic systems of less developed regions, because approximately 80% of all cases reported occur within these territories (Arnold, *et al.,* 2015; Ferlay, *et al.,* 2013).

In South Africa, studies have shown oesophageal cancer to be the third most commonly diagnosed cancer amongst the male population, with a high mortality rate (<10% survival rate within 3 months of diagnosis) due to the late diagnosis of the disease (Mqoqi, *et al.,* 2004; Somdyala, *et al.,* 2010). Furthermore, the WHO identified Southern Africa as the region with the second highest incidence of oesophageal cancer in males in the world (See figure 2.1; published by: Torre, *et al.,* 2015). Patients with oesophageal cancer frequently develop resistance to currently used chemotherapeutic regime, underscoring the need to develop more effective and efficient tools to diagnose and treat this form of cancer, at an early stage.

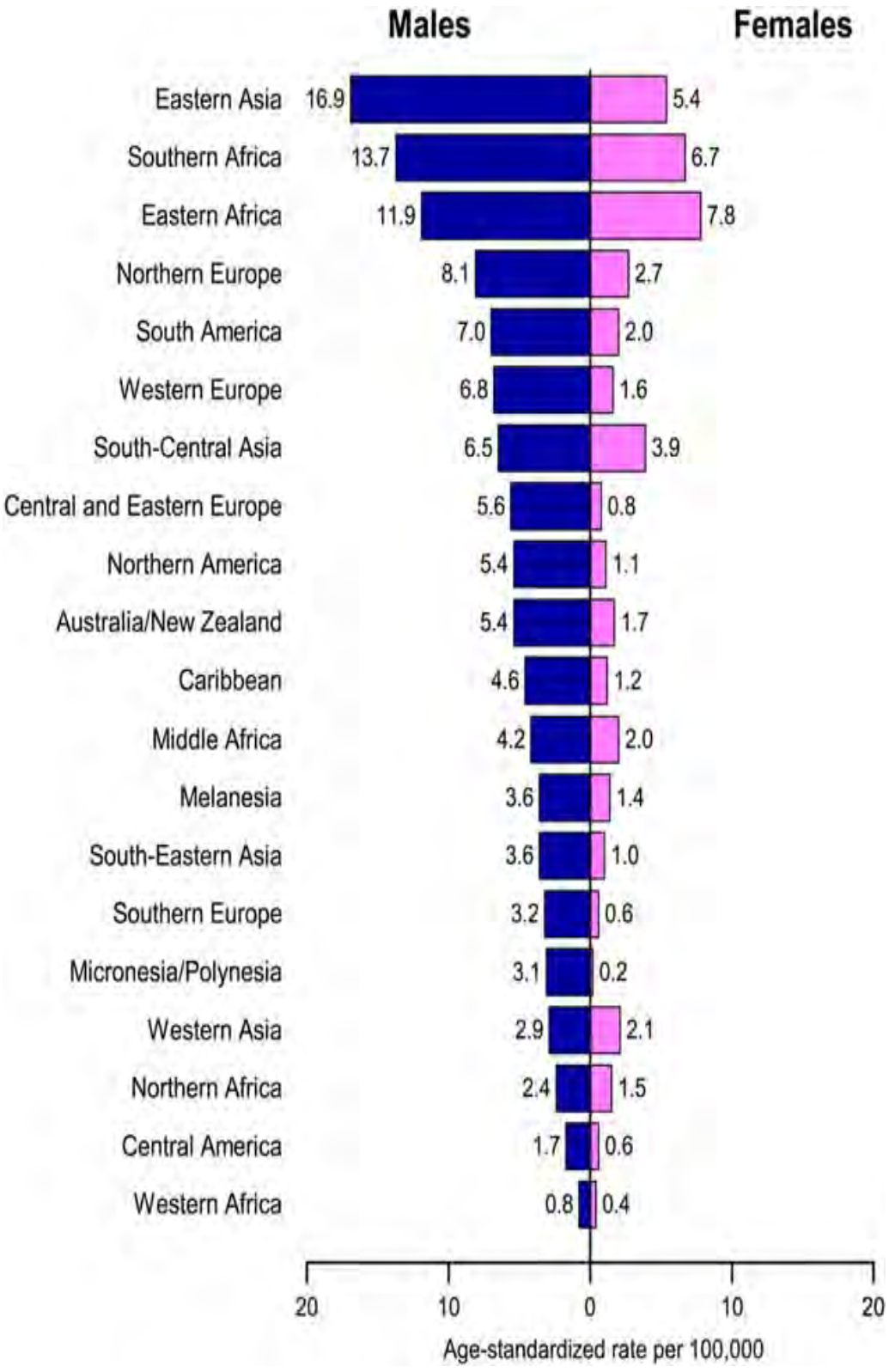

Figure 1.2: Incidence rate of oesophageal cancer worldwide, WHO. This data spread depicts the incidence rates of oesophageal cancer in men and women worldwide. The graph shows Eastern Asia, Southern Africa and Eastern Africa, with the highest incidence rates of oesophageal cancer (Torre, *et al.,* 2015).

1.4 Hallmarks of cancer

Cancer is a multifaceted disease and in 2000, Hanahan and Weinberg initially described six hallmarks of cancer. In 2011, Hanahan and Weinberg proposed the addition of two emerging hallmarks of cancer, namely: “deregulating cellular genetics,” and, “avoiding immune destruction”. Two important enabling characteristics of neoplastic acquisition were identified; genomic instability and mutation, as well as tumour promoting inflammation (Hanahan and Weinberg, 2011; Cavallo, *et al.,* 2011). Figure 1.3 below, graphically displays the Hallmarks of Cancer.

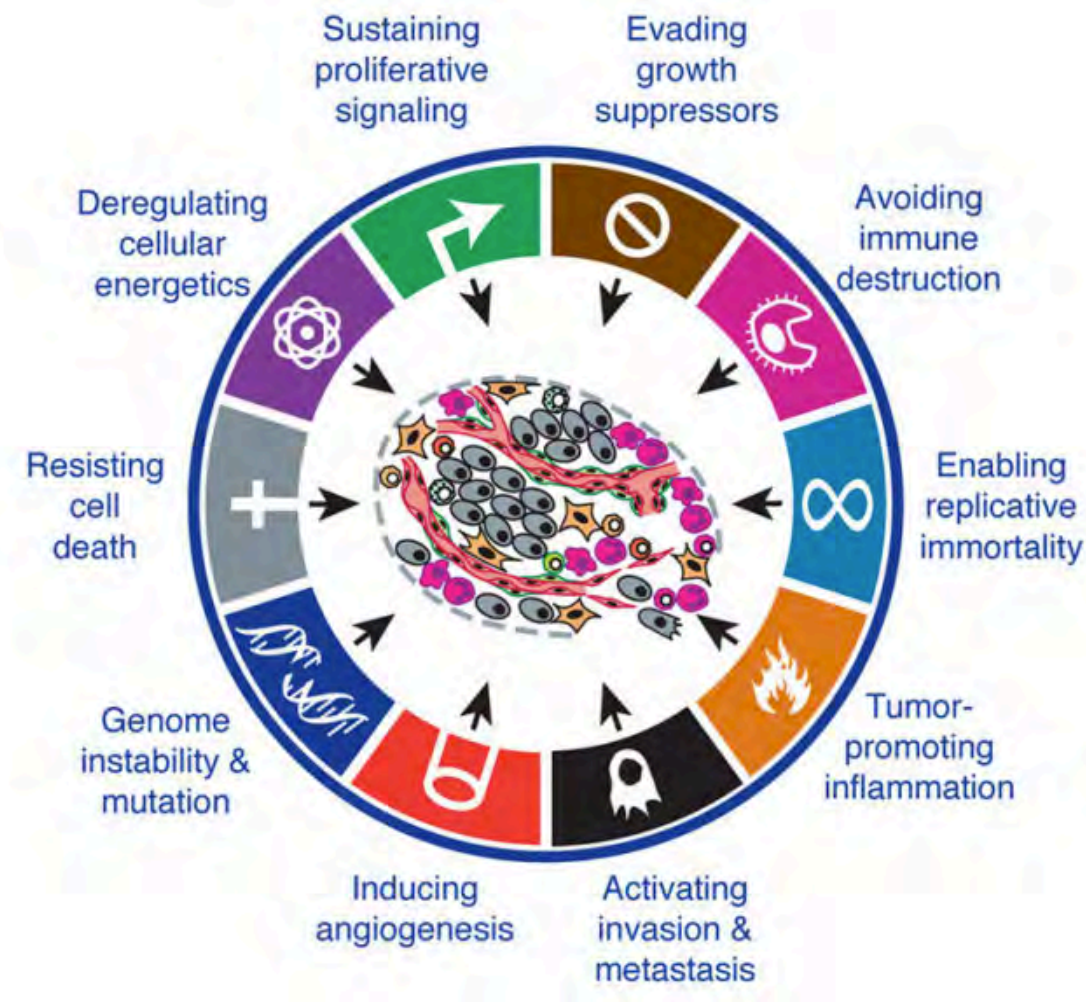

Figure 1.3: The Hallmarks of Cancer. (Hanahan and Weinberg, 2011).

The role played by the Hallmarks relevant to this study are reviewed below:

i. Growth factor independence or self-sufficiency of growth factors:

The binding of a ligand to a specific receptor leads to the eventual transfer of a signal from the membrane towards the nucleus via a cascade of multiple intermediary messengers in the case of membrane-bound receptors (Harrington, 2016). Under normal cellular conditions, the synthesis and activation of ligands responsible for growth factor receptor activation is tightly monitored and regulated; however, cancer cells are able to achieve self-sufficiency of growth signal by ubiquitously deregulating this signaling pathway, thereby using these signals to drive unrestrained cellular division (Harrington, 2016; Rogers, *et al.,* 2005; Hanahan and Weinberg, 2011; Cavallo. *et al.,* 2011).

ii. Insensitivity to anti-growth signals:

Anti-growth signals counteract the growth signals by either forcing cells into a quiescent state (G0 phase of the cell cycle) or by initiating a terminal differentiation state of the cell thereby ensuring a permanent inability of the cell to re-enter the cell cycle. Abnormalities in these signaling pathways are commonplace in cancer thus ensuring progress of the cancer cells through the cell cycle (Hanahan and Weinberg, 2011; Harrington*,* 2016).

iii. Avoidance of cell death:

Within normal cells, if DNA damage occurs during replication (endogenous DNA damage) or due to a genotoxic event (exogenous DNA damage), cell cycle arrest would take place whilst the repair of DNA is executed (Hanahan

and Weinberg, 2011; Harrington, 2016). If the damage to DNA exceeds the capacity for repair, the cell undergoes a form of programmed cell death (apoptosis or autophagy) (Harington, 2016). Tumorigenesis involves the loss of normal regulated cell death signaling pathways, thereby evading programmed cell death. By circumventing apoptosis or autophagy, cancer cells are able to survive and proliferate despite DNA damage, consequently passing the damaged DNA on to the daughter cells (Adam and Cory, 2007; Hanahan and Weinberg, 2011; Harrington, 2016).

iv. Sustained angiogenesis:

Growth of new blood vessels (angiogenesis) is regulated tightly by pro-angiogenic and anti-angiogenic cellular signals (Harrington, 2016). The ability of pre-neoplastic cells to develop into full-blown cancer cells is related to its' capability to attract and secure a new blood supply. Tumorigenesis involves activating an "angiogenic phenotype" by means of increasing and up-regulating the production of pro-angiogenic factors e.g. vascular endothelial growth factor (VEGF), whilst simultaneously down-regulating the production and release of anti-angiogenic proteins such as angiostatin (Hanahan and Weinberg, 2011; Harrington, 2016).

v. Invasion and metastasis:

The invasion-metastasis cascade comprising of discrete sequential steps includes the detachment of tumorigenic cells from within the immediate surrounding microenvironment, coupled with an enzymatic-driven degradation of the extracellular matrix (ECM) allowing for mobility of cells (Harrington, 2016). Following motility of cancer cells, intra-vasation of blood or lymphatic

vessels occur, causing tumour to embolize (Hanahan and Weinberg, 2011; Harrington, 2016). Survival of the tumour emboli is essential until a favourable colonization site is located. Once such a site is identified, attachment of the emboli and subsequent extravasation through the vessel wall takes place. The successful proliferation and ensuing invasion of the new locality is achieved through inducing angiogenesis. (Alizadeh, Shiri and Farsinejad, 2014; Hanahan and Weinberg, 2011).

Some of the key processes explored in this project relate to altered cell morphology, motility and invasion, key elements of metastasis. These are also key elements of another important cellular process termed epithelial to mesenchymal transition (EMT).

1.5 Epithelial to Mesenchymal Transition (EMT)

Epithelial to mesenchymal transition (EMT) is that process where polarized epithelial cells undergo a host of changes (morphology, cellular architecture, adhesive properties and migratory capacity) resulting in detachment and release of highly motile, fibroblast-like mesenchymal cells (Kalluri and Weinberg, 2009). This transitional process is regulated by gene expression changes and subsequent degradation of adherens junctions, causing an increased ability of cells to migrate and subsequently invade surrounding tissue (Figure 1.4) (Kalluri and Weinberg, 2009; Lee and Nelson, 2012; Thiery, 2002; Thiery, *et al.,* 2009).

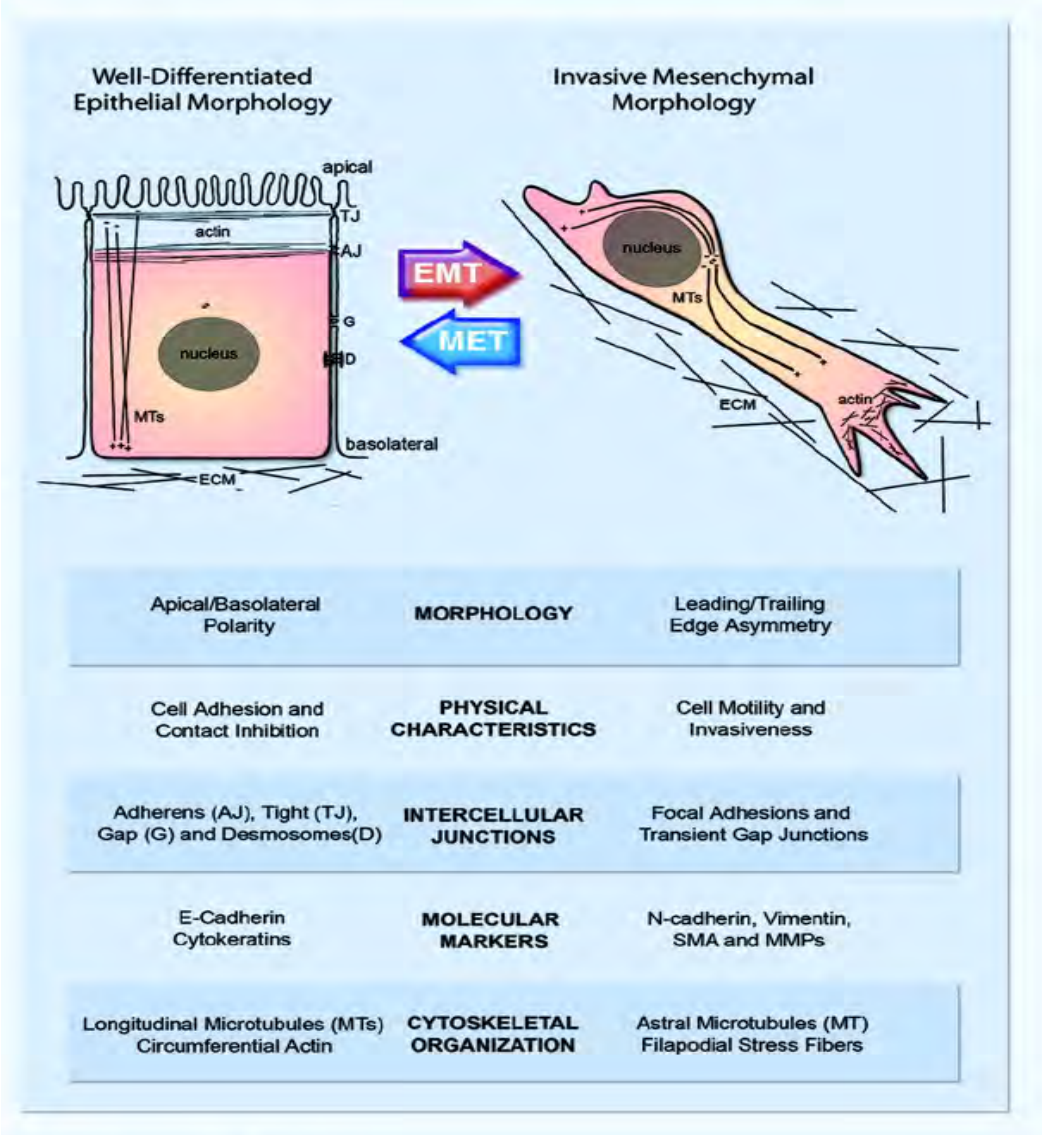

Figure 1.4 Morphologic, phenotypic, and molecular marker differences between epithelial cells and highly invasive mesenchymal cells. Epithelial cells posses a highly polarized morphology with distinct apical and baso-lateral plasma membrane domains. During the process of EMT, well-differentiated epithelial cells acquire an invasive mesenchymal morphology. Mesenchymal cells do not form extensive intercellular junctions. These cells possess different cytoskeletal arrangements and express a different profile of genes, relative to epithelial cells (Figure adopted from: Christiansen, and Rajasekaran, 2006).

Physiologically, EMT plays important roles during embryonic development and wound healing. Loss of proper control over EMT can lead to fibrosis, organ dysfunction, tissue dysfunction and in the case of cancer, metastasis.

This often reversible transition process in cell phenotype has been classified into three types, namely: Type I – Embryogenesis and organ development, Type II – Fibrosis (wound healing and tissue regeneration); and Type III – Metastasis (Klymowsky and Savagner, 2009; Shook and Keller, 2003; Cervantes-Arias, *et al.,* 2013).

The induction of Type-III EMT involves both extrinsic and intrinsic stimuli where the surrounding microenvironment of tumour cells acts as an extrinsic stimulus in facilitating further cancer development and metastasis (Cervantes-Arias *et al.,* 2013).

A critical step in the progression of EMT activation involves the reduction of E-cadherin expression on epithelial cells (Thiery, 2003; Acloque, *et al.,* 2009; Cervantes-Arias, *et al.,* 2013). The Snail family of proteins (an E-Cadherin repressing family) are known EMT inducing factors, which promote the interaction of the tumour cell with its microenvironment (Voulgari and Pintzas, 2009; Moustakas and Heldin, 2005).

Coupled to its central role in cell adhesion, E-Cadherin is known for its cell signaling activity with a range of regulatory proteins, such as β-Catenin, a stabilizing factor within adherens junctions located between adjacent cells (Thiery, 2003; Acloque, *et al.,* 2009). Wnt pathway signaling has been reported to result in β-Catenin release from E-Cadherin and translocation to

the nucleus where β-Catenin has been shown to increase the levels of numerous transcriptional factors of EMT-related proteins, which include Twist, Slug and Snail (Cervantes-Arias, *et al.,* 2013).

1.6 The ADAMs family

1.6.1 Background

The ADAMs (**A D**isintegrin **A**nd **M**etalloproteinase) is a family of proteins present in invertebrate species and all vertebrates (Edwards, *et al.,* 2008). ADAMs are implicated in the control of multiple cellular and developmental activities that include cytokine and growth factor shedding, membrane fusion, cellular migratory as well as invasive properties (Seals and Courtneidge, 2003; Fu, *et al.,* 2014; Edwards, *et al.,* 2008; Rocks, *et al.,* 2008). Extensive literature reviews have also highlighted the involvement of ADAMs in pathologies such as pro-inflammatory microenvironment development as well as tumourigenesis (Giebeler and Zigrino, 2016; Seals and Courtneidge, 2003).

The members of the ADAM family were first identified in guinea pig sperm studies. These studies aimed to identify membrane surface proteins targeted by the monoclonal antibody PH30 (Giebeler and Zigrino, 2016; Seals and Courtneidge, 2003; Primakoff, *et al.,* 1987). These sperm surface proteins contained both metalloproteinase-like and disintegrin-like domain regions, structurally similar to that of the snake venom metalloproteinase protein (SVMP) domain (See figure 1.5) (Giebeler and Zigrino, 2016; Seals and Courtneidge, 2003; Wolfsberg, *et al.,* 1995). The identification of these two

domains, led to their combination, in name, giving rise to the term ADAM, as it contained both ‘A Disintegrin’ and ‘A Metalloproteinase’ domain within its structure (Giebeler and Zigrino, 2016; Wolfsberg, *et al.,* 1995). Belonging to the metzincin superfamily of proteases, ADAMs, also known as MDC proteins (metalloproteinase / disintegrin / cysteine-rich), are zinc-dependent proteinases (Giebeler and Zigrino, 2016).

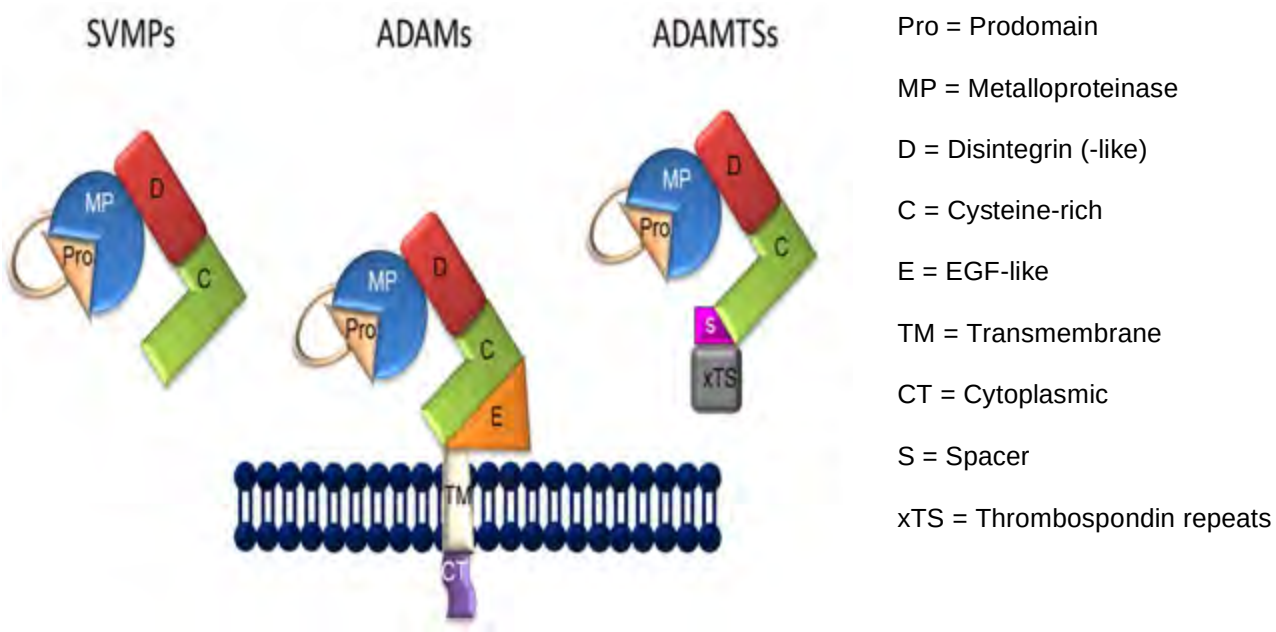

Figure 1.5: A topographic representation of the ADAMs and related metalloproteinases. Generalized domain structures of the ADAMs, SVMPs, and ADAM-TS, families are shown above. Note that ADAM-TS family members have a variable number of thrombospondin-like (TS) motifs (Giebeler and Zigrino, 2016).

1.6.2 Structural overview

The ADAMs is a family of type 1 transmembrane bound and secreted proteins of approximately 750 amino acids in length, with documented functions in cell adhesion and ectodomain shedding of a variety of cell surface receptors and

signaling molecules (Duffy, *et al.,* 2009). The ADAMs are essential in cellular fate determination, wound healing, cell migration, proliferation and angiogenesis (Fu, *et al.,* 2014; Edwards, *et al.,* 2008; Rocks, *et al.,* 2008). A member of the metzincin superfamily of metalloproteinases (zinc protease subfamily), ADAM is structurally composed of six domains, each performing a specific function (Seals and Courtneidge, 2003).

The structural domains of ADAM include: a prodomain region, noted for its ability to assist as a intra-molecular chaperone, as well for its' ability to block potential protease activity (Edwards, *et al.,* 2008; Roghani, *et al.*, 1999); a metalloproteinase region (regulates protease activity, as well as guiding substrate specificity); a disintegrin domain (assists in cellular adhesion activity), an epidermal growth factor (EGF)- like domain (reported to stimulate and aid in membrane fusion) and a cytoplasmic-tail domain, a region rich in proline residues, shown to interact with Src homology 3 domain-containing proteins (Duffy, *et al.,* 2009), and shown in Figure 1.6. ADAM presents as a pro-enzyme (enzymatically inactive precursor protein) due to a cysteine residue (located within the pro-domain site) interacting with a zinc ion at the catalytic site (Edward, *et al.,* 2008; Duffy, *et al.,* 2009; Duffy, *et al.,* 2011). To ensure full metalloproteinase activation, the prodomain region is removed either by means of a furin-like convertase reaction, or via autocatalysis both resulting in proteolytic cleavage (Edwards, *et al.,* 2008, Murphy, 2008; Duffy, *et al.,* 2011).

Approximately 50% of ADAMs contain a highly conserved catalytic region, with a consensus sequence of – HEXGHXXGXXHD – constituting a Zinc binding motif within its protease domain region (Duffy, *et al.,* 2009; 2011). The successful hydrolytic processing of protein substrates of ADAM require this zinc-binding motif consisting of three histidine residues as well as a highly conserved methionine region within the active site of the helix region (Reiss, Ludwig and Saftig, 2006).

Downstream of the proteolytic domain, is the disintegrin region comprising ~90 amino acids (Duffy, *et al.,* 2009; 2011). The disintegrin domain is important for cellular adhesion activities, key in directing binding of ADAMs to the integrins (Duffy, *et al.,* 2009; 2011). The cysteine rich domain located on the C-terminal side of the disintegrin domain regulates the catalytic activities of ADAM. It is the cysteine region that controls substrate targeting as well as the cleavage of the pro-domain region from the catalytic region of the ADAM structure (Duffy, *et al.,* 2009; Duffy, *et al.,*2011; Reiss, Ludwig and Saftig, 2006). The cytoplasmic C-terminal tail of ADAMs vary in sequence length. This particular region is known to be rich in proline residues thus it possesses binding site motif structures for Src homology 3 (or SH3) domain-containing protein, with potential sites for phosphorylation (Reiss, Ludwig and Saftig, 2006). Functionally, this domain site is reported to be involved in the regulation of protease function (Duffy, *et al.,* 2009; Duffy, *et al.,* 2011; Reiss, Ludwig and Saftig, 2006).

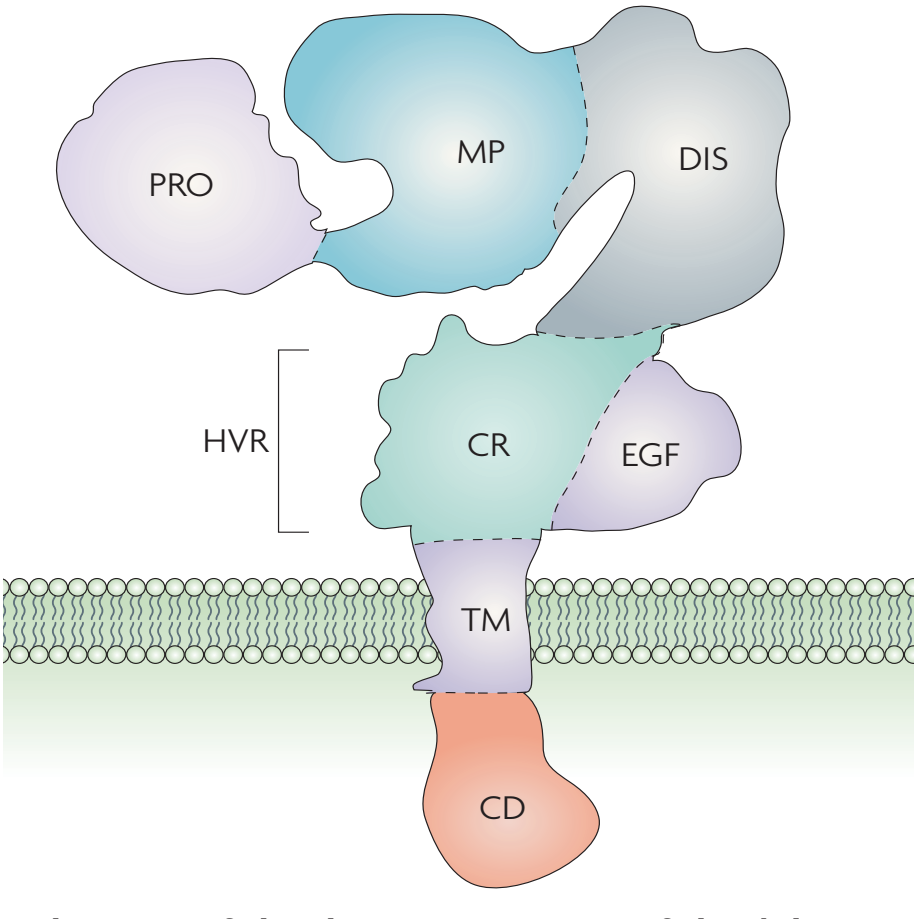

Figure 1.6: Schematic diagram of ADAM. A large amino-terminal propeptide (PRO) (Edwards *et al.,* 2008; Murphy, 2008); a metalloproteinase domain (MP) a carboxy-terminal region split into three segments, namely: a disintegrin domain (DIS), cysteine-rich region (CR) and an epidermal growth factor-like repeat (EGF). The ADAM - DIS and CR domains are documented to form a disulphide bonded entity exposing a hypervariable region (HVR) in the CR domain. The remaining domains within ADAM are the cytoplasmic domain (CD) and the transmembrane domain (TM) (Murphy, 2008).

1.6.3 ADAM and cancer expression levels

Considering the wide range of biological processes that the ADAM protein are involved in, it is perhaps unsurprising that ADAMs have also been implicated in tumorigenesis (Duffy, *et al.,* 2009). These activities include tumour necrosis

factor alpha (TNF-α) release, as well as the shedding of HER/ EGFR ligands (Duffy, *et al.,* 2009). Epidermal growth factor receptor (EGFR) and HER2, members of the EGFR family, are involved in cellular survival, growth, migration and invasion activities, as well as pro-angiogenic activities (Duffy, *et al.,* 2009). Due to their role in these cellular processes, any altered elevated expression level of ADAM on the surface of cells have been implicated in cancer progression and proliferation (Duffy, *et al.,* 2009; Lu, *et al.,* 2008).

Described as a pluripotent peptide, TNF- α assists in activities key to tumour formation and progression (Duffy, *et al.,* 2009; Lu, *et al.,* 2008). These processes include its ability to up-regulate matrix metalloproteinase (MMP) expression levels, thereby enhancing cellular migration, promotion of epithelial to mesenchymal transition, induction of pro-angiogenic growth and development factors, as well as the release of reactive oxygen species known to damage DNA (Duffy, *et al.,* 2009; Lu, *et al.,* 2008).

Overexpression of members of the ADAMs family have been reported in cancer of the brain, breast, colon, lungs, oesophagus, stomach and prostate. Overexpression of ADAM-8 has been associated with renal, lung and brain cancer (Mochizuki and Okada, 2007). In primary brain carcinoma, ADAM-8 associates with an increase in invasiveness and rapid progression (Wildeboer, *et al.,* 2006). The association between invasive metastatic spread and high levels of ADAM-8 expression in tissues has also been seen in patients with pancreatic cancer (Valkovskaya, *et al.,* 2007; Lu, *et al.,* 2008). These results show that ADAM-8 is associated with tumour migration and invasion properties. ADAM-8 has also been reported to be a potential

biomarker for prognosis in lung adenocarcinoma, since greatly elevated levels of ADAM-8 were observed in cancer patient serum samples compared to healthy patient controls (Lu, *et al.,* 2008; Mochizuki and Okada, 2007).

ADAM-9 overexpression has been reported to associate with cancers of breast, pancreas, skin, and lung origin (Lu, *et al.,* 2008; Mochizuki and Okada, 2007). Elevated levels of ADAM-9 in breast cancer have been reported to contribute to the release of HB-EGF (O'Shea, *et al.,* 2003). ADAM-9 overexpression has also been reported in pancreatic ductal adenocarcinoma (PDAC), distinguishing it from other pancreatic tumours (Edwards, *et al.,* 2008; Lu, *et al.,* 2008; Mochizuki and Okada, 2007). In lung carcinoma, ADAM-9 up-regulation assists in the enhancement of invasion properties of non-small cell lung cancer, done so by modulating, altering adhesive molecular properties and, in so doing, promoting metastasis (Edwards, *et al.,* 2008; Lu, *et al.,* 2008; Mochizuki and Okada, 2007).

Increased levels of ADAM-12 have been reported in breast tumour proliferation (Lu, *et al.,* 2008; Mochizuki and Okada, 2007), as well as in bladder, colon and lung carcinoma development (Lu, *et al.,* 2008; Mochizuki and Okada, 2007).

Increased expression levels of ADAM-15 have been associated with cancer development and progression in the breast, prostatic, stomach and lung tissues respectively (Mochizuki and Okada, 2007). Known to have a role in metastasis, ADAM-15, aids both in the detachment of cells from the ECM via

its disintegrin-like domain, and by means of degrading the ECM through its metalloproteinase structural region (Lu, *et al.,* 2008).

ADAM-17 overexpression has been identified within cancers of breast, renal, ovary and prostate origin (Mochizuki and Okada, 2007). Reportedly responsible for the release of proteins such as tumour necrosis factor alpha (TNF-α) and Amyloid Precursor Protein (APP), ADAM-17 has been shown to be a potentially viable biomarker and target for drug therapy (Moss, *et al.,* 2001; Mochizuki and Okada, 2007). Sharing a ~35% identity to ADAM-10 gene sequence, ADAM-17 has been shown to perform similar functions to ADAM-10 (Mochizuki and Okada, 2007). In breast carcinoma, ADAM-17 overexpression has been reported to cause significant increases in cell proliferation and invasion, whilst down-regulation of ADAM-17 results in a decrease in invasive properties (Lu, *et al.,* 2008; Mochizuki and Okada, 2007).

ADAM-19 has been reported to be up-regulated in human primary brain tumours, and associate with invasive properties in glioma cells (Wildeboer, *et al.,* 2006).

ADAM-28, is expressed as two forms, anchored to a membrane, as well as in a short secreted form (Lu, *et al.,* 2008). ADAM-28 is found to be overexpressed in human breast carcinoma, suggesting an involvement in both cellular proliferation as well as invasion and migration properties (Lu, *et al.,* 2008).

Previous work done in our laboratory using microarray analysis identified differentially expressed genes that associate with cervical cancer (Van der Watt, *et al.,* 2009; Ward, *et al.,* 2011). Amongst the genes identified and validated further, ADAM-10 was found to show significant increased expression in both cervical and oesophageal cancer tissue samples when compared to normal tissue samples.

1.6.4 ADAM-10 and cancer

1.6.4.1 Structural features

Described as a membrane sheddase protein, ADAM-10 has an inactive (85kDa) and active mature (65kDa) protein size (Tousseyn, *et al.,* 2009). Although similar in structural domain features, ADAM10 is known to possess both the cysteine rich and EGF-like domain, prevalent in other ADAM proteins (Reiss, Ludwig and Saftig*,* 2006).

1.6.4.2 Role of ADAM-10 in cancer development and progression

ADAM-10 has been reported to be overexpressed in cancers, including colon, prostate and ovarian (Arribas, *et al.,* 2006; Zhang, *et al.,* 2014; Zhao, *et al.,* 2014). ADAM-10 is involved in the intramembranous proteolytic processes of mediating ectodomain shedding of various membrane-bound receptors, growth factors, adhesion molecules and cytokines (Endres and Fahrenholz, 2010; Mochizuki and Okada, 2007). ADAM-10 substrates include betacellulin, epidermal growth factor (EGF), Notch, collagen IV, CD-44 and E-Cadherin (Duffy, *et al.,* 2011; Moss, *et al.,* 2008; Moss, *et al.,* 2007). There is evidence

in the literature that ADAM-10 substrates aid in the development and progression of tumours.

A well-studied example of active ADAM-10 involvement in intramembraneous proteolytic activation is seen in the solubilisation of a range of cell adhesion molecules, including E-Cadherin, and the proteolytic cleavage of CX_3CL1 (Caolo, *et al.,* 2015). Increased levels of B-Catenin freed from a complex of E-Cadherin-B-Catenin, activates cyclin D1, thus enhancing cellular proliferation (Caolo, *et al.,* 2015; Maretzky, *et al.,* 2005); increasing epithelial to mesenchymal transition; enhancing cellular migration, essentially enabling opportunities for tissue invasion and metastasis of tumour cells (Ma, *et al.,* 2007). As ADAM-10 is associated with various processes linked to cancer development, it presents a promising target for cancer therapy.

1.7 Small molecule inhibitors of ADAMS family

1.7.1 Development of ADAM-10 targeted small molecule inhibitor

The inhibition of ADAM-10 is considered a promising strategy aimed at targeting cellular proliferation, invasion and migration in cancer. Several synthesized inhibitors for ADAM-10, i.e. batimastat and marimastat, which belong to the peptidomimetic hydroxamic acid inhibitors for metalloproteinase, have been investigated (Groves, *et al.,* 2006; Hoettecke, *et al.,* 2010; Hundhausen, *et al.,* 2003). Recent studies have demonstrated that although these inhibitors can affect numerous metalloproteinase, they lack in protein

receptor selectivity, hence contributing to their failure in clinical trials (Groves, *et al.,* 2006; Hoettecke, *et al.,* 2010).

The GI254023X (see figure 1.7 of its chemical structure) compound was designed to fit the active cleft site (catalytic domain) of the available ADAM-17 X-ray crystal structure (Ludwig, *et al.,* 2005), whilst using a hydroxamate ligand as a peptidic backbone template. The modeling program used, showed the hydroxamate group binding to the catalytic zinc site, with its P1" isobutyl substituent (leucine-like side-chain) directed into the S1' pocket (Ludwig, *et al.,* 2005). Despite being modeled as an inhibitor against ADAM-17, GI254023X displays a stronger potency to ADAM-10, than ADAM-17. Molecular modeling analysis illustrate that amino acid differences in the active site between ADAM-10 and ADAM-17 contribute to enhanced hydrophobic interaction between GI254023X and ADAM-10, improving its potency in ADAM-10 (Ludwig, *et al.,* 2005).

Therefore, the molecular modelling GI254023X shows a clear distinction at the P1' position within the pseudopeptidic part of the molecule, therefore differing from a broad- spectrum metalloproteinase inhibitors, due to a large hydrophobic substitution (Ludwig, *et al.,* 2005). The lipophilic substitution within this P1' position of GI254023X hydroxymate inhibitor contributes to the compounds' specificity profile for ADAMs (Hundhausen, *et al.,* 2003; Ludwig, *et al.,* 2005), and the greater specificity for ADAM-10.

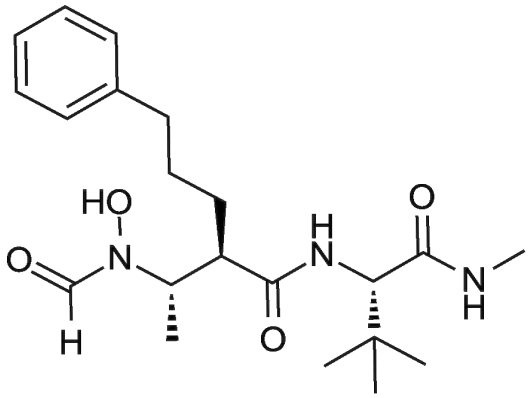

Figure 1.7: GI254023X (Chemical formula: $C_{21}H_{33}N_3O_4$), an inhibitor of ADAM-10 activity. This small molecule inhibitor of ADAM-10 binds to the pocket of activated ADAM-10, thereby inhibiting the function of ADAM-10.

Notably, ADAM-10 differs from other ADAMs four side-chains, which are located in the lining of the S1' pocket, thus causing slight alterations in size and surface charge of the pocket (Hundhausen, *et al.,* 2003; Ludwig, *et al.,* 2005). These surface changes aid in the P1' phenpropyl substitutent of GI254023X attaching enhancing its potency for ADAM-10 S1' pocket over other ADAMs (Ludwig, *et al.,* 2005). Prior research attributes this enhanced fit to the compound's higher potency for ADAM-10 over other ADAMs (Hundhausen, *et al.,* 2003; Ludwig, *et al.,* 2005). The involvement of ADAM-10 in oesophageal cancer and cervical cancer remains unclear. This study aims to examine this role by testing the effect of GI254023X inhibitor and two compounds, SN-311 and SN-254, which were developed as part of a synthetic process to synthesize GI254023X in a laboratory at UCT.

1.8 Research rationale

1.8.1 Aim

Investigate the effects of inhibiting ADAM-10 activity in oesophageal and cervical cancer cells using small molecule inhibitors.

1.8.2 Objective

- To investigate the effect of inhibiting ADAM-10 activity using the small molecule GI254023X and its precursors: SN-254 and SN-311 on cancer cell survival.
- To investigate the ability of the small molecule GI254023X and its precursors: SN-254 and SN-311 to inhibit epithelial to mesenchymal transition in cancer cells.

Chapter 2:
Materials and Methods

2.1 Mammalian cell culture

2.1.1 Cell lines

In order to determine ADAM-10 endogenous expression in normal and cancerous cell lines grown in culture, a range of cell lines were used. Cervical cancer cell line include: HeLa (HPV18 positive), obtained from the American Type Culture Collection (ATCC) (Rockville, MD, USA). An oesophageal cancer cell line was also used, WHCO5 South African oesophageal cancer cells line (Veale and Thornley, 1989). Normal cell lines used included, normal lung fibroblast cell line, WI38 (obtained from the ATCC) and the FG_0 normal skin fibroblast was also assessed (obtained from the Department of Medicine, UCT).

2.1.2 Non-primary cell line growth conditions

All non-primary cancer and normal cell lines used in this study were grown and cultured at 37°C within a humidified incubator, supplied with a mixture of 5% carbon dioxide and 95% air gas. These cell lines were cultured with Gibco® Dulbecco's Modified Eagle Medium (DMEM) (Invitrogen, USA) containing 10% heat-inactivated foetal bovine serum (FBS), penicillin

(100U/mL), and streptomycin (100µg/mL).

2.1.3 Subculturing cells

Cells grown in a 100 mm tissue culture dish to a confluence of 60 – 80% were washed with 2 mL of trypsin –EDTA laboratory prepared trypsinisation solution, thereafter, the solution was washed off. Thereafter, four millilitres of fresh trypsin-EDTA solution was pipetted onto the cells. The culture plates where returned to the incubators, left inside to aid in the process of trypsinisation. When 70-90% of cells were trypsinised (determined by monitoring with use of a microscope), the reaction was stopped with the addition of 4 mL of fresh complete media (DMEM, 10% FCS and 1% P/S). This cell suspension was transferred into a 12 mL Greiner tube, and centrifuged at 250 x g for 3 minutes at room temperature. Post centrifugation, this complete media / trypsin-EDTA combined solution was aspirated off, and the cell pellet was re-suspended in 1 mL of complete media. Approximately 150 µL of this cell suspension was then inoculated into 10 mL of fresh complete medium within a 100 mm tissue culture dish.

2.1.4 Freezing and thawing cells

A confluent dish (70 – 80% fully grown dish) of cells was trypsinised, neutralised with fresh complete media, and following centrifugation, carefully removed from this combined trypsin-EDTA / full media solution. These cells were then re-suspended in 5 mL of freezing media (70% complete culture

media, 20% FCS and 10% dimethylsulfoxide (DMSO)) and 1 mL of this solution was added to individual cryotubes. The cryotubes were stored at -80°C for 24 hours, thereafter transferred to liquid nitrogen for long-term storage.

Thawing of frozen stocks (whether from -80°C stocks, or liquid nitrogen) involved quickly thawing the cryotube contents in a 37°C water-bath, thereafter transferring the cryotube cell suspension contents into a 100 mm tissue culture dish containing 10 mL pre-warmed complete media. Cells were left in the incubator at 37°C overnight, thereafter change of complete media occurred.

2.1.5 Mycoplasma testing

All cell lines were tested twice a year for Mycoplasma contamination. The protocol to test involved culturing of cells in penicillin and streptomycin-free culture media for 3 days. Continuing with the same culture media conditions, cells were then plated onto recently sterile flamed coverslips, and left to settle and grow for a further 24 hours. Cells were then fixed and stained with Hoechst fluorescent DNA-binding stain for approximately 30 seconds, thereafter washed and then mounted with mowiol on microscopy slides. Stained slides were visualised on the Zeiss Axiovert 200 Fluorescent microscope (Carl Zeiss, Jena, Germany). The absence off small fluorescent speckling / spots between the stained nuclei, indicated that cells were Mycoplasma- free.

2.2 Drug and inhibitor preparation

2.2.1 GI254023X

GI254023X, a hydroxymate derived inhibitor of ADAM-10, was purchased from Tocris Biosciences (Catalogue #3995/1). A 1 mg sample of the drug was dissolved into a stock solution concentration of 100 mM in DMSO and stored at -20°C (as per manufacturer's instruction).

2.2.2 Precursor derivatives: SN254 and SN311

During the initial synthesis plan for GI254023X inhibitor, the UCT Chemistry Department developed two new precursor derivatives of GI254023X, namely SN-254 and SN-311 compounds. Synthesis of SN-254 and SN-311 compounds were carried out by UCT Chemistry Department. Briefly, 1 mg sample of each drug was dissolved into a stock solution concentration of 100 mM in DMSO and stored at -20°C.

2.3 Protein analysis

2.3.1 Preparation of whole cell lysates and protein quantification

After various *in-vitro* experiments (i.e. detection of epithelial to mesenchymal transition markers, or VEGF expression detection post treatment with ADAM-10 inhibitors), protein was isolated from the plated cells. The existing media removed, and cells washed twice with PBS, which was cooled to 4°C. a Radioimmunoprecipitation assay buffer (RIPA) containing 0.5 mM PMSF,

complete protease inhibitor cocktail (Roche, Basel, Switzerland), and 50 mM NaF, 2mM NA_3VO_4 to inhibit the action of phosphatases was added to the cells. Cells were then scraped using a cell scraper and transferred to a 1.5 mL Eppendorf tube. The cell lysate was then subjected to sonication for 10 seconds, followed by centrifugation at 10000 x g at 4°C for 10 minutes, in order to remove any cellular debris. The supernatant was aspirated and transferred to a clean Eppendorf 1.5 mL tube. Protein concentration was quantified using the Bicinchoninic acid (BCA) Protein Assay Kit (Thermo Scientific, USA), as per manufacturer's instructions. Both the BCA samples and the protein samples absorbance was read at 595 nm, and protein concentration of the isolated protein samples harvested, was calculated using the standard bovine serum albumin concentrations (BSA) readings at 595 nm. The isolated protein samples were stored at -80°C for long-term storage.

2.4 Western blot analysis

2.4.1 Sodium dodecyl sulphate polyacrylamide gel electrophoresis (SDS-PAGE) and protein transfer

All gels were cast and proteins were separated using the Mini Protean II System (BIO RAD). 10 – 35 µg of protein sample size was prepared by adding 5X Laemmli loading dye (see solutions) and made up to a specific volume with distilled autoclaved H_2O. The prepared samples were heat-denatured at 90°C for 1 minute using a heating block. Heating of the protein sample when combined with β-mercaptoethanol and sodium dodecyl sulphate (SDS) ensures that the protein sample is denatured, into a reduced state, thus

allowing for the successful separation of the proteins present within the sample based on their respective size.

Gels were cast in 1.5 mm glass plates using the BIO-RAD system. Resolving and stacking gels were prepared as described in table 2.1. The resolving gel was poured first, and left to set. Thereafter the stacking gel was cast above the set resolving gel, and carefully the 10-well comb was inserted into the stacking gel mixture. Prepared protein samples were loaded into the cast wells within the stacking gel. A protein molecular weight marker was run concurrently with the samples, in order to determine the size of the separated proteins (Kaleidoscope, BIO RAD, USA). Protein samples were then electrophoresed at 180V for 1.5 hour in 1X Running Buffer (see solutions). Following this process, the separated proteins within the resolving gel were transferred onto a Hybond™-ECL™ nitrocellulose membrane (Amersham Life Sciences, UK) using the wet/tank transfer system (BIO RAD, USA). The transfer occurred at 100V for 70 minutes in 1X Transfer Buffer (see solutions).

Table 2.1: Solutions with specified volume as per gel condition for Western blot analysis.

Resolving gel (cast in 1.5mm glass plate):				
Contents:	**12%**	**10%**	**7.5%**	**15%**
dH_2O	2150 µL	2850 µL	7280 µL	3300 µL
1M Tris pH8.8	3750 µL	3750 µL	3750 µL	3900 µL
10% SDS	50 µL	50 µL	150 µL	150 µL
30% Acrylamide/ bis	4000 µL	3300 µL	3750 µL	7500 µL
10% Ammonium persulphate (APS)	50 µL	50 µL	75 µL	150 µL
TEMED*	5 µL	5 µL	7.5 µL	15 µL

Stacking gel (cast in 1.5mm glass plate):	
Contents:	**4%**
dH_2O	3650 µL
1M Tris pH6.8	625 µL
10% SDS	50 µL
30% Acrylamide/ bis	650 µL
10% Ammonium persulphate (APS)	60 µL
TEMED*	6 µL

***(N,N,N',N'tetramethylethylenediamine)**

2.4.2 Immunoblotting and chemi-luminescent detection

Following the transfer of the protein samples onto the nitrocellulose membrane, the membrane was blocked in 5% low fat milk dissolved in Tris-buffered saline with 0.1% Tween (TBST) for 1 hour at room temperature. Thereafter, the membrane was probed with the specific primary antibody at 4°C over night with agitation. Post primary antibody incubation, the membrane was washed three times with TBST for 10 minutes each, thereafter the

nitrocellulose membrane had horseradish peroxidase-conjugated secondary antibody added onto it for 1 hour at room temperature with agitation. Following the incubation of the membrane with the secondary antibody, excess secondary antibody was removed with three 10 minute TBST washes. The protein bands were detected using the LumiGLO or LumiGLO reserve chemiluminescent substrate system (KPL Inc.). For detection procedure, AGFA CU-BR Medical X-ray film (AGFA, Belgium) were exposed onto the membrane. Thereafter, the X-ray film was developed until the band(s) of interest were seen, before the X-ray film was fixed in a fixative reagent.

2.4.3 Antibody concentrations and conditions

Below, is a table summarising the blocking conditions for all primary antibodies used, along with their corresponding secondary antibody conditions (table 2.2)

Table 2.2: Blocking and immunoblotting conditions for primary and secondary antibodies

CONDITIONS FOR ANTIBODY USAGE IN WESTERN BLOT DETECTION:										
PRIMARY ANTIBODY	TYPE	SPECIES	BLOCK	DILUTION	DILUENT	COMPANY	CATALOGUE NUMBER	SECONDARY ANTIBODY	DILUTION	DILUENT	COMPANY	CATALOGUE NUMBER
ADAM-10	Monoclonal	Mouse	5% Milk	1:500	5% Milk in TBST	Santa Cruz	Sc-28358	Goat anti-mouse IgG (H+L) HRP conjugate	1:1000	5% MILK in TBST	Abcam	170-6516
E-Cadherin	Polyclonal	Rabbit	5% Milk	1:1000	5% Milk in TBST	Santa Cruz	Sc-7870	Goat anti-rabbit IgG-HRP-conjugate	1:5000	TBST	Abcam	170-6515
B-Catenin	Monoclonal	Mouse	5% Milk	1:1000	TBST	Santa Cruz	Sc-7963	Goat anti-mouse IgG (H+L) HRP conjugate	1:2000	5% MILK in TBST	Abcam	170-6516
GAPdH	Monoclonal	Mouse	5% Milk	1:2000	5% Milk in TBST	Santa Cruz	Sc-47724	Goat anti-mouse IgG (H+L) HRP conjugate	1:5000	5% MILK in TBST	Abcam	170-6516
PARP-1	Polyclonal	Rabbit	5% Milk	1:1000	TBST	Santa Cruz	Sc-7150	Goat anti-rabbit IgG-HRP-conjugate	1:5000	5% MILK in TBST	Abcam	170-6515
β-tubulin	Polyclonal	Rabbit	5% Milk	1:1000	5% Milk in TBST	Santa Cruz	Sc-9104	Goat anti-rabbit IgG-HRP-conjugate	1:2000	5% MILK in TBST	Abcam	170-6515
VEGF-1	Monoclonal	Mouse	5% Milk	1:500	2.5% Milk + 2.5% BSA in TBST	Santa Cruz	Sc-7269	Goat anti-mouse IgG (H+L) HRP conjugate	1:1000	5% MILK in TBST	Abcam	170-6516
Vimentin	Monoclonal	Mouse	5% Milk	1:1000	TBST	Santa Cruz	Sc-6260	Goat anti-mouse IgG (H+L) HRP conjugate	1:5000	TBST	Abcam	170-6516

2.4.4 Densitometry analysis

Once X-ray radiographic detection (using AGFA radiofilm) of membranes were performed, the developed band intensities of proteins probed were quantified by densitometry using ImageJ software, following the manufacturer's instructions. The protein expression of each band was quantified relative to the intensity to β-tubulin or GAPdH bands (which served as the loading control).

2.4.5 Stripping and reprobing blots

To re-probe the membrane for another protein, the membrane was stripped using 10% acetic acid for 30 minutes at room temperature with agitation. Following stripping, the membrane was then washed 4 times with TBST for 5 minute intervals at room temperature each time with agitation. Thereafter, the membrane was again blocked in 5% milk, and primary antibody conditions as stipulated in table 2.2 were applied.

2.5 Drug efficacy assessment

2.5.1 MTT EC_{50} determination assay

The EC_{50} value of GI254023X, and the two newly synthesized precursors, SN-254 and SN-311 were determined in a two normal cell lines (FG_0 and WI38), and two independent cancer cell lines, namely HeLa cervical cancer cell line and WHCO5 oesophageal cancer cell line respectively. Cells were

grown in complete media (DMEM, 10%FCS, 1%P/S) and seeded at a density of 1000 cells per well for HeLa, and 3000 cells per well for WHCO5, FG_0 and WI38 cells, and plated into a 96-well tissue culture plate. Cells were treated the following day with varying concentrations of the small molecule inhibitors of ADAM-10 (0, 10, 50, 75, 100, 200, 300 and 400 µM), all performed in triplicate. 24 hours after drug treatment of the individual cell lines, 10 µL MTT reagent (Sigma) was added to each well, and four hours later the crystals formed were solubilised by the addition of Solubilisation Solution Reagent (10 % SLS in 0.01 M HCl). Absorbance readings were measured at 595nm the following day using a BioTek microplate spectrophotometer (Winooski, VT, USA). The EC_{50} determined assay curves were generated with use of GraphPad 6.05 Prism (Mac compatible edition).

2.5.2 Anchorage-dependant (MTT) proliferation assay

Cell growth and death as a result of either ADAM10 knockdown transfection assays or treatment with GI254023X, SN-311 and SN-254 was numerically determined using the MTT proliferation assay, which analysis cell viability and proliferation by the addition of a yellow reagent, MTT (3-(4,5-dimethylthiazole-2-yl)-2,5-diphenyl tetrazolium bromide) (Sigma). MTT is a positively charged tetrazolium salt, which readily penetrates the cell membrane of viable cells, and in the process the salt is reduced to a purple formazan product by means of the active metabolism of the viable cells, it penetrates (Berridge and Tan, 1993). Furthermore, the MTT reagent is solubilised by the addition of a solubilisation reagent (10 % SLS in 0.01 M HCl) and quantified by reading

absorbance at 595nm using a BioTek microplate spectrophotometer (Winooski, VT, USA). The proliferation assay was performed over a five-day period. HeLa cervical cancer cell line and WHCO5 oesophageal cancer cells were seeded into 96-well tissue culture plates at 1000 cells per well. The EC_{50}, 2X EC_{50} and the volume required to dissolve the drug at 2X EC_{50} in DMSO (control) was selected for each of the small molecule inhibitors and treated to each cell line for each day, and treatment was performed in triplicate. On each day that the assay was performed, 10 µL of MTT was added to each of the treated wells, thereafter, 4 hours later, 100 µL of solubilization solution was subsequently added. The next day the 96-well tissue culture plate was read at 595 nM using a BioTek microplate spectrophotometer (Winooski, VT, USA).

2.5.3 Clonogenic colony formation assay

Clonogenic colony formation assay is described as an *in vitro* cell survival assay, This assay monitors the ability of a single cell to grow into a colony of at least 50 cells. This assay is widely used to assess the number and size of cancer cell colonies that remain post cytotoxic agent administration / treatment. Briefly, 1000 cells were seeded into each well within a 6-well plate.

Both HeLa cervical cancer cell line and WHCO5 oesophageal cancer cell line were seeded to 1000 cells per 6-well plate, plated in triplicate, and treated 24 hours later with EC_{50} value, 2X EC_{50} value of each of the small molecules under investigation individually per cell line, as well as the equivalent volume

of DMSO required to dissolve 2X EC_{50} concentration of each drug, serving as a control variable. The treated cells were left to grow in the incubator at 5% CO_2, 37°C for a period of 9 days. Thereafter, cells were stained with 0.5% crystal violet staining solution (see solutions), and cell colonies formed were quantified under the stereomicroscope. High definition (HD) resolution photographs were taken of each well, and colonies were quantified using the ColonyArea ImageJ Plugin, as described by Guzman and colleagues (2014). Plating efficiency and survival fraction was calculated using the following equations:

- Plating efficiency %: (PE%) = number of colonies / number of cells plated x100
- Survival fraction %: (SF%) = PE of treated sample / PE of control x100
- Cell survival = number of counted colonies / [number of seeded cells x PE control / 100]

2.6 ADAM10 functional assay

2.6.1 Human CX_3CL1 fractalkine immunoassay – enzyme linked immune-sorbent assay (ELISA)

The CX3C chemokine fractalkine (CX_3CL1) exists both as a membrane protein, enhancing cell-cell adhesion, as well as a soluble molecule form, aiding in chemotaxis (Hundhausen, *et al.,* 2003). The trans-membrane CX_3CL1 is converted into its soluble form by the process proteolytic cleavage (shedding). Cleavage of the 95 – 100 kDa type 1 transmembrane form of

fractalkine into its soluble 60 – 80 kDa form, is conducted by ADAM10 (Hundhausen, *et al.,* 2003).

This assay, the Quantikine® ELISA Human CX_3CL1/ fractalkine Immunoassay (catalogue number: DCX310, R&D Systems, USA), utilizes the quantitative sandwich enzyme immunoassay technique. Plates were precoated with a human fractalkine monoclonal antibody. Both standards (employed within this kit) and samples tested were collected according to the manufacturer's requirements. Briefly, 100 µL of the Assay diluent RD1-88 (kit provided) was pipetted into each of the wells used in the 96-well plate provided. Thereafter within 15 minutes, a 100 µL of the standard control and tested samples collected post EC_{50}, 2X EC_{50} and DMSO (control) treatment of all compounds assessed in HeLa and WHCO5, were added to the wells, and left to incubate for 3 hours at 4°C.

Post washing away any unbound substances with the washing buffer (kit provided), 200 µL of the cold enzyme-linked monoclonal antibody specific for human fractalkine was added to each of the wells within the 96-well plate, and left to incubate for a further 1 hour at 4°C. Following another wash to remove any unbound antibody-enzyme reagent, 200 µL of a substrate solution (kit provided) was added to each of the wells. At this stage, the plate was stored away from light and left to incubate at room temperature for 30 minutes. Lastly, 50 µL of a kit provided stop solution was added to each well, resulting in a colour change, with intensity of the colour change correlating to the amount of fractalkine bound within the initial step. This colour intensity was

measured at 450 nm, and corrected to 570 nm, as per manufacturer's instructions, using the BioTek microplate spectrophotometer (Winooski, VT, USA).

2.7 Microscopy and immunofluorescent analysis

2.7.1 Immunocytochemistry detection in cell lines – actin staining

250000 HeLa cervical and WHCO5 oesophageal cancer cells were plated and left to grow on flamed sterilised glass coverslips in a 6-well tissue culture treated plate in complete media (DMEM, 10%FCS, 1%P/S). The following day, once the cells had settled on the coverslips, they were treated with EC_{50}, 2X EC_{50} of GI254023X, SN-254 and SN-311. For control variables, equivalent volumes of DMSO required to dissolve 2X EC_{50} of each small molecule inhibitor was used.

Following treatment of the cells, the treated media was removed and the cells were washed with PBS, thereafter the cells were fixed with 4% paraformaldehyde (PFA), which was then followed by three intervals of 5 minute washes in PBS. Following fixation, the treated cells were permeabilised with 0.5% Triton-X 100, and subsequently washed in PBS for 5 minutes. The permeabilised cells were then quenched with 50mM NH_4Cl made up in PBS for 5 minutes, thereafter blocking of the quenched cells were performed using 0.2% gelatin dissolved in PBS for 30 minutes at room temperature. After blocking, cells were incubated with fluorescently labelled

50ng/mL Phalloidin-Tetramethylrodamine B isothiocyanate (Sigma-Aldrich) in 0.2% gelatin dissolved in 1X PBS, and incubated for 45 minutes at room temperature, by means of inverting the coverslips onto 100µl drop of the antibody dilutions. All incubation periods were conducted within a humidifying chamber in the dark. Following phalloidin incubation, the coverslips were washed 3 times for 5 minute intervals with 1X PBS. Thereafter, the cell nuclei were stained with 100ng/ml Hoechst staining in 1X PBS for 10 minutes at room temperature. The coverslips were finally washed 1X PBS at room temperature and mounted onto slides with Mowiol® -88 (Polysciences Inc., USA). Slides were stored at 4°C in a dark, slide storage chamber for long-term storage. Images of the slides were captured using a Zeiss inverted fluorescence microscope under 100 X oil immersion.

2.7.2 Phase- contrast microscopy

Phase contrast microscopy technique was used to capture any possible morphological changes associated with transformation and the effect of ADAM-10 inhibition in HeLa and WHCO5 cell lines post treatment with GI254023X, (and also with SN-254 and SN-311. Cells were plated onto sterilized cover slips in 60 mm dishes, and allowed to settle overnight following adherent growth conditions. The next day, cell lines were treated with either one of the compounds, at either the EC_{50}, 2X EC_{50} concentrations, or with DMSO volume equivalent to 2X EC_{50} required volume to dissolve the drug. 48 hours after treatment, the various cell lines were fixed in 4% paraformaldehyde for 20 minutes at room temperature and mounted on slides

using Mowiol® -88 (Polysciences Inc., USA). Slides were stored at 4°C in a dark, slide storage chamber for long-term storage. Cells were viewed under visual light and phase contrast, and numerous pictures were taken using a standard fluorescence microscope.

2.8 Monitoring cellular killing effects

2.8.1 PARP1 (Poly (ADP-Ribose) Polymerase 1) detection assay

Poly(ADP- Ribose) polymerase (PARP), is a well known caspase cleaved substrate (Bock and Chang, 2016; Kotsopoulos, 2016), therefore induced cleavage of its protein, indicates that the cell is undergoing apoptosis. PARP is therefore involved in regulating cellular responses to stresses, which are induced by DNA damage response (DDR), unfolded protein response (UPR), and cytoplasmic stress response (Bock and Chang, 2016). 350 000 HeLa and WHCO5 cancer cells were seeded per 60mm dish into 4ml of complete media (DMEM, 10%FCS, 1%P/S) and incubated overnight at 37°C. The following day, treatments with GI254023X, SN-311 and SN-254 were performed with an EC_{50} and a 2X EC_{50} concentration value of the compounds. DMSO only treatment served as the control variable for each of the small molecule treatments. 48 hours after treatment, cells were harvested by collecting both adherent and floating cells (within the media). The initial step involved aspirating the media bathing the treated cells, and decanting it into a sterile 12 mL tube. The 12 mL tubes were centrifuged at 10 000 RPM to harvest the floating cells. After suctioning off gently the supernatant after centrifuging the

12 mL tube, the formed pellet of floating cells was gently washed and re-suspended with PBS and placed in sterile 1.5 mL eppendorf tube. Thereafter, another round of centrifugation was performed with the 1.5 mL eppendorf tubes at 10 000 RPM for 15 minutes at 4°C. The PBS was removed and the eppendorf tubes were placed on ice.

The remaining adherent cells to the dishes were harvested using RIPA mix and a cell scraper as described in section 2.3.1. Following the process of sonication and centrifugation, the cell lysate of both adherent and floating cells supernatant was transferred into a clean 1.5ml eppendorf tube and proteins were quantified as described in section 2.3.1. PARP-1 cleavage was detected via western blot analysis and radiographically viewed with LumiGLO chemiluminescent substrate system (KPL Inc.). The presence of a 89kDa cleaved PARP band from the 116kDa full length PARP band, was an indication of apoptotic activity.

2.8.2 Caspase GLO 3/7 Apoptosis assay

Caspases 3 and 7 are known mediators of the apoptosis. Their enzymatic activity levels can be determined using a luminogenic substrate system, whereby the luminescence produced in this activity assay is proportional to caspase activity, and thus apoptosis. The extent of apoptotic activity was determined by measuring the Caspase-3/7 activity, using the Caspase-Glo® 3/7 Assay (Promega), according to the manufacturer's instructions. Cells were seeded into tissue culture 96-well plates, at a final volume of 90 µL with a cell

concentration value of 8000 cells/well. The following day, these cells were treated either with GI254023X, SN-311 or SN-254 at EC_{50} and 2X EC_{50} concentrations respectively at a final volume of 10 µL. DMSO only treatment served as the control variable for each small molecule treatments. 48 hours after treatment, 100 µL of Caspase-Glo 3/7 reagent was added to each well. The plate was left at room temperature for 1 hour, protected from light. Thereafter, 100 µL of this cell/Caspase 3/7 suspension was transferred to a white 96-well plate (Nunc, Rochester, NY, USA). Luminescence was measured and quantified using the Glomax 96 Microplate Luminometer (Promega).

2.9 Cellular adhesion assays

2.9.1 Fibronectin-coated adhesion assay.

All cell lines (HeLa and WHCO5) were treated with GI254023X, SN-311 and SN-254 at concentrations of EC_{50}, and 2X EC_{50}, and at 0 µM (served as the control – DMSO only treatment). In a 96 well plate, 40 µL of 20µg/mL fibronectin was coated on the base of each well and incubated at 4^{o}C overnight. Post fibronectin coating, all wells were washed twice with 200 µL wash buffer (0.1% BSA in antibiotic and serum free media) and blocked in 200 µL binding block buffer (0.5% BSA in DMEM only) for 1 hour at 37^{o}C. The binding block buffer was discarded with the addition of 200 µL wash buffer and incubated on ice for 10 minutes. A total of $8x10^4$ cells was plated into each of the 6 well plate per treatment and incubated at 37 ^{o}C for 30 minutes, with gentle tapping every 3 minutes. The unbound cells were rinsed away by

200 µL wash buffer. The remaining bound cells were fixed in 50 µL 4% paraformaldehyde for 15 minutes at room temperature. Thereafter the plate was again rinsed with 200 µL of washing buffer per well. The wells were then stained with 60 µL crystal violet (5mg/mL in 2% EtOH) for 10 minutes at room temperature. Excess crystal violet was rinsed off with 100 µL dH_2O and left to dry overnight in a fume hood. The next day, 50 µL 2% SDS was added to solubilise stained cells and a colorimetric intensity was analysed on a microplate reader at 595 nm.

2.9.2 Non—coated adhesion assay

All cells (both HeLa and WHCO5) were seeded and pre-treated with the established EC_{50} and 2X EC_{50} value of GI254023X, SN-311 and SN-254 compounds respectively. DMSO only treatment served as the control variable for each small molecule treatments. Thereafter, treated cells were trypsinised and recounted to be seeded to a total number of $5x10^4$ cells within a total volume of 500 µL and added into a 24-well plate, in which the cells were incubated for 1 hour at 37^{o}C. Thereafter, all media was removed from these wells. Half the wells of each treatment were washed with 300 µL of PBS, whilst the remainder of the wells remained unwashed, hence served as a total cell control. Then both washed and unwashed wells were fixed with 100 µL of 4% paraformaldehyde for 15 minutes and stained with crystal violet for 5 minutes. Thereafter, all the wells were rinsed three times with dH_2O (to eradicate excess crystal violet), and allowed to dry overnight at room

temperature. A range of fields of view was reviewed for each treatment and subsequently calculated in relation to the unwashed wells accordingly.

2.10 Motility assays

2.10.1 Transwell migration assay

Transwell migration assays are commonly used for studying motility of metastatic cancer cells. The principle behind this assay is based on two-medium containing chambers, employing a permeable layer of support (usually tissue-culture treated microporous membrane) through which metastatic cancer cells transmigrate. Each compartment mimics different microenvironments for cell survival.

A Transwell inserts with 8 µM pores were used in this assay (Greiner bio-one, Solingen, Germany). Cells were plated at $3x10^5$ cells per 60 mm dish. The following day, the cells were treated with the various compounds under review, at concentrations of the determined EC_{50} and 2X EC_{50} value. DMSO only treatment served as the control variable for each small molecule treatments. 24 hours after treatment, treated cells were trypsinised and counted so that 2.5 x 10^5 cells were re-plated in triplicate within a 24-well plate in 0.5 mL of 1% FCS-containing media onto the porous membrane of the inserted chamber (within the upper chamber), allowing for vertical directed migration of the cells through the pores of the membrane into the lower

chamber containing a chemo-attractant agent (higher serum concentration of 20% FCS-containing media).

These cells were incubated at 37°C and allowed to migrate through the porous membrane to the underside of the insert for a 24 hour period. After the 24-hour incubation period, cells, which had not migrated, and found on top of the membrane, were removed with a cotton swab. Motile treated cells, which moved to the underside of the membrane, were fixed in 1 mL of methanol for a 5 minute period, thereafter was stained with 1 mL of crystal violet (0.2% w/v in 2% methanol) for 5 minutes. The inserts were then rinsed five times with dH_2O, and at every interval, cotton swabs were used to ensure that the sides and edges of the inserts were cleaned and dried properly.

Along with every treatment condition assessed, which was performed in triplicate, and repeated independently twice, a fourth chamber of cells were plated, and served as a total cell number control between the various drug treatment conditions applied. The cells plated in this fourth chamber were not removed with a cotton swab, instead were stained on either side of the membrane with crystal violet (0.2% w/v in 2% methanol) for 5 minutes.

The total number of migrated cells was normalized for each condition to the control insert (the 4^{th} chamber of each drug treatment condition), which was then further normalized to the control –DMSO only treated wells, as DMSO treatment served as the control variable for each small molecule treatments (as each of the drugs assessed were dissolved in DMSO). The stained

membranes were left to dry overnight at room temperature, following which the stained cells were viewed under a microscope and images were taken in ten random fields under view. The cells in each of the fields were counted and quantified to determine the number of migrated cells using ImageJ software. Furthermore, an additional quantitation method was applied whereby the stained cells were solubilised with 50% acetic acid and the absorbance read at OD595.

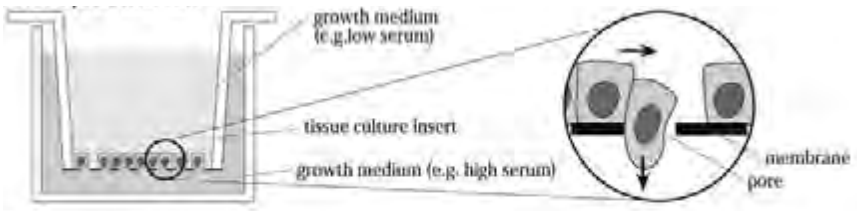

Figure 2.1: Transwell migration assay (Boyden chamber assay). Migration of a cell through a pore in the membrane is depicted (Kramer, *et al.,* 2013).

2.10.2 Transwell matrigel invasion assay

To analyse carcinoma invasion, HeLa cervical and WHCO5 oesophageal cancer cell lines respectively, were pre-treated with the GI254023X, SN-311 and SN-254, at the individual determined concentrations of EC_{50}, and 2X EC_{50} per drug. 24 hours after treatment, treated cells were trypsinised and counted so that $2.5x10^5$ cells were re-plated in triplicate within 0.5 mL of 1% FCS-containing media onto the membrane of the inserted matrigel-coated chamber (Corning Matrigel Invasion Assay kit, USA).

The matrigel serves as a basement membrane, which functions as an extracellular matrix. The matrigel chambers were initially incubated in a 37°C

incubator for 4 hours to allow for the matrigel coated membrane to solidify. Thereafter 1 mL of complete media containing 20% FCS was added to each 12 well. Then, $5x10^5$ of recently suspended treated cells were added into the matrigel chamber within a volume of 500 µL of 0.5% FCS media. Cells were incubated at 37°C, 5% CO_2 for 24 hours to allow for invasion of the cancer cells, moving through the matrigel membrane toward the underside of the matrigel chamber, following which, the matrigel member chambers were fixed and stained with crystal violet as mentioned 2.10.1. Random image fields of the matrigel depicting invaded cells were captured (10 images per condition) via the microscope camera, counted and analysed accordingly.

2.11 Statistical analysis

All experiments were performed in triplicate and repeated at least two independent times. Results are presented as the mean value ± standard error of mean (SEM) unless stated otherwise. The Student's *t*-test (paired and unpaired) was applied to calculate statistically significant differences between samples. A two-tailed distribution was used. Statistical significance was defined using a type I error or p-value of 0.05 where the p-value is the probability of rejecting the null hypothesis when it is assumed to be true. All calculations were performed in Microsoft Excel for MAC 2011 and GraphPad Prism MAC compatible (GraphPad Prism 6.05 Software, La Jolla, CA, USA).

Chapter 3:
Investigating the effects of GI254023X, SN-311 and SN-254, on cancer cell survival and proliferation.

3.1 Introduction

The ‘magic bullet’ concept, formulated first by Paul Ehrlich in the late 1800s, formed the basis of current direct chemical therapy (Imai and Takaoka, 2006). Ehrlich postulated the ability of a chemical to specifically target a given microorganism (Imai and Takaoka, 2006). Since the publication of his theory, targeted drug therapeutics have been combined with established cancer treatment regiment affecting specific molecular biomarkers (Imai and Takaoka, 2006; Charlton and Spicer, 2016). The development of ground-breaking cancer therapeutic approaches, includes a monoclonal antibody (mAbs) molecular targeting technique, able to induce a specific mechanism of action by targeting a tumour-selective cell-surface protein (Imai and Takaoka, 2006). These novel treatment techniques also include small-molecule inhibitors, peptide mimics and antisense nucleotides (Imai and Takaoka, 2006).

The discovery of new small molecule inhibitors targeting cancer has revolutionised prevailing treatment approaches (Hoelder, Clarke and Workman, 2012). The historical use of cytotoxic chemotherapy where a one-size fits all therapeutic approach on the systemic application to disrupt cancer cell mitosis, is

often associated with broad tissue and organ based toxicities (Charlton and Spicer, 2016; Hoelder, Clarke and Workman, 2012).

Research in molecular targeted cancer therapy is generating treatment regimens, which may have positive impacts in the lives of many cancer patients. Initial advancement into targeted therapy development was based on the treatment of haematologically derived malignancies (Charlton and Spicer, 2016). The first reported cancer-targeted monoclonal antibody therapeutic was rituximab. Rituximab, an antibody to the antigen CD20 on the B-cell, was used to treat B cell non-Hodgkin's lymphoma (Druker, *et al.,* 2001; Charlton and Spicer, 2016). Further molecular studies into another blood based malignancy, chronic myeloid leukaemia (CML), identified a BCR-ABL translocation between the chromosomes 9 and 22, signalling the overexpression of active tyrosine kinases (Druker, *et al.,* 2001; Charlton and Spicer, 2016). Imatinib, the first FDA approved small molecule inhibitor target therapy for cancer was developed to bind and block the mutated tyrosine kinase activity (Charlton and Spicer, 2016).

ADAM-10 is an established biomarker in neurodegenerative diseases (Hoettecke, *et al.,* 2010), and has been implicated in the involvement of cancer and pro-inflammatory activities (Hoettecke, *et al.,* 2010). Therefore, the targeting and direct inhibition of ADAM-10 is seen as a promising strategy to target cell proliferation, migration and invasion in cancer (Hoettecke, *et al.,* 2010; Ludwig, *et al.,* 2005).

ADAM-10 small molecule inhibitors have come under investigation, with several of them belonging to the peptidomimetic hydroxamic acid inhibitors for metalloproteinase (Hoettecke, *et al.,* 2010; Ludwig, *et al.,* 2005). Among these hydroxamate inhibitors, are batimastat and marimastat, which exhibit a lack of selectivity due to their ability to inhibit a broad spectrum of metalloproteinases; thereby dramatically affecting its potency (see Figure 3.1 A, B, C) (Hoettecke, *et al.,* 2010; Ludwig, *et al.,* 2005).

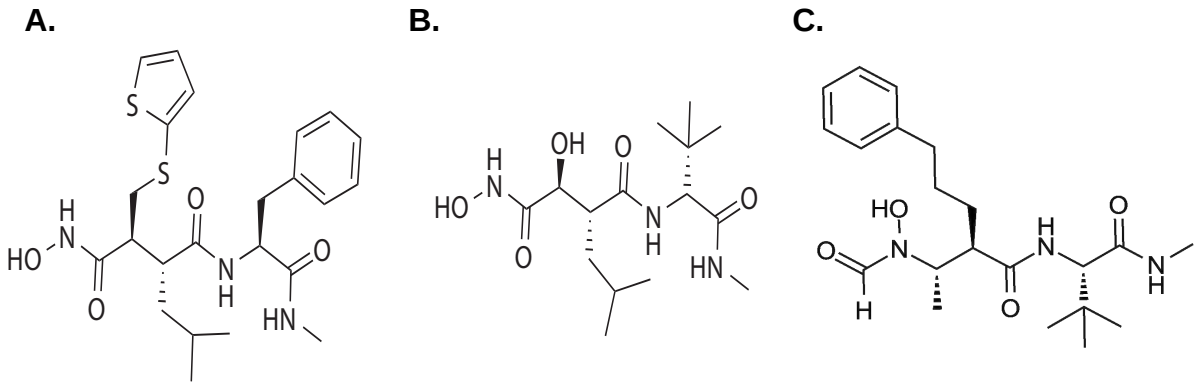

Figure 3.1: ADAM inhibitors. A- Batimastat; B- Marimastat; C- GI254023X (Hoettecke, *et al.,* 2010).

Glaxo Smith Kline described a newly synthesized targeted inhibitor of ADAM-10, namely GI254023X (see Figure 3.1C). The molecular modelling of GI254023X showed a P1' position alteration within the pseudopeptidic part of the molecule when compared to Batimastat and Marimastat (Figure 3.1A-B), therefore differing from a broad- spectrum of metalloproteinase inhibitors, due to a large hydrophobic substitution (Ludwig, *et al.,* 2005). The lipophilic substitution within this P1' position of GI254023X enhanced the compounds' specificity profile for ADAM-10 (Hundhausen, *et al.,* 2003; Ludwig, *et al.,* 2005).

Given the interest to determine the effects of specifically targeting ADAM-10, we were interested in determining the effects of GI254023X and other similar molecules on markers of tumorgenicity in cancer cells. Whilst synthesizing GI254023X, UCT Chemistry Department was able to generate two molecules en route to synthesizing GI254023X, named SN-254 and SN-311 respectively. A comparison of GI254023X and its two precursor derivatives is shown in: figure 3.2, and table 3.1.

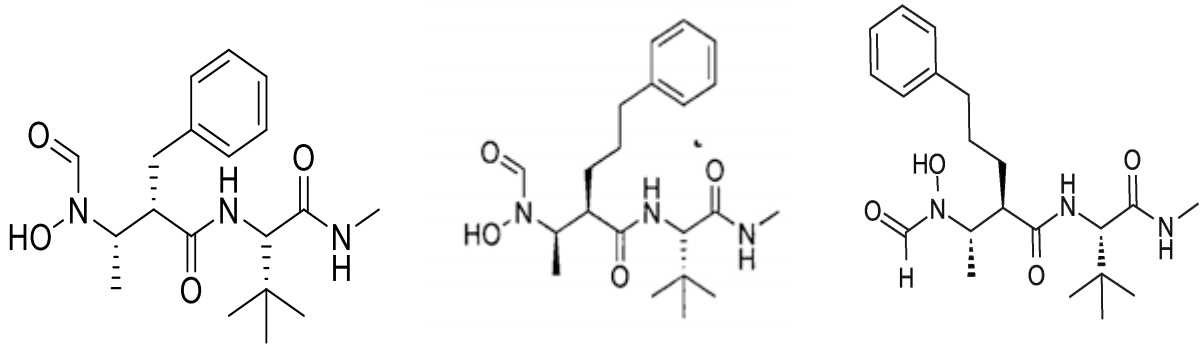

1. SN-254 2. SN-311 3. GI254023X

Figure 3.2: Structural comparison between GI254023X, SN-254 and SN-311. GI254023X molecular structure and the two newly synthesized molecules, SN-254 and SN-311, respectively.

Table 3.1: Structural difference between GI254023X, SN-254 and SN-311. (Nair, S, 2015 unpublished data).

ADAM-10 inhibitors:	**SN-254**	**SN-311**	**GI254023X**
i. At C3 side chain length:	1 carbon chain	3 carbon chain	3 carbon chain
ii. Phenyl ring position:	Positioned closer to main chain	Positioned further from main chain – similar to GI254023X	

In this study we investigated whether the two newly synthesized small molecules, SN-311 and SN-254, have effects on the biology of cancer cells in a similar manner as GI254023X. Experiments to determine whether SN-254 and SN-311 inhibited ADAM-10 associated activities and other markers of tumorigenicity of cancer, which GI254023X is known to inhibit, was performed.

3.2 Results

3.2.1 The effect of GI254023X, SN-311 and SN-254 on cancer cell growth and proliferation

The small molecule inhibitor of ADAM-10, GI254023X, and two newly synthesized small molecules, namely SN-254 and SN-311, were tested in biological assays to determine their effect in inhibiting cell growth and proliferation. EC_{50} values of all three small molecules was determined in a panel of cell lines, including cervical (HeLa), oesophageal (WHCO5) cancer and in non-cancer cell lines (WI38 and FG_0). The EC_{50} or effective concentration value was determined using GraphPad Prism. This program proximate's this EC_{50} curve by means of applying 4 parameter non-linear logistic equation, called the Hill equation (Gadagkar and Call, 2015). The HeLa cervical cancer cell line, and the WHCO5 oesophageal cancer cell line were chosen because previous studies had shown significant ADAM-10 expression in these cells (Williams, 2013). The 3-(4,5-Dimethylthiazol-2-yl)-2,5-diphenyltetrazolium bromide (MTT) assay was used in EC_{50} determination. This colourimetric assay is able to assess cell number based on the colour change of yellow tetrazolium salts (the MTT reagent) to form a reduced dark purple formazan crystal. This assay measures cell metabolic activity, whereby a yellow to purple colour change is catalyzed by mitochondrial dehydrogenase in living cells, thus providing an indication of living cell numbers (Berridge and Tan, 1993).

EC_{50} data were obtained for GI254023X (Tocris Biosciences), and compared to the UCT generated SN-254, and SN-311. Hill plots used to determine the EC_{50} values for GI254023X, SN-254 and SN-311 are shown in figure 3.3. The EC_{50} values are summarized in Tables 3.2, 3.3, 3.4 and shows EC_{50} values within similar range for all three compounds in HeLa and WHCO5 cells. Interestingly all three small molecules produced EC_{50} values 3 – 4 fold times higher in the non-cancer WI38 and FG_0 cells compared to the cancer cells (Tables 3.2; 3.3 and 3.4). These results show that SN-254 and SN-311 have EC_{50} in a similar range to that of the commercially available GI254023X, and that HeLa and WHCO5 cancer cells are therefore sensitive to treatment with these molecules.

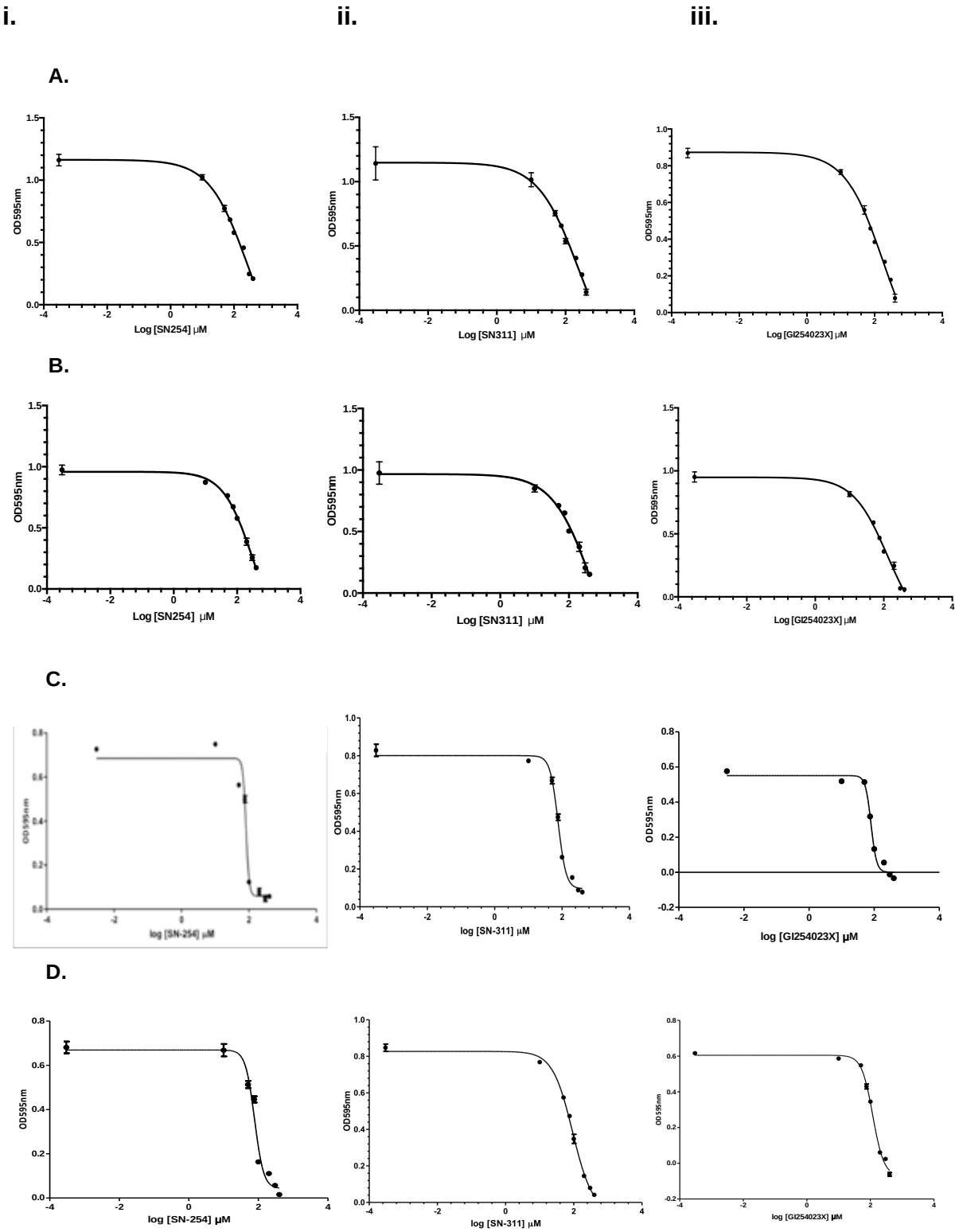

Figure 3.3: Hill plots for EC_{50} determination in (A) FG_0 and (B) WI38 normal cell lines; (C) HeLa; and (D) WHCO5 with varying concentrations of (i.) SN-254, (ii.) SN-311 and (iii.) GI254023X drugs respectively. All experiments were performed in triplicate and repeated three independent times. Results are the mean ± SEM.

Table 3.2: Small molecule SN-254 EC_{50} value in a panel of cell lines.

SN-254 compound:

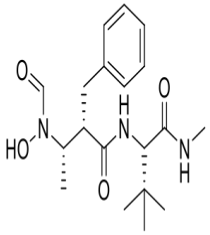

IC_{50} values for SN-254 against cancer and normal cell lines

Cell line:	IC_{50} (μM):	95% Confidence Interval
FG_0	306	162 - 1833
WI38	304	147 - 1970
HeLa	61	59 - 95
WHCO5	77	58 - 101

Table 3.3: Small molecule SN-311 EC_{50} value in a panel of cell lines.

SN-311 compound:

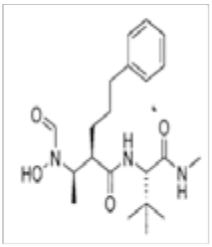

IC_{50} values for SN-311 against cancer and normal cell lines

Cell line:	IC_{50} (μM):	95% Confidence Interval
FG_0	239	226 - 2243
WI38	501	358 - 7018
HeLa	76	66 - 86
WHCO5	92	68 - 124

Table 3.4: Small molecule GI254023X EC_{50} value in a panel of cell lines.

GI254023X compound:

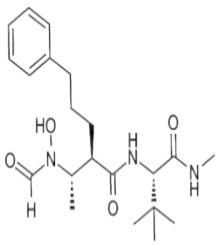

IC_{50} values for GI254023X against cancer and normal cell lines

Cell line:	IC_{50} (μM):	95% Confidence Interval
FG_0	172	135 - 893
WI38	128	123 - 511
HeLa	80	69 - 92
WHCO5	111	94 - 132

3.2.2 The effect of small molecules GI254023X, SN-311 and SN-254 on ADAM-10 activity – Human CX_3CL1 fractalkine immunoassay

The human fractalkine chemokine CX_3CL1 exists both as a membrane bound protein, aiding in enhancing cell-cell adhesion as well as a soluble form, inducing chemotaxis (Hundhausen, *et al.,* 2003). ADAM-10 has been described as a candidate protease for CX_3CL1 cleavage. Previous studies showed that GI254023X significantly inhibited CX_3CL1 cleavage by preferentially blocking ADAM-10 (Hundhausen, *et al.,* 2003). To assess whether treating cancer cells with SN-254 and SN-311, newly synthesized precursor derivatives of GI254023X would be able to target the ADAM-10, and therefore affect its function, a functional assay based on detecting levels of cleaved, solubilized CX_3CL1 was performed. This immunoassay allowed us to assess whether the newly synthesized derivatives inactivated ADAM-10.

HeLa and WHCO5 were treated with GI254023X (as a positive control), SN-254 and SN-311 respectively. Our results show a significant reduction in CX_3CL1 cleavage in both HeLa and WHCO5 cell lines treated with GI254023X (Figure 3.4A and B). Our results also showed a decrease in cleaved CX_3CL1 with SN-254, SN-311 treatment in HeLa and WHCO5 respectively, (Figure 3.4A and B). These results suggest that the SN-254 and SN-311 have inhibitory effects in ADAM-10 activity similar to that of GI2540234X.

A. HeLa

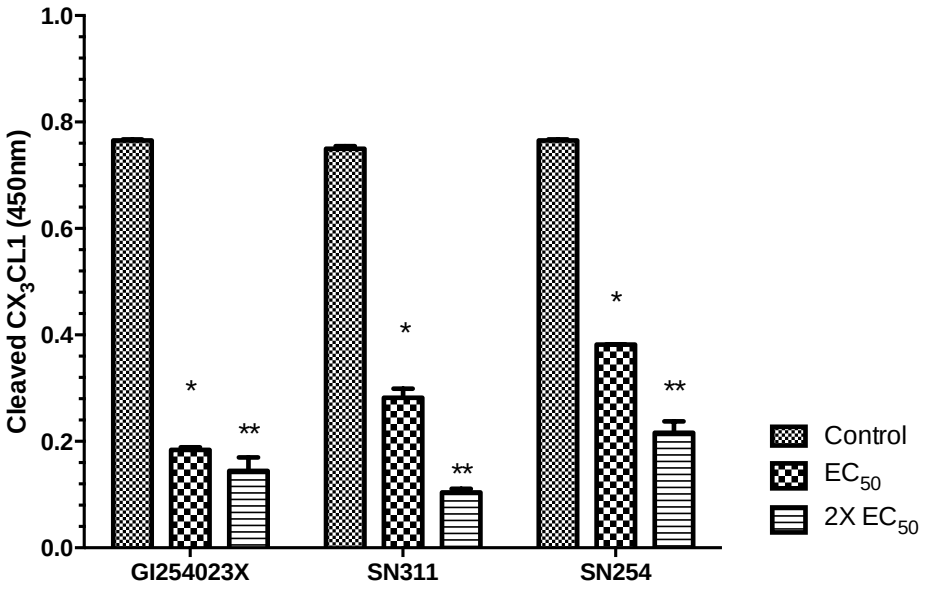

B. WHCO5

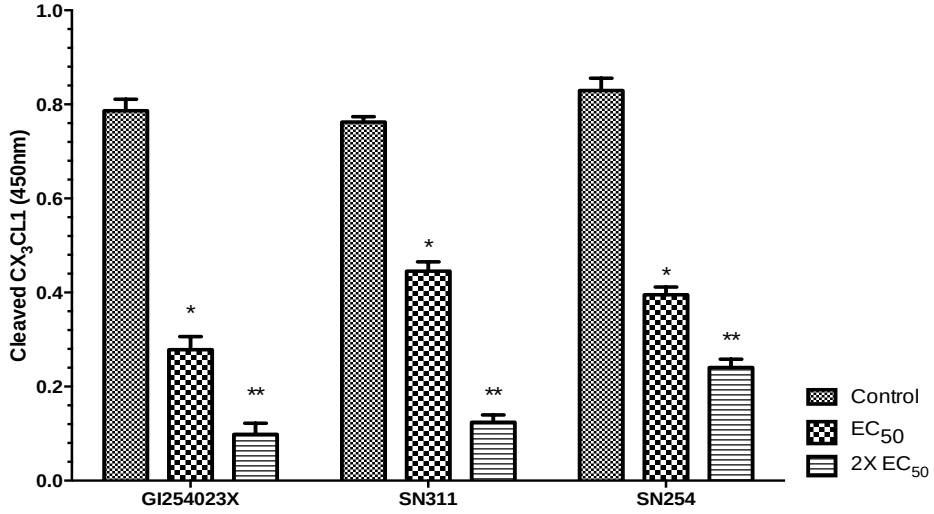

Figure 3.4: Effect of test compounds on ADAM-10 activity: Human CX_3CL1 Fractalkine immunoassay. HeLa cervical cancer cell line (A) and WHCO5 oesophageal cancer cell line (B) were treated with the calculated EC_{50}; 2 X EC_{50}; and a vector control (DMSO equivalent to EC_{50} concentration of the compound under investigation applied) of SN-254; SN-311 and GI254023X respectively. Cell lysate and media of each treatment condition was collected and plated into a pre-coated CX_3CL1 ELISA plate. Results are the mean ± SEM of experiments performed in triplicate. The set of results show a decrease in cleaved CX_3CL1 post SN-254, SN-311 and GI254023X treatment in HeLa and WHCO5 respectively. *$p<0.05$; **$p<0.001$.

3.2.3 Characterisation of the effect of GI254023X, SN-311 and SN-254 on the growth and proliferation of cancer cells

3.2.3.1 Anchorage dependent proliferation

Having established that GI254023X, SN-254 and SN-311, behave in a comparable manner in terms of IC_{50} and ADAM-10 inhibitory activity, further assays were performed to characterize its effect on cancer cell proliferation.

HeLa and WHCO5 cells were treated with the EC_{50} and, 2X EC_{50} concentration of each of the small molecules, as well as the equivalent amount of DMSO to that of the 2X EC_{50} concentration, as a control. Cellular proliferation was monitored over a five-day period by the MTT assay. Results showed that GI254023X and SN-311 in HeLa caused a significant inhibition in proliferation from as early as 48 hours after both EC_{50} and 2X EC_{50} treatment (Figure 3.5A and B). A less pronounced effect was observed with SN-254 (Figure 3.5C).

Similar results were obtained with WHCO5 cells showing significant inhibitory effect with all three small molecules (Figure 3.6A-C). From this data, it can be deduced that GI254023X, SN-311 and SN-254, produced a significant inhibitory effect on the proliferation of both HeLa and WHCO5 cell lines respectively.

A. GI254023X

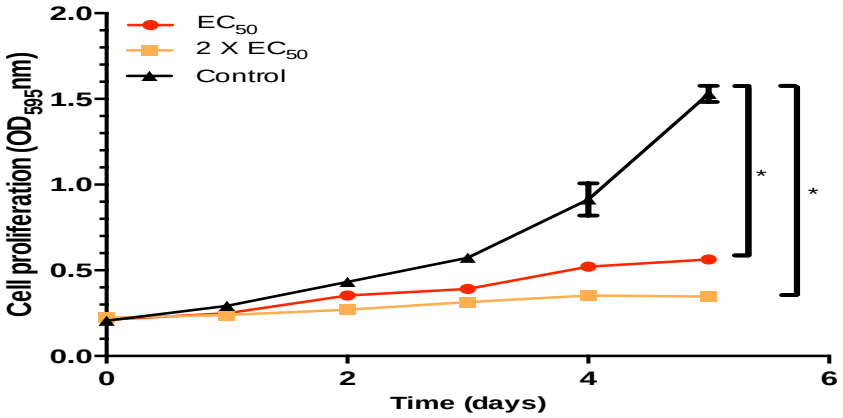

B. SN-311

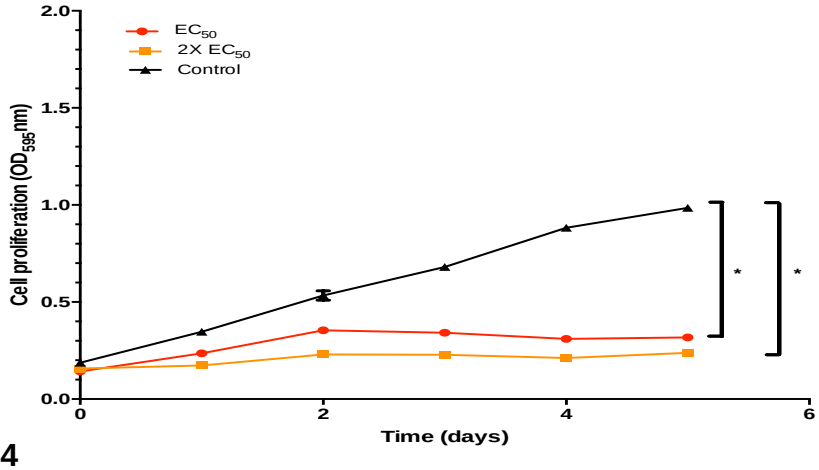

C. SN-254

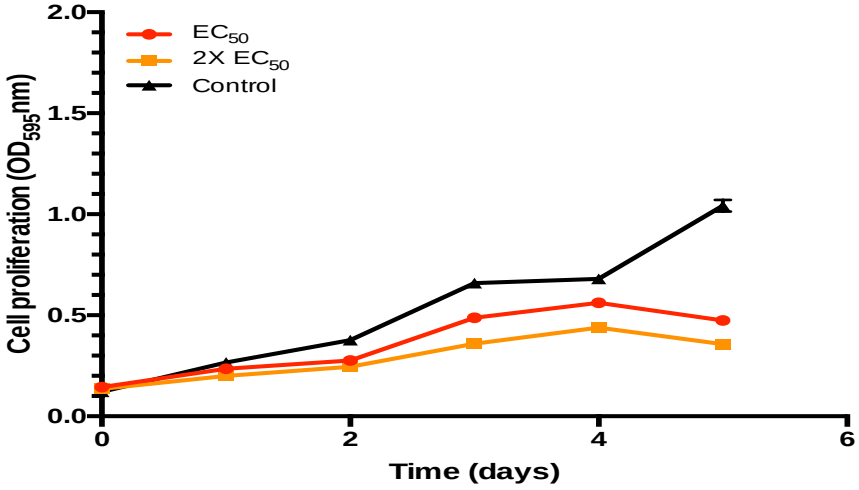

Figure 3.5: Proliferation assay, treating HeLa cervical cancer cell line with the EC_{50}; 2 X EC_{50}; Control (DMSO equivalent to 2X EC_{50} concentration of compound) of (A) GI254023X; (B) SN-311 and (C) SN-254 respectively. Cellular proliferation was monitored over a 5-day period. Results are the mean ± SEM of experiments performed in quadruplicate (*p<0.05). The results show that GI254023X and SN-311 had a significant inhibitory effect.

A. GI254023X

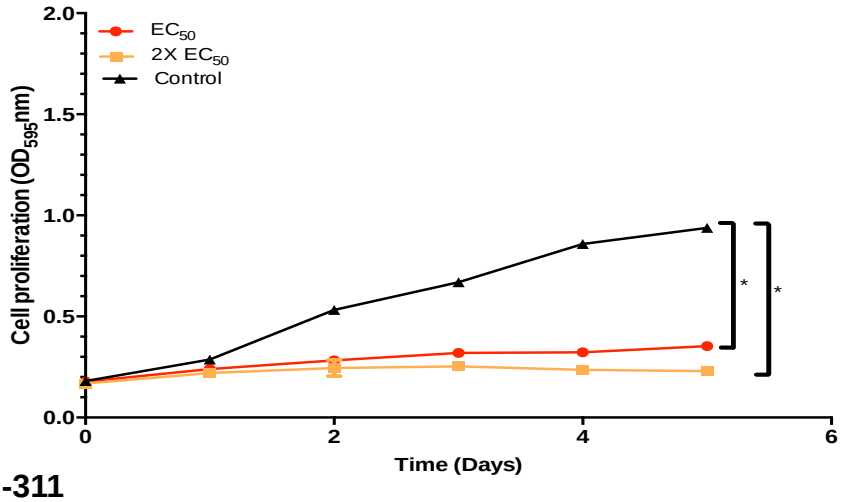

B. SN-311

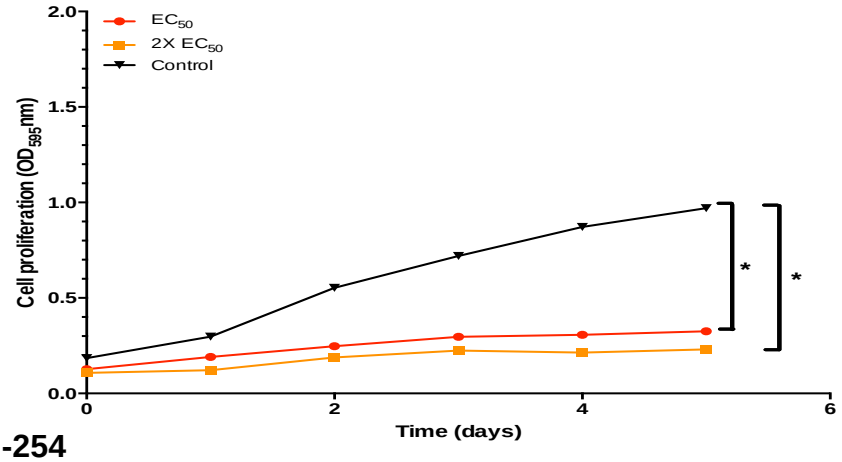

C. SN-254

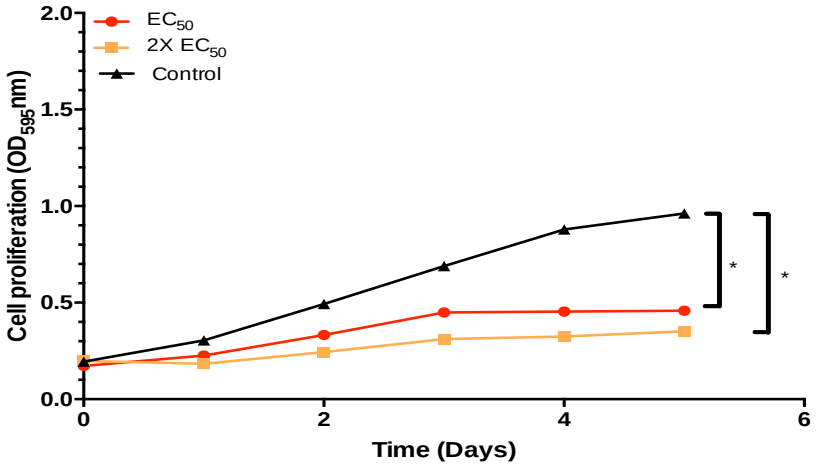

Figure 3.6: Proliferation assay, treating WHCO5 oesophageal cancer cell line with the IC_{50}; 2 X IC_{50}; Control (DMSO equivalent to 2X IC_{50} concentration of compound) of (A.) GI254023X; (B.) SN-311 and (C.) SN-254 respectively. Cellular proliferation was monitored over a 5-day period (*p<0.05). Results are the mean ± SEM of experiments performed in quadruplicate. The results show that GI254023X, SN-311 and SN254 had a significant inhibitory effect on the proliferation of WHCO5 oesophageal cancer cells.

3.2.3.2 The effect of GI24023X, SN254 and SN-311 on the clonogenic potential in cancer cells

Clonogenic colony formation assay is described as an *in vitro* cell survival assay, This assay monitors the ability of a single cell to grow into a colony of at least 50 cells (Franken, *et al.,* 2006). The clonogenic assay is a widely used assay of tumorigenicity, and in this context, this assay was used to test the effect of certain agents on clonogenicity, a widely used marker of tumorigenicity

Both HeLa and WHCO5 cancer cell lines were plated at 100 cells per 6-well plate, and treated 24 hours later with EC_{50} value, 2X EC_{50} value of each of the small molecules. The treated cells were left to grow for a period of 9 days. Thereafter, cells were stained with 0.5% crystal violet staining solution, and cell colonies formed were quantified under the stereomicroscope. Photographs were taken of each well, and colonies were quantified using the ColonyArea ImageJ Plugin, as described by Guzman and colleagues (2014). Plating efficiency and survival fraction was calculated (see methods).

The result obtained showed a decrease in HeLa colonies with a concentration-dependent increase in GI254023X (Figure 3.7A). The survival fraction percentage (%)for HeLa treated with GI254023X over 9 days is shown graphically, and shows a decrease in cell survival with increasing drug concentration (Figure 3.7).

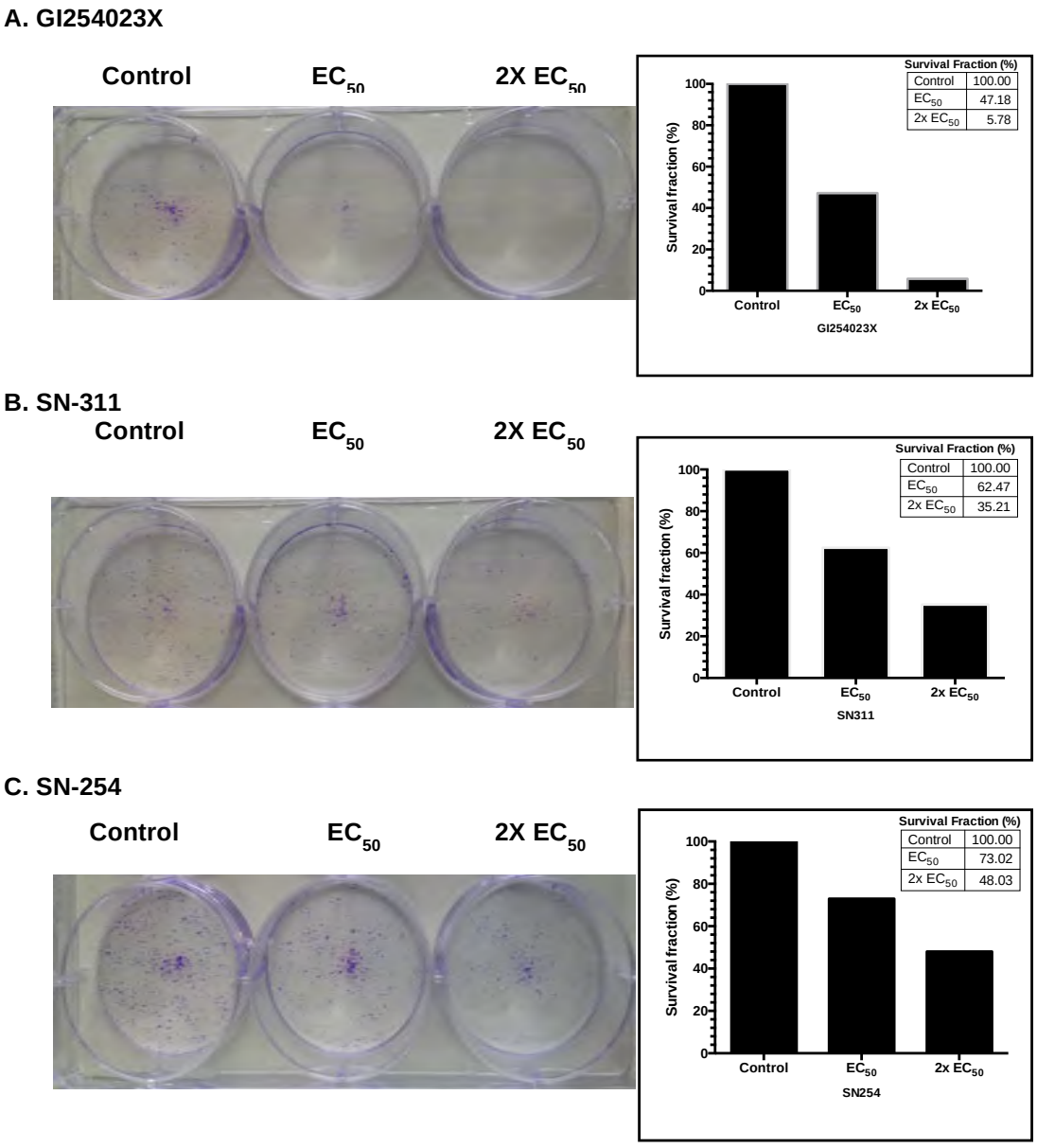

Figure 3.7: Clonogenic colony formation assay in HeLa, treating HeLa cervical cancer cell line with the EC_{50}; 2 X EC_{50}; and DMSO equivalent to 2X EC_{50} concentration of compound under investigation applied of (A) GI254023X; (B) SN-311 and (C) SN-254 respectively. Colony formation assay was monitored over a 9-day period. Results are the mean ± SEM of experiments performed in quadruplicate. The results show that GI254023X, SN-311 and SN254 had a significant inhibitory effect on the survival fraction and cellular survival of HeLa cells. Tabulated figures represents Survival Fraction % (SF%). SF% = (Plating efficiency of treated sample/ Plating efficiency of control) X 100.

A. GI254023X

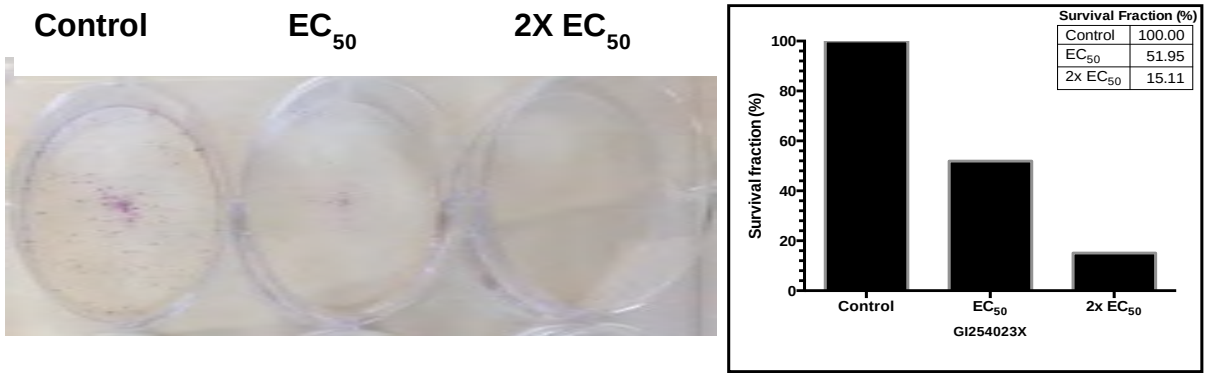

B. SN-311

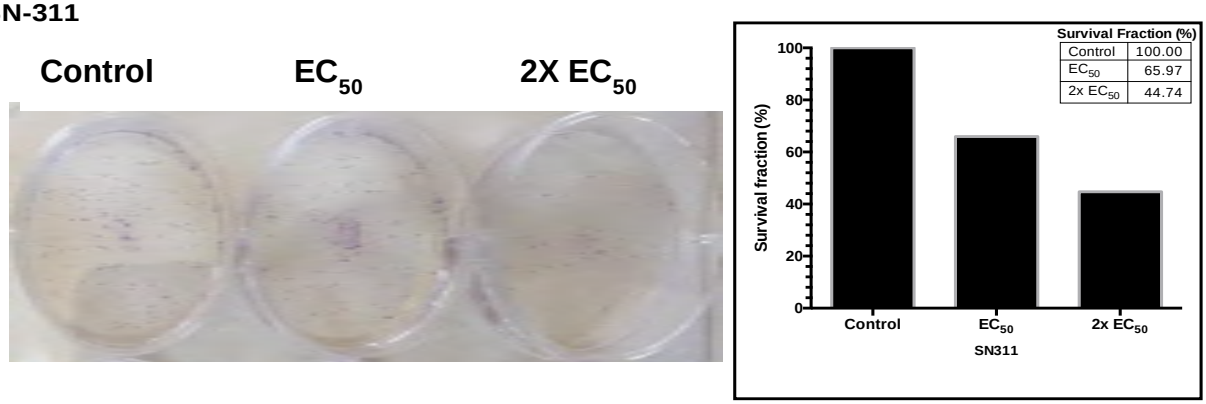

C. SN-254

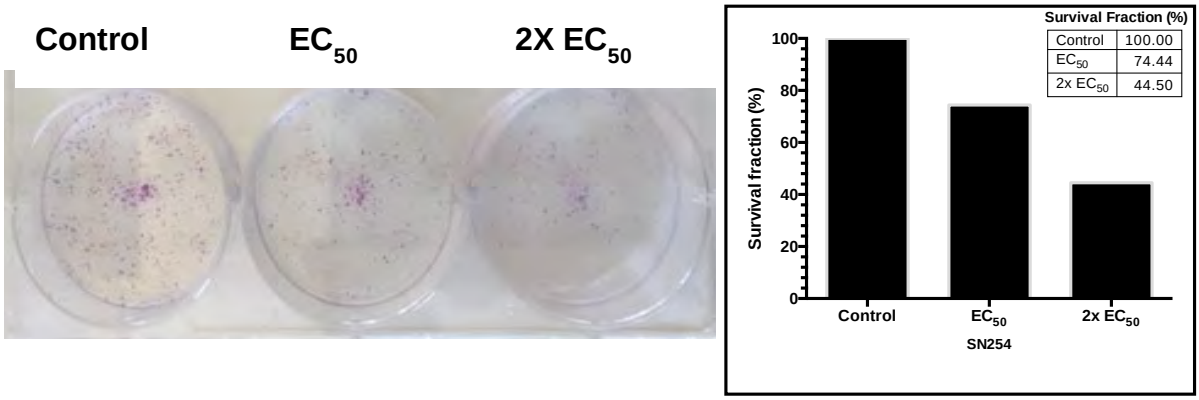

Figure 3.8: Clonogenic colony formation assay in WHCO5, treating WHCO5 oesophageal cancer cell line with the EC_{50}; 2 X EC_{50}; and DMSO equivalent to 2X EC_{50} concentration of compound under investigation applied of (A) GI254023X; (B) SN-311 and (C) SN-254 respectively. Colony formation assay was monitored over a 9-day period. Results are the mean ± SEM of experiments performed in quadruplicate. The results show that GI254023X, SN-311 and SN254 had a significant inhibitory effect on the survival fraction and cellular survival of WHCO5 cells. Tabulated figures represents Survival Fraction % (SF%). SF% = (Plating efficiency of treated sample/ Plating efficiency of control) X 100.

The survival fraction percentage (%) calculated for HeLa treated with GI254023X over 9 days, showed, a decrease in colonies formed with an increase in treatment concentrations, reaching a value of 5.78% with 2X EC_{50} treatment concentration (Figure 3.7A). In SN-311 treated HeLa wells, a 32.5% and 62.4% decrease for EC_{50} and 2X EC_{50} respectively was noted in colonies when compared to the control wells, (Figure 3.7B). SN-254 treatment too showed a decrease in colonies compared to untreated cells (Figure 3.7C). While SN-254 inhibited colony formation, it was not as effective an inhibitor as GI254023X and SN-311. SN-254 had reduced to 73.02% in EC_{50} concentration treatment, and 48.02% in 2X EC_{50} concentration treatment (Figure 3.7C). These results are in line with what was observed in the proliferation assays.

Similar results were obtained for WHCO5 cells, which showed that GI254023X and SN-311 inhibited WHCO5 colony formation to a greater extent than that of SN-254 (Figure 3.8A-C).

3.2.4 Cell death associated with GI254023X, SN-311 and SN-254 targeting ADAM-10 activity

3.2.4.1 Effect of GI254023X, SN-311 and SN-254 on mode of cell death

Having shown that GI254023X, SN-311 and SN-254 compounds resulted in the inhibition of HeLa and WHCO5 cell proliferation and growth, we next set out to investigate whether this inhibition associates with cell death via apoptosis. Apoptosis, described as a type 1 method of programmed cell death, regulates cellular self-destruction in response to a variety of stimuli (Portt, *et al.,* 2011; Man and Kanneganti, 2016). Known too as a non- inflammatory form of programmed cell death, apoptosis is mediated by a family of proteases, called Cysteinyl aspartate-specific proteinases, or Caspases (Elmore, 2007; Man and Kanneganti, 2016). Thus, once Caspases are proteolytically activated, they generally activate a cascade of events that result in cell death through targeted cleavage of specific substrates (Elmore, 2007). Morphologically, cells undergoing apoptosis appear to undergo cell shrinkage or pynknosis, membrane blebbing as well as DNA fragmentation (Elmore, 2007; Man and Kanneganti, 2016).

In this study, a commercially available Caspase 3/ 7 activity assay kit (Promega), was used to assess the levels of caspase – 3 and 7 enzyme activity, using a luminogenic tetrapeptide substrate. The level of luminescence detected is directly proportional to that of substrate cleavage by the Caspase- 3 and 7 enzymes, thus reflecting a level of apoptotic activity.

Caspase 3/7 activity assay results obtained in HeLa showed a significant increase in response to GI254023X and SN-311 treatment at both IC_{50} and 2X IC_{50} (Figure 3.9A and 3.9B). A significant increase in levels of caspase 3/7 activities was only observed at the 2X IC_{50} treatment with SN-254 treatment in HeLa(Figure 3.9C).

Significant increase in caspase 3/7 activity was detected across all three compound treatments, GI254023X, SN-311 and SN-254 in WHCO5 oesophageal cancer cell line for both IC_{50} and 2X IC_{50} treatment conditions respectively (Figure 3.10A – C).

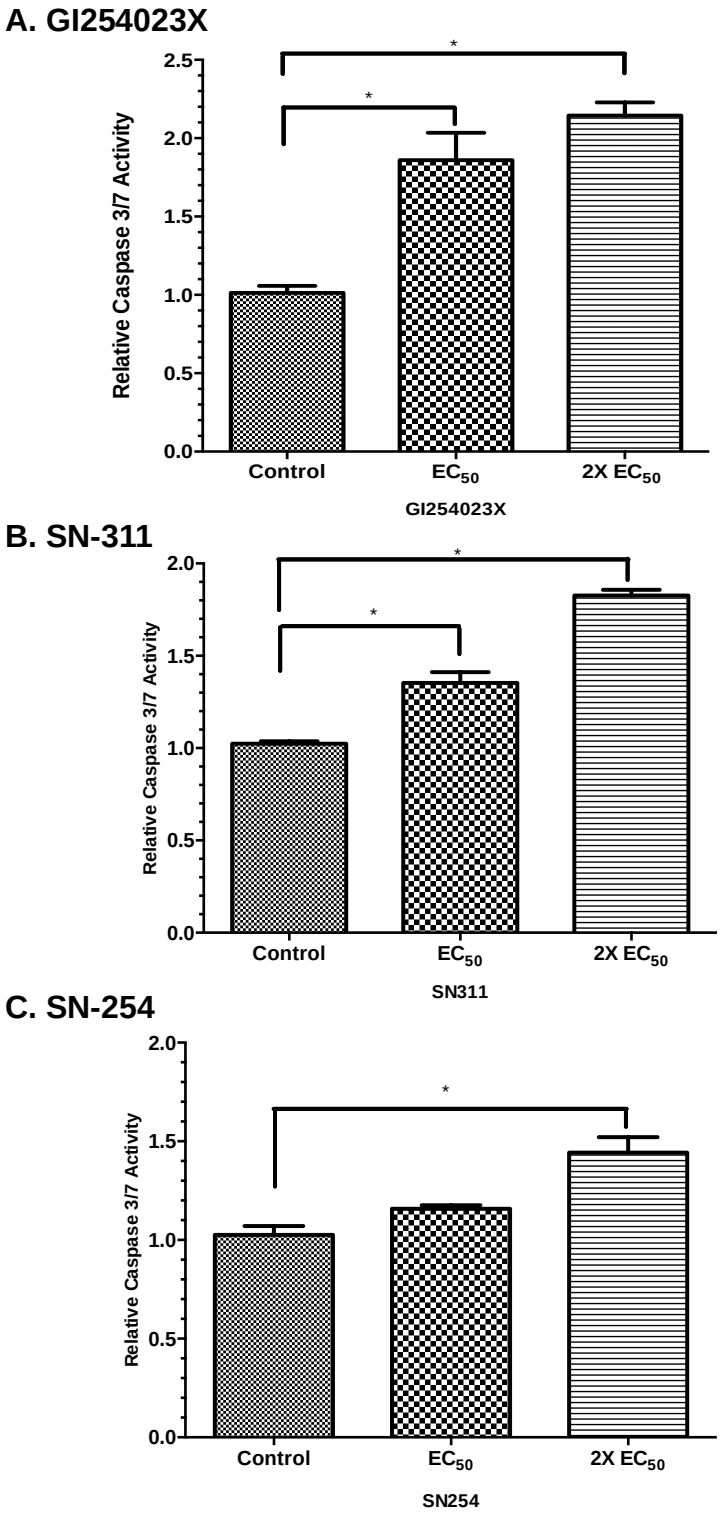

Figure 3.9: The effect of GI254023X, SN-311 and SN-254 on induction of apoptosis in HeLa cells. HeLa cells were treated with 1X EC_{50}; 2 X EC_{50}; and DMSO only equivalent to 2XEC_{50} concentration of **(A)** GI254023X; **(B)** SN-311 and **(C)** SN-254 respectively. The data above shows an increase in caspase 3/ 7 activation with an increase in selected drug treatments. (*p.<0.05).

A. GI254023X

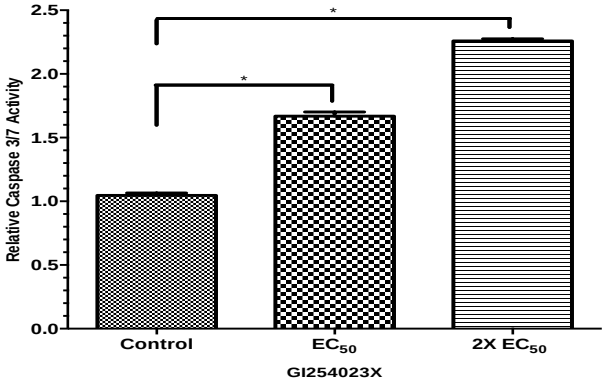

B. SN-311

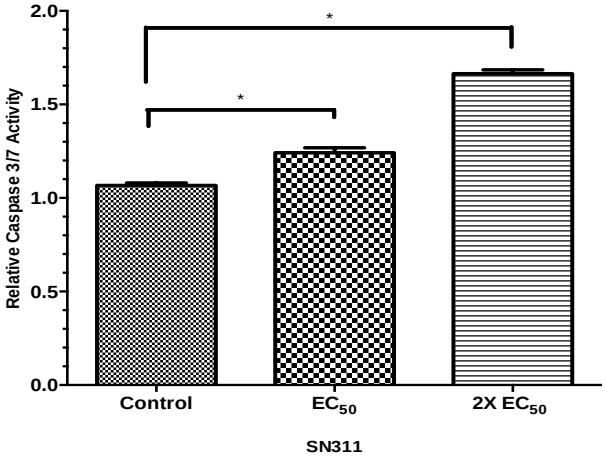

C. SN-254

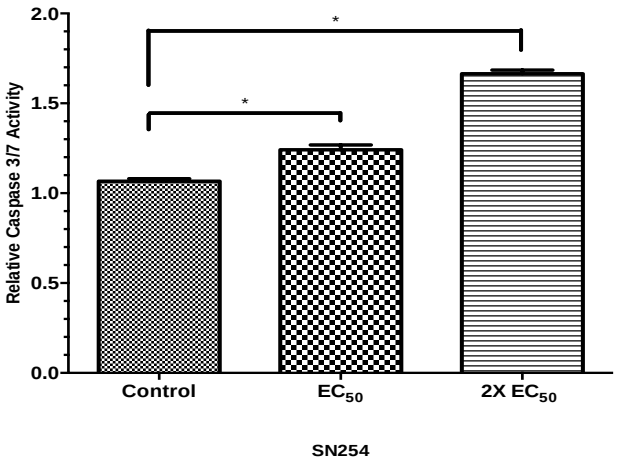

Figure 3.10: The effect of GI254023X, SN-311 and SN-254 on induction of apoptosis in WHCO5 cells. WHCO5 cells were treated with 1X EC_{50}; 2 X EC_{50}; and DMSO only equivalent to 2XEC_{50} concentration of **(A)** GI254023X; **(B)** SN-311 and **(C)** SN-254 respectively. The data above shows an increase in caspase 3/ 7 activation with an increase in selected drug treatments. (*p.<0.05).

3.2.4.2 The effect of GI254023X, SN-311 and SN-254 on Poly(ADP-Ribose) Polymerase-1 activation

We next determined the extent of PARP cleavage as an alternate measure of apoptosis. PARP is a known substrate of activated caspase (Bock and Chang, 2016; Kotsopoulos, 2016). Referred to also as ADP-ribosyltransferases (ART), humans express 17 such enzymes, which aid in altering targeted proteins by the unique modification of ADP-ribose attachment (Bock and Chang, 2016; Hottiger, *et al.,* 2010; Kotsopoulos, 2016). PARP is involved in a range of cellular functions which include transcription regulation, cell division and mRNA stability (Bock and Chang, 2016).

Better-understood and studied roles of PARP involve regulating cellular responses to stresses, which are induced by DNA damage response (DDR), unfolded protein response (UPR), and cytoplasmic stress response (Bock and Chang, 2016). Damage of DNA activates PARP-1and PARP-2 enzymes, which both assist in base excision repair (BER) pathway activities. These enzymes create an ADP-ribose homopolymer, ‘flagging’ the damaged area (Kotsopoulos, 2016; Robert *et al.,* 2013). This action driven by PARP induces histone release, loosening chromatin at the affected site, allowing for recruitment of additional mechanisms to repair and restore the DNA (Kotsopoulos, 2016; Robert *et al.,* 2013).

A PARP cleavage assay was performed by Western blot analysis. In response to activated caspase activity, PARP is cleaved from a 116kDa form to a 89kDa protein size (Kauffman, *et al.,* 1993). PARP cleavage was analysed in HeLa and WHCO5 cell lines 48 hours after treatment with 1X IC_{50} and 2X IC_{50} concentration values of GI254023X, SN-311 and SN-254, respectively. After the 48-hour treatment interval, both floating cells and attached cells were collected and lysed with RIPA buffer (see Appendix I Solutions). The harvested cell lysates of HeLa and WHCO5 were subjected to Western Blot analysis with an α-PARP antibody.

Both HeLa and WHCO5 cells showed PARP cleavage with EC_{50} and 2X EC_{50} concentrations of GI254023X, SN-311 and SN-254 respectively (Figures 3.11 A and B). These results further confirm, that GI254023X, SN-311 and SN-254 treatment of HeLa and WHCO5 cells results in cell death via apoptosis.

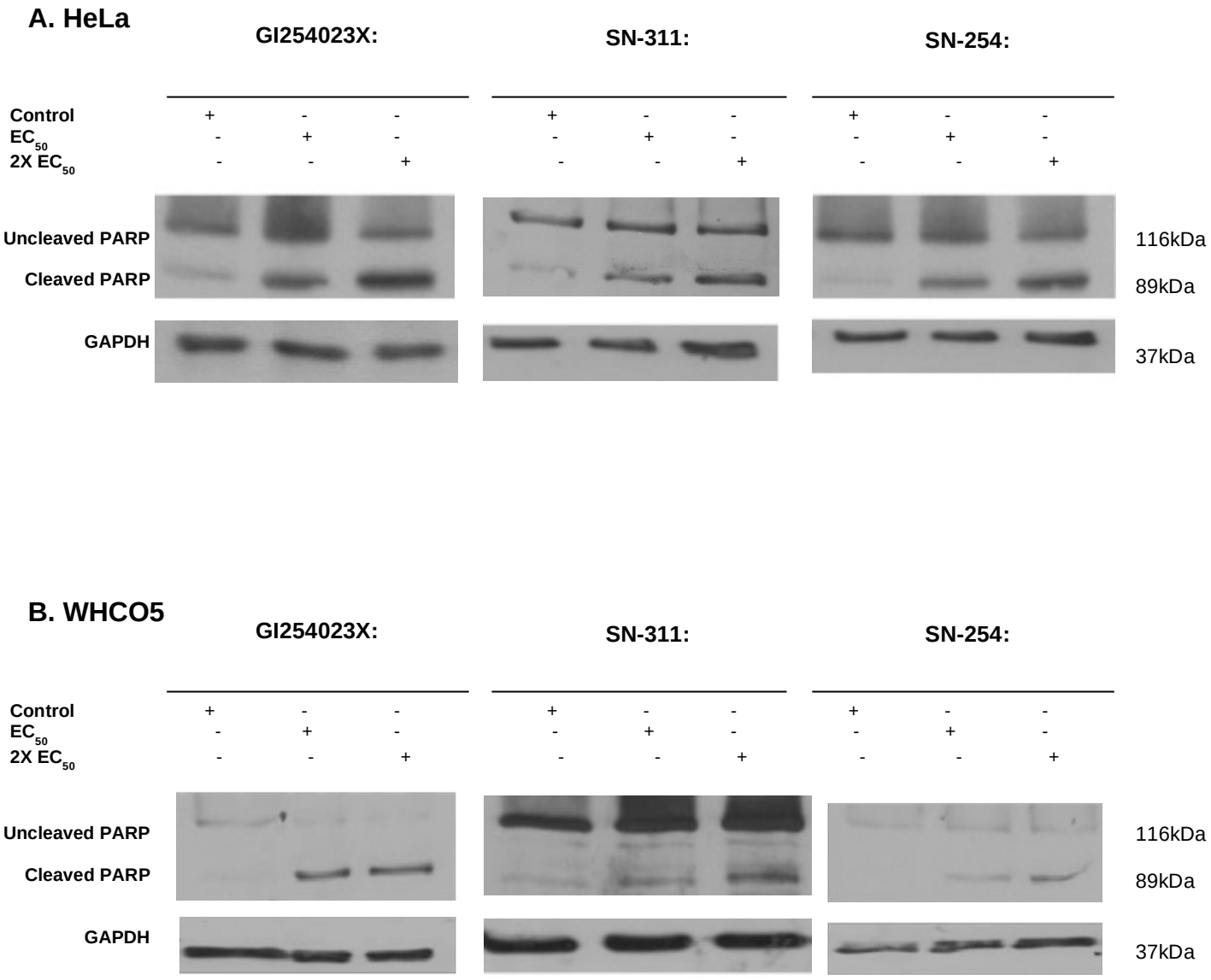

Figure 3.11: Poly (ADP-Ribose) Polymerase (PARP) cleavage detection in (A.) HeLa, and (B.) WHCO5. Uncleaved (precursor/ full length) PARP-1 (116kDa) and cleaved PARP-1 (89kDa) was detected in HeLa and WHCO5 cell lines post treatment with the indicated concentration of 1X EC_{50} and 2 X EC_{50} varying concentrations of **(i)** GI254023X, **(ii)** SN-311 and **(iii)** SN-254. DMSO only treatment served as the control variable for each small molecule treatment. The data shows that, when compared to the control band– both concentrations of each small molecule inhibitor induced significant PARP cleavage. GAPDH was used as a control for protein loading.

3.3 Discussion

In this study we investigated the potential of ADAM-10 as a therapeutic target in oesophageal cancer and cervical cancer, using a known small molecule inhibitor of ADAM-10, GI254023X, as well as the novel small molecules SN-254 and SN-311. This study was carried out given the evidence in the literature that tumour tissue express higher levels of ADAM-10, as well as previous data generated in our laboratory confirming this elevated ADAM-10 expression in cancer cells (Arribas *et al.,* 2006; Camodeca, *et al.,* 2016; Saftig and Reiss, 2011; Zhang, *et al.,* 2014; Zhao, *et al.,* 2014; Ward, 2011; Williams, 2013).

Previous reports (Hundhausen, *et al.,* 2003; Ludwig, *et al.,* 2005; Moss, *et al.,* 2007; Hoettecke, *et al.,* 2010) had cited GI254023X IC_{50} value at a range between 5 and 10 μM. Using this concentration of GI254023X in our laboratory had proven ineffective to induce cell death (Williams, 2013 unpublished data). Recently, a research group investigating ADAM-10 involvement in cell junction assembly during early porcine embryo development had established an IC_{50} concentration of GI254023X to be 100 μM (Kwon, *et al.,* 2016). Camodeca and colleagues (2016) using Hodgkin's lymphoma cells established an IC_{50} of GI254023X to be 27 μM. Comparisons of EC_{50} values in our laboratory of the three compounds had shown the EC_{50} value obtained in GI254023X in HeLa is 80 μM, and WHCO5 is 111 μM. The newly synthesized precursor compounds SN-254, and SN-311 generated EC_{50} values within a similar range to that for

GI254023X, as the 95% Confidence Interval range of all three compounds overlapped.

Having determined the concentration where the novel compounds block cell growth, we next set out to assess whether SN-311 and SN-254 would be able to target and subsequently inhibit a known ADAM-10 function. As such, the human fractalkine CX_3CL1 immunoassay was performed. ADAM-10 is described throughout literature as a candidate for constitutive cleavage of CX_3CL1, thus solubilizing this transmembrane protein via shedding activity (Hundhausen, *et al.,* 2003). Prior research has also shown that GI254023X is able to reduce significantly the cleavage of human fractalkine by preferentially blocking ADAM-10 activity (Hundhausen, *et al.,* 2003). To assess whether treating cancer cells with SN-254 and SN-311, is able to target ADAM-10 activity, a functional assay based on detecting levels of cleaved, solubilized CX3CL1 was performed. In accordance with literature, the levels of CX_3CL1 cleaved to its shed soluble form in both HeLa and WHCO5 cell lines treated with GI254023X decreased significantly. Furthermore, we were able to show that both SN-311 and SN-254 were able to induce a decrease in cleaved soluble CX_3CL1 levels, suggesting that the newly derived precursor small molecule compounds are able to target ADAM-10 (like GI254023X) by inactivating its shedding function. The ability of SN-311 and SN-254 to target and inhibit an ADAM-10 functional activity, similar to GI254023X, could stem from the structural similarity that these three compounds share.

After establishing that SN-311 and SN-254 were able to induce a comparable inhibitory effect on cancer cell growth, and, moreover, that the two new compounds were able to target and inhibit an ADAM-10 functional activity like that of GI254023X, by inactivating its' shedding function, further assays were performed to characterize its effect on cancer cell proliferation. Results obtained post treatment with GI254023X, SN-311 and SN-254 in both HeLa and WHCO5 cells had showed a significant inhibition in proliferation. The result obtained in GI254023X treatments was in accordance with literature, citing it as a small molecule able to decrease proliferation in a range of cancers, including breast, hepatocellular carcinoma and tongue squamous cell carcinoma (Duffy, *et al.,* 2011; Fu, *et al.,* 2014; Zhang, *et al.*, 2013; Shao, *et al.,* 2015).

Literature cites the ability of different ADAMs family members able to perform compensatory roles for each other, which, may explain why 100% cell death was not achieved. ADAM-10 is described as structurally and functionally related to ADAM-17, and both are shown to be leading proteases in trans-membrane protein ectodomains (Mullooly, *et al.,* 2016; Bzowska*, et al.,* 2009). Research has further linked ADAM-10 and ADAM-17 as able to compensate functionally in the absence of the other (Bzowska*, et al.,* 2009). ADAM-10 and ADAM-17 are known to activate epidermal-like growth factor receptor (EGFR), which contributes to cancer proliferation (Mullooly, *et al.,* 2016, Sahin, *et al.,* 2004). It is, therefore possible that in the presence of an inhibited ADAM-10 in HeLa and WHCO5 cells induced by a small molecule, GI254023X, which is known to possess a 100 fold

biological affinity to ADAM-10 over ADAM-17, ADAM-17 would functionally compensate for the inhibited ADAM-10 activity (Mullooly, *et al.,* 2016).

Having shown that treatment with GI254023X, SN-311 and SN-254 compounds resulted in the suppression of HeLa and WHCO5 cell proliferation and growth, we investigated whether this inhibition was due to cell death induced by apoptosis. A quantitative caspase 3/7 assay and PARP cleavage assay was performed. Our results obtained in HeLa and WHCO5 cancer cell lines had shown significant increases in caspase 3/7 activity levels and PARP cleavage in treatments with GI254023X and SN-311.

Furthermore, the results obtained of cell death induced by GI254023X, SN-311 and SN-254 treatment in HeLa and WHCO5 cells, suggest that apoptosis was a mechanism involved. Our findings for GI254023X correspond with literature, where GI254023X was shown to not only block cell proliferation, but also induced apoptosis within acute T-lymphoblastic leukaemia Jurkat cells (Mullooly, *et al.,* 2016; Ma, *et al.,* 2015).

In summary, the current study has established that the two newly derived precursor derivatives of GI254023X, namely SN-311 and SN-254 has a similar IC_{50} concentration range in the two cancer cell lines studied here, and that SN-311 and SN-254 is able to inhibit ADAM-10 cellular functions (shedding of CX_3CL1). Furthermore, the derivatives are able to inhibit cellular proliferation,

although producing a weaker effect to that of GI254023X. This study has also shown that SN-311 and SN-254, are able to induce cell death by activating caspase 3/7 activity and increasing cleavage of PARP.

Chapter 4:
Investigating the effects of GI254023X, SN-311 and SN-254 on cancer biology and progression

4.1 Introduction

In the previous chapter, we reported that GI254023X and precursors SN-311 and SN-254, were able to reduce cell proliferation of HeLa cervical and WHCO5 oesophageal cancer cell lines, as well as induce cell death via apoptosis. In this chapter we assess whether GI254023X, SN-311 and SN-254 affect other cancer hallmarks such as migration, invasion, adhesion, and activation of epithelial transition markers in oesophageal and cervical cancer cells.

Recently, GI254023X was shown to inhibit migration and invasion of breast cancer cell lines, as well as in cancer cell lines of the stomach, oral cavity and the ovary (Mullooly, *et al.,* 2016; Mullooly, *et al.,* 2015; Mochizuki and Okada, 2007). Furthermore, GI254023X has also been reported to induce different effects on cancer biology i.e. inhibition of cell growth, proliferation, migration and invasion in different cell lines shown in *in vitro* studies (Mullooly, *et al.,* 2016). This suggests that the biological activities affected by ADAM-10 may well be cell-type specific, and probably largely dependent on the ectodomain substrates it acts on (Mullooly, *et al.,* 2016). This was illustrated when GI254023X reduced pancreatic cancer cell line migration and invasion, but

failed to affect proliferation (Gaida, *et al.,* 2010; Mullooly, *et al.,* 2016); whilst in skin cancer cell lines and bladder cancer cell lines, this small molecule induced significant suppression of both cellular proliferation and migration (Lee, *et al.*, 2010; Fu, *et al.,* 2014). In addition, GI254023X has been shown to reduce the cleavage of E-cadherin, a biomarker of cell-cell communication and adhesion (Reiss, et al., 2005; Mullooly *et al.,* 2016).

4.2 Results

4.2.1 Effect of GI254023X, SN-254 and SN-311 on actin levels in cancer cells

Since its discovery within non-muscular cells, the filamentous actin (F-actin) cytoskeletal network has been well studied and shown to be a critical role-player in regulating numerous biophysical and biochemical signals to control a variety of cell processes, such as cellular adhesion, migration, invasion as well as proliferation (Byron and Frame, 2016; Stricker, Falzone, and Gardel, 2010). ADAM-10 has been linked with the ectodomain cleavage of many adhesion related factors, impacting on cell-cell adhesiveness and tethering to the extracellular matrix (ECM), as well as ectodomain surface binding, and shedding receptor targets such as E-cadherin, and B-catenin translocation (Maretzky, *et al.,* 2005). These factors can affect the overall size and shape of cells, the cytoskeletal arrangement as well as whether cells exhibit a more mesenchymal or epithelial phenotype (Byron and Frame, 2016; Stricker, Falzone, and Gardel, 2010).

To investigate the effect of blocking ADAM-10 activity by GI254023X on the cytoskeletal arrangement, size and cell shape of HeLa and WHCO5 cells, an actin staining assay was performed using phalloidin. These cells were also treated with SN-311 and SN-254 to determine the effect of these agents on the parameters assessed. Phalloidin fluorescent stains for the polymeric filamentous –actin (F-actin). Briefly, HeLa and WHCO5 cell lines were

cultured on coverslips, and once the cells had settled, they were treated with 1X EC_{50} and 2X EC_{50} of GI254023X, SN-254 and SN-311. 24 hours after treatment, the cells were fixed and stained for F-actin with phalloidin. Phalloidin staining revealed F-actin distribution shown in red, whilst Hoechst was used to stain for cellular nuclei (shown in blue). This was viewed by fluorescence microscopy.

Our results in both HeLa and WHCO5 cells displayed a decrease in F-actin staining in response to treatment with increasing concentrations of the agents tested (Figure 4.1 and Figure 4.2). Results obtained showed a significant decrease in F-actin staining at both 1X EC_{50} and 2X EC_{50} for all of the compounds tested (bar graphs Figure 4.1 and Figure 4.2). With the exception of SN-254, where the effect of this compound on phalloidin staining in WHCO5 cells was not significant at 1X EC_{50}.

These results suggest that SN-311 and SN-254 is able to suppress F-actin forming, similar to that of GI254023X in both WHCO5 and HeLa cell lines (with the note that SN-254 was less active in WHCO5 cells).

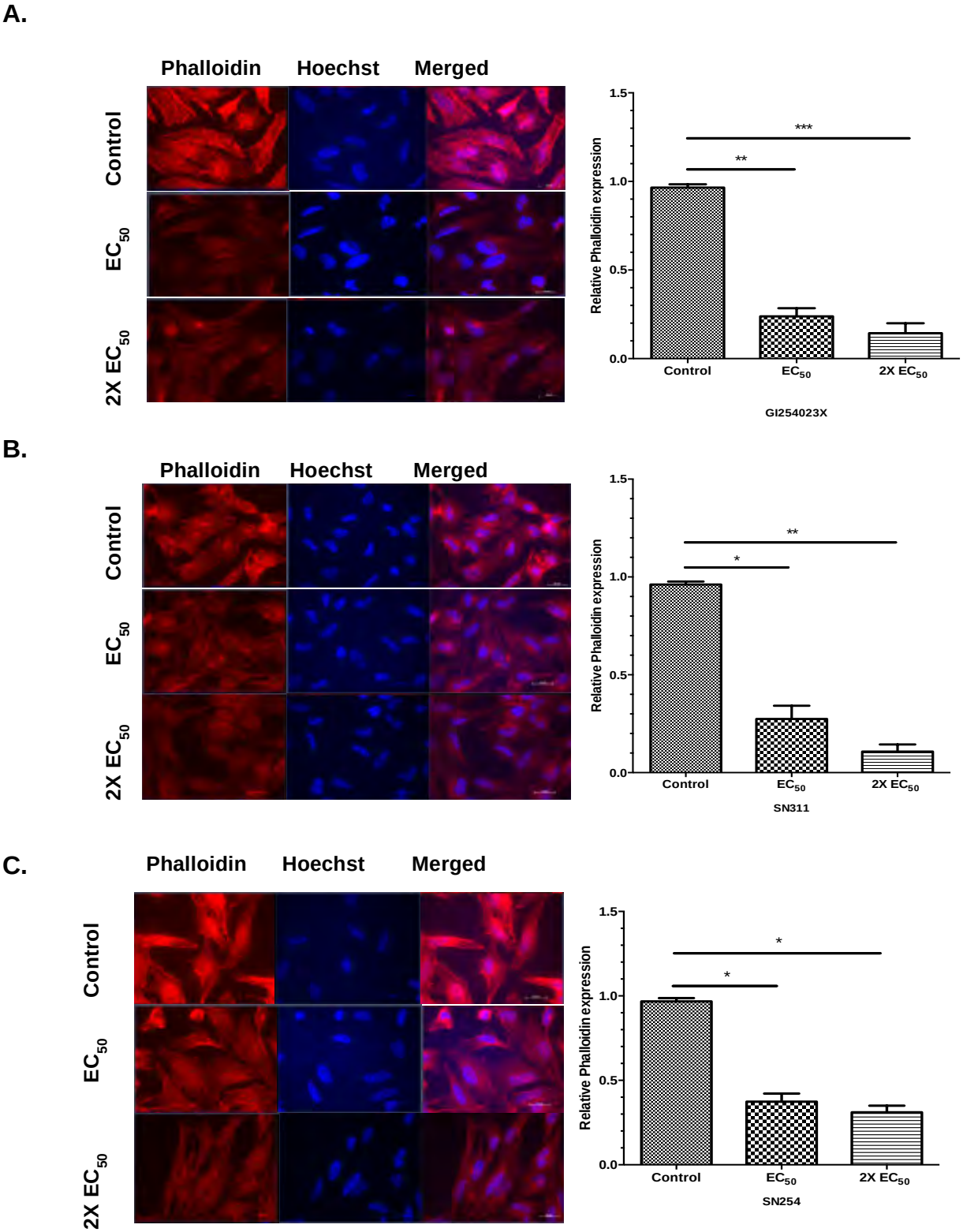

Figure 4.1: Phalloidin staining revealed Filamentous (F) actin distribution (shown in red), and Hoechst was used to stain for cell nuclei (blue) in HeLa post treatment with (A) GI254023X, (B) SN-311 and (C) SN-254 respectively. Results show a global decrease in F-actin expression levels in response to treatment with increasing concentrations of the indicated compounds (*p.<0.05; **p<0.01; ***p<0.001).

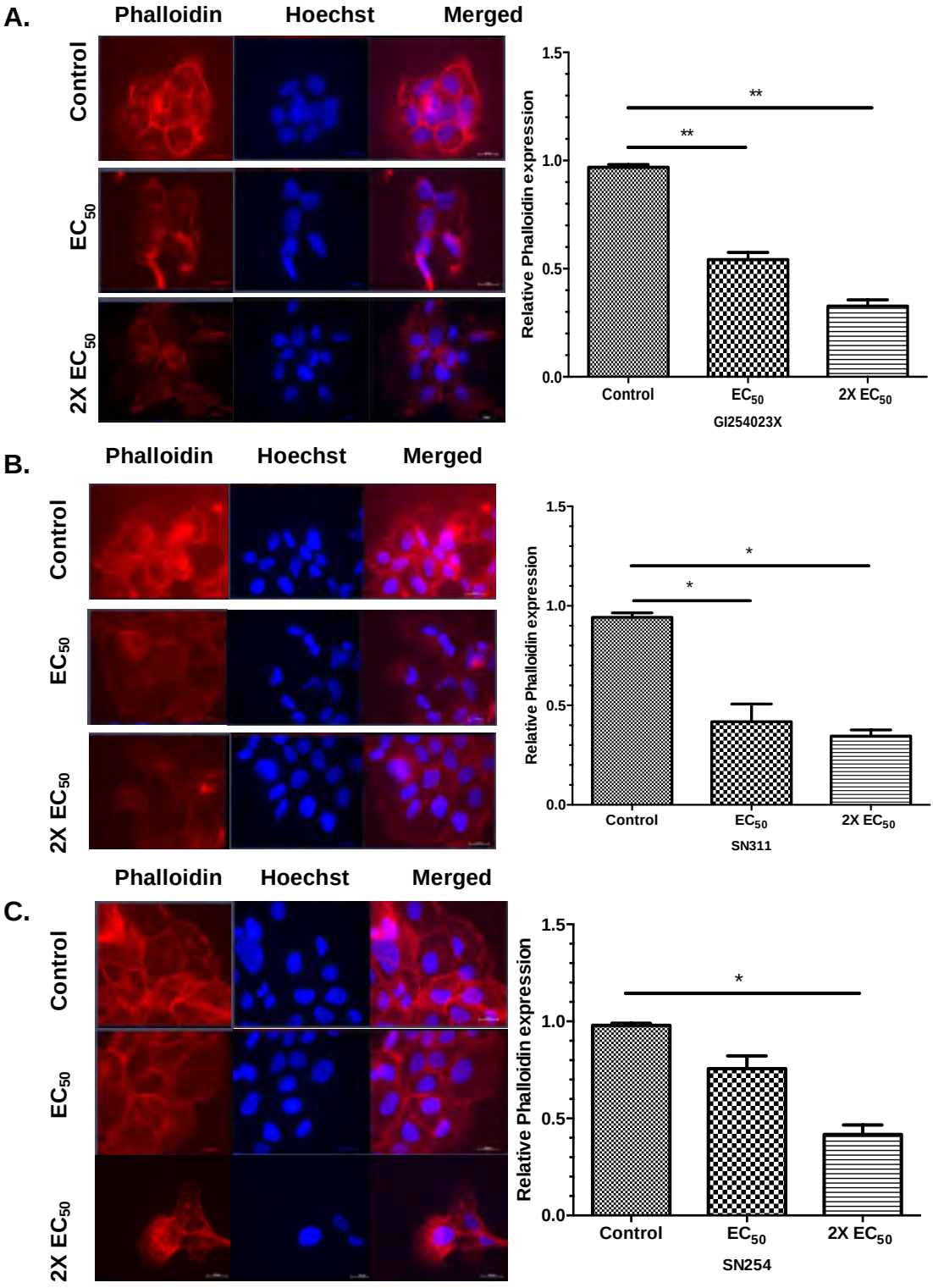

Figure 4.2: Phalloidin staining revealed Filamentous (F) actin distribution (shown in red), and Hoechst was used to stain for cell nuclei (blue) in WHCO5 post treatment with (A) GI254023X, (B) SN-311 and (C) SN-254 respectively. Results show a decrease in F-actin expression levels in response to treatment with increasing concentrations of the GI254023X and SN-311 compounds, however only a 2X EC_{50} treatment of SN-254 caused a significant decrease in F-actin expression (*p<0.05; **p<0.01).

4.2.2 Effects of ADAM10 inhibition on cancer cell adhesion

The decrease in F-actin expression observed on treatment with GI254023X, SN-311 and SN-254 suggested that inhibiting ADAM-10 activity, may affect cell adhesion, migration, as well invasion properties since Filamentous (F) actin has been linked with multiple biophysical cellular processes, including cellular adhesion (Byron and Frame, 2016; Stricker, Falzone, and Gardel, 2010). We consequently investigated the effects of GI254023X, SN-254 and SN-311 on cell adhesion in HeLa and WHCO5 cells.

Previous work conducted in our laboratory using ADAM-10 shRNA treatment showed a significant increase in cell adhesion in both cervical and oesophageal cancer cell lines (Williams, 2013, unpublished thesis). In this study we wanted to assess whether GI254023X, a small molecule inhibitor of ADAM-10 has similar effects, and also assess the effects of the novel molecules, SN-311 and SN-254 To assess the effect of these small compounds on cell adhesion, two adhesion assays were performed: non-coated and a fibronectin-coated adhesion assays. These two experimental conditions were used to analyse two types of adhesion, cell – cell adhesion modelled in the fibronectin assay, and cell-surface (ectodomain) adhesion modelled in the non-coated assay. Fibronectin is a widely distributed large extracecellular matrix (ECM) glycoprotein molecule implicated in several cellular adhesive functions, such as cell – to – cell attachment, cell –to – basement membrane attachment (Proctor, 1987; Wang, *et al.,* 2016). Furthermore, as fibronectin is described too as a mechanoregulator of the

ECM, the use of a fibronectin coated adhesion assay has been reported to assess whether the ADAM-10 small molecule inhibitors have the ability to stop the remodelling of the tumour stroma microenvironment that facilitate cancer invasion and metastasis (Wang, *et al.,* 2016).

Briefly, both HeLa and WHCO5 cell lines were treated with: GI254023X, SN-311 or SN-254 at EC_{50} and 2X EC_{50} concentrations. Thereafter, non-coated as well as fibronectin-coated adhesion assays were performed using 96-well tissue culture plates, as described in Materials and Methods.

Results obtained from both the non-coated (Figure 4.3A) and fibronectin-coated adhesion (Figure 4.3B) assay conditions showed a significant increase in cell adhesion in HeLa cells after treatment with GI254023X, SN-311, and SN-254. A similar increase was detected in the WHCO5 cell line, after treatment with all three of the small molecule inhibitors (Figure 4.4). Our data therefore suggests that an inhibition of ADAM-10 activity with GI254023X, leads to an increase in HeLa and WHCO5 cellular adhesion. Furthermore, treatment with SN-311 and SN-254 in HeLa and WHCO5 showed a similar result.

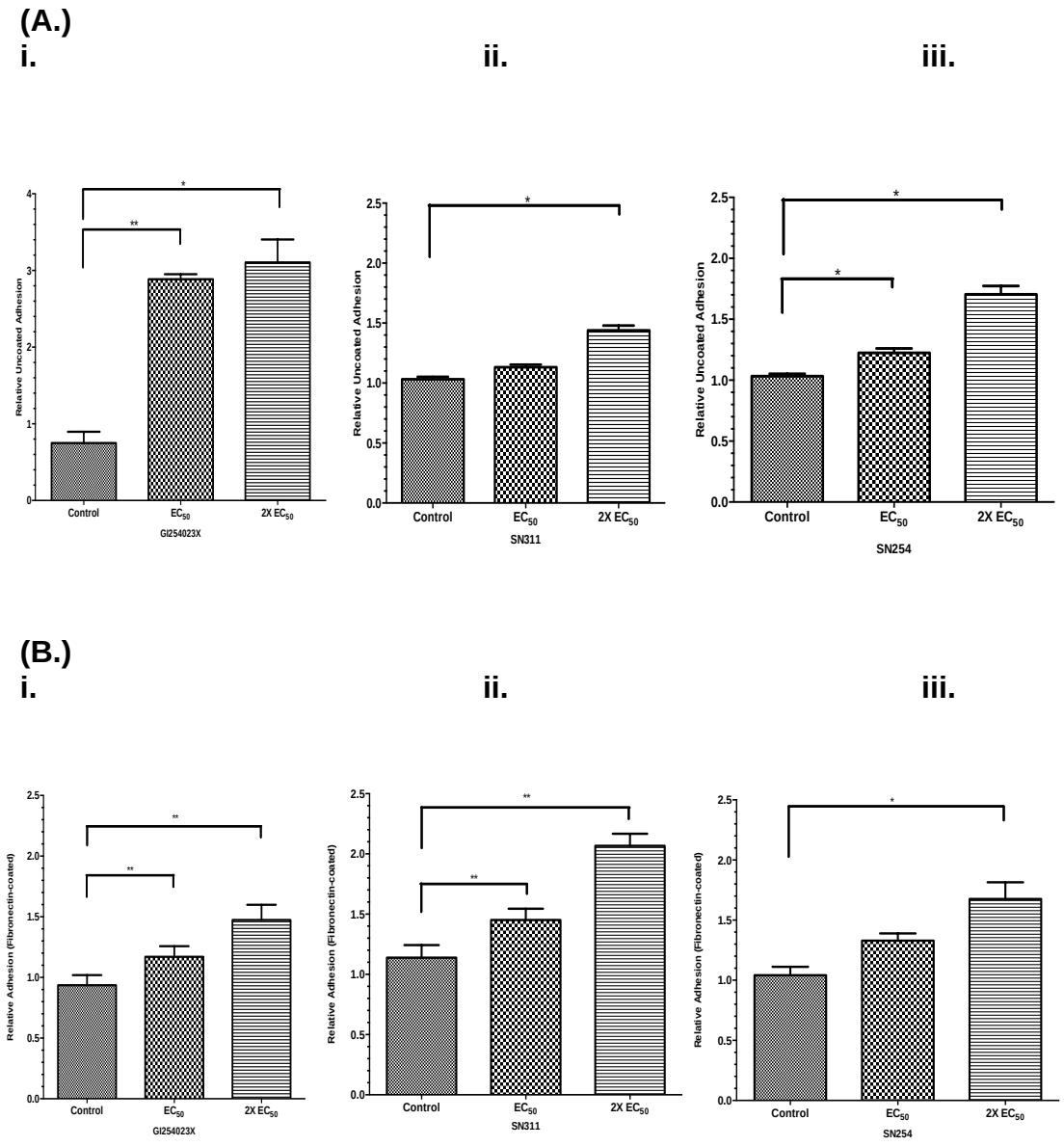

Figure 4.3: The effect of GI254023X, SN-311 and SN-254 on HeLa cervical cancer cell line cellular adhesion – (A) non-coated and (B) fibronectin-coated. GI254023X (4.3Ai & 4.3Bi), SN-311 (4.3Aii & 4.3Bii) and SN-254 (4.3Aiii &4.3Biii) treatment caused an increase in HeLa cell adhesion. HeLa cell line was treated with EC_{50} and 2 X EC_{50} values of GI254023X, SN-311 and SN-254; and DMSO equivalent to 2X EC_{50} concentration of the compound under investigation applied (serving as the control). Experiments were performed in quadruplicate and repeated at least three independent times. Results are presented as the mean ± standard error of mean (SEM). Data presented above was normalized to the experiment control. Adherent cells were expressed relative to total cell number, and the control variables were normalised to a value of 1. (*$p<0.05$; **$p<0.01$).

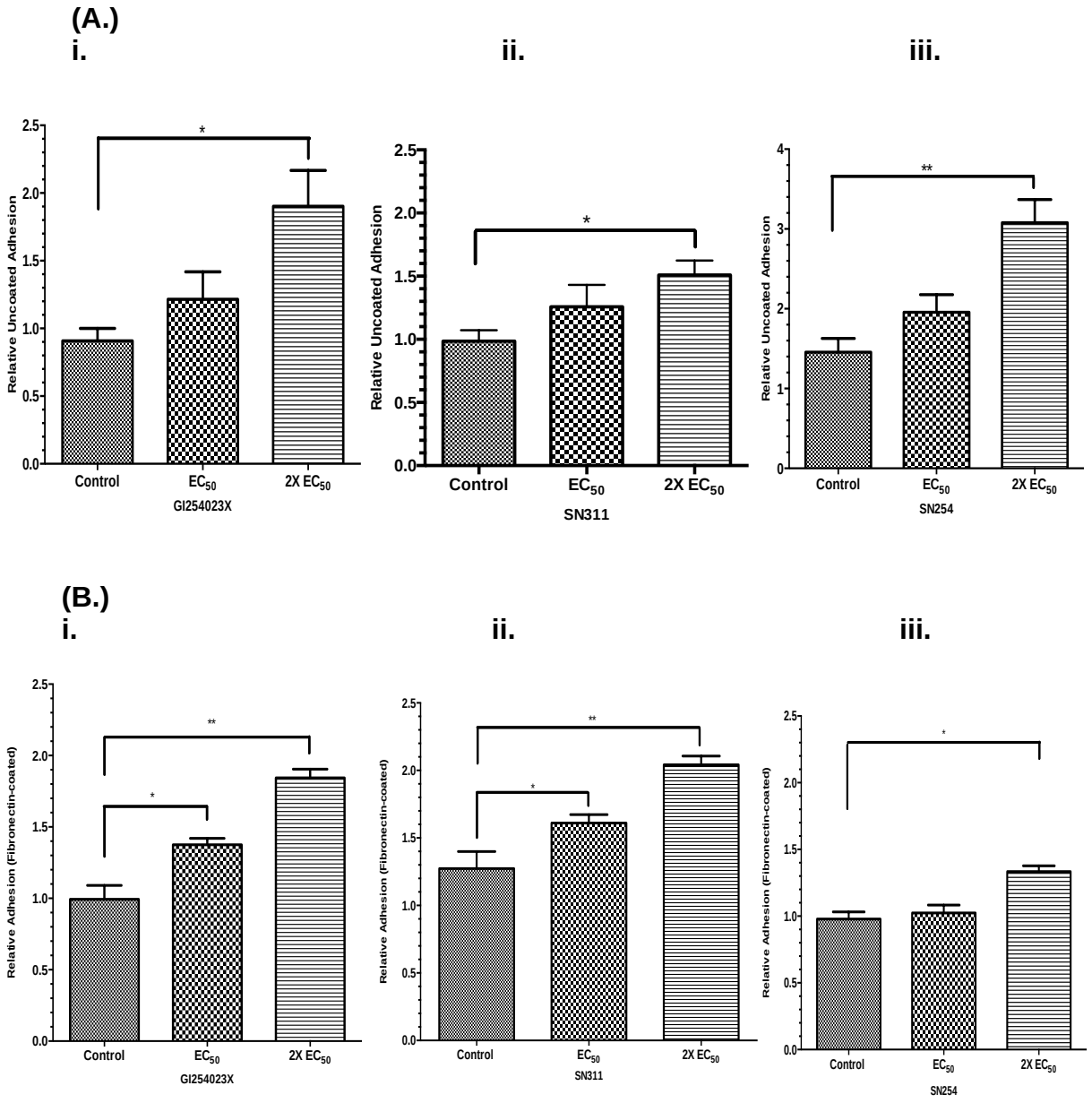

Figure 4.4: The effect of GI254023X, SN-311 and SN-254 on WHCO5 oesophageal cancer cell line cellular adhesion – (A) non-coated and (B) fibronectin-coated. GI254023X (4.4Ai & 4.4Bi), SN-311 (4.4Aii & 4.4Bii) and SN-254 (4.4Aiii &4.4Biii) treatment caused an increase in WHCO5 cell adhesion. WHCO5 cell line was treated with EC_{50} and 2 X EC_{50} values of GI254023X, SN-311 and SN-254; and DMSO equivalent to 2X EC_{50} concentration of the compound under investigation applied (serving as the control). Experiments were performed in quadruplicate and repeated at least three independent times. Results are presented as the mean ± standard error of mean (SEM). Data presented above was normalized to the experiment control. Adherent cells were expressed relative to total cell number, and the control variables were normalised to a value of 1. (*$p<0.05$; **$p<0.01$).

4.2.3 The effect of GI254023X, SN-311, and SN-254 on cancer cell migration

Cell migration is described as a complex process that is required for physiological growth and development, as well as repair and regeneration of tissue (Arribas, Bech-Serra and Santiago-Josefat, 2006). Cell migration also plays a critical role in metastasis and invasion (Arribas, Bech-Serra and Santiago-Josefat, 2006; Clark and Vignjevic, 2015).

A range of *in vitro* studies has identified several factors regulating cancer migration mode and dynamics. These factors include, single-cell migration, multicellular streaming as well as collective migration (Clark and Vignjevic, 2015). Single cell migration is caused by a lack of cell-cell interaction during migration activity. When increased contractility, whilst under the intrinsic factor regulation of the Rho-pathway is favoured, an amoeboid-like motility is experienced (Clark and Vignjevic, 2015; Wolf, *et al.,* 2003). Other individually moving cells may present as a mesenchymal phenotype, characterised by their spindle shaped cell body and protrusions (Clark and Vignjevic, 2015). Multicellular streaming is seen in non-adherent cells able to migrate along a similar path (Friedl and Gilmour, 2009; Friedl and Alexander, 2011). Collective migration describes groups of cells retaining the cell-cell adhesion and moves either as a narrow strand or as irregular multiple sheets of mixed phenotype cells (Khalil and Friedl, 2010; Clark and Vignjevic, 2015).

Having established that treatment with GI254023X induced a decrease in F-actin formation in HeLa and WHCO5 cancer cell lines, we next investigated whether this compound would inhibit migration. We also tested the effects of SN-311 and SN-254 in the assay. For this, we performed a Transwell migration assay. The principle behind this assay is based on two- medium containing chambers, separated by a permeable membrane (usually tissue-culture treated microporous membrane) through which cells can transmigrate. Cells are plated in one chamber, and separated from the other chamber that contains a chemoattractant, that should trigger cell migration. In this experiment, HeLa and WHCO5 cells were plated and treated with the indicated concentrations of GI254023X, SN-311 and SN-254.

24 hours later, treated cells were re-plated in triplicate into Transwell 8µM pore inserts containing 1% FCS media, allowing for vertical directed migration of the cells through the pores of the membrane into the lower chamber of the 24-well plate containing a higher serum concentration medium (20% FCS), serving as a chemo-attractant. After 24 hours, cells that had migrated across to the underside of the membrane were fixed with methanol and stained with crystal violet. The total number of migrated cells was normalised for each condition to controls.

A.

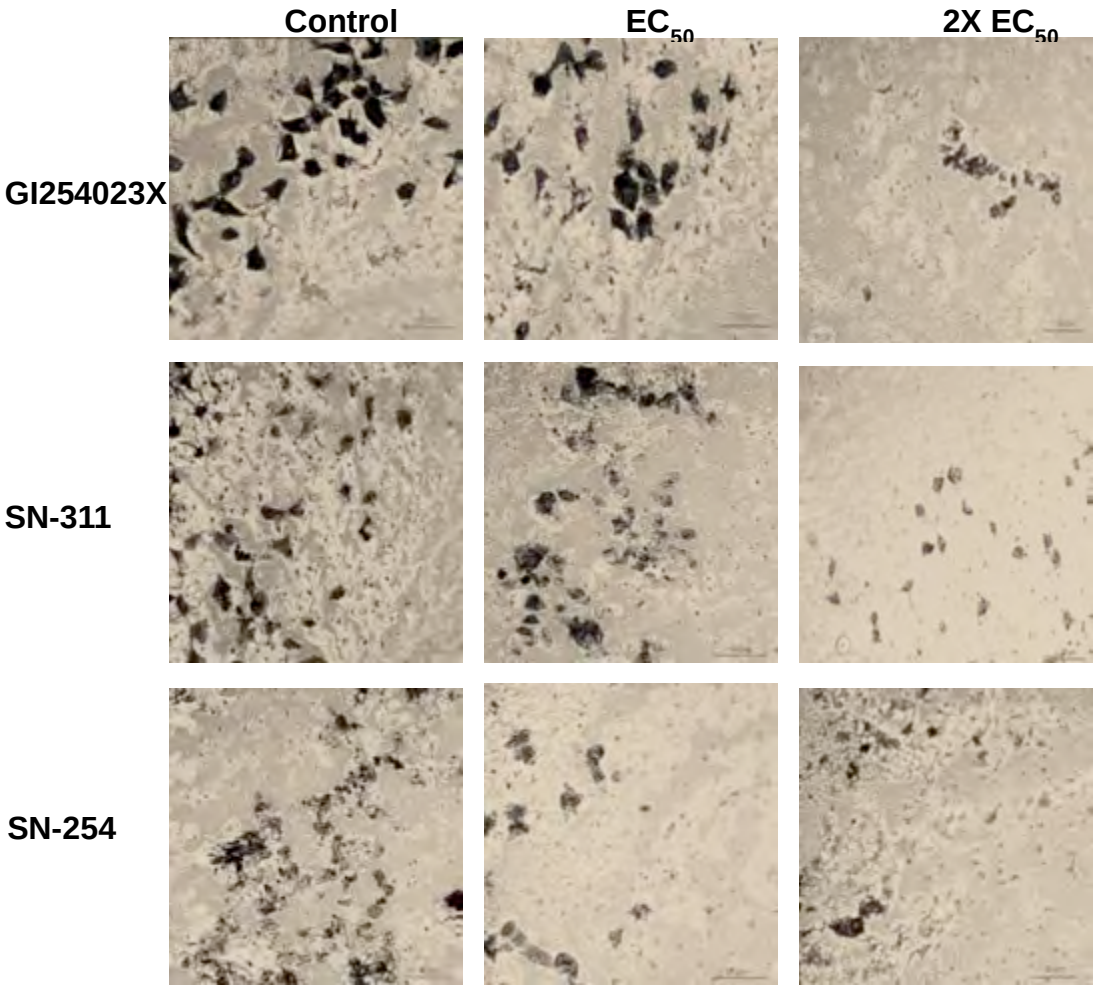

B.

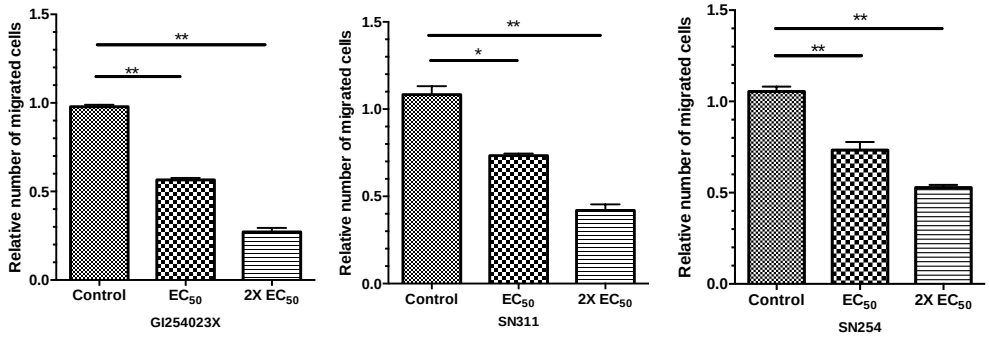

Figure 4.5: The effect of GI254023X, SN-311, and SN-254 on HeLa cervical cancer cell line migration. (A) Photographs of 8µM pore inserts after different treatment, taken with a phase contrast Zeiss microscope (X100 magnification). **(B)** Quantified densitometric analysis of relative number of cells migrated through the insert per treatment condition. Experiments were performed in quadruplicate and repeated at least two times. Results are presented as the mean ± standard error of mean (SEM). Data presented was normalized to the experiment control. Adherent cells were expressed relative to total cell number, and the control variables where normalised to a value of 1. * $p<0.05$; ** $p<0.01$. Size bar represents 50 µM.

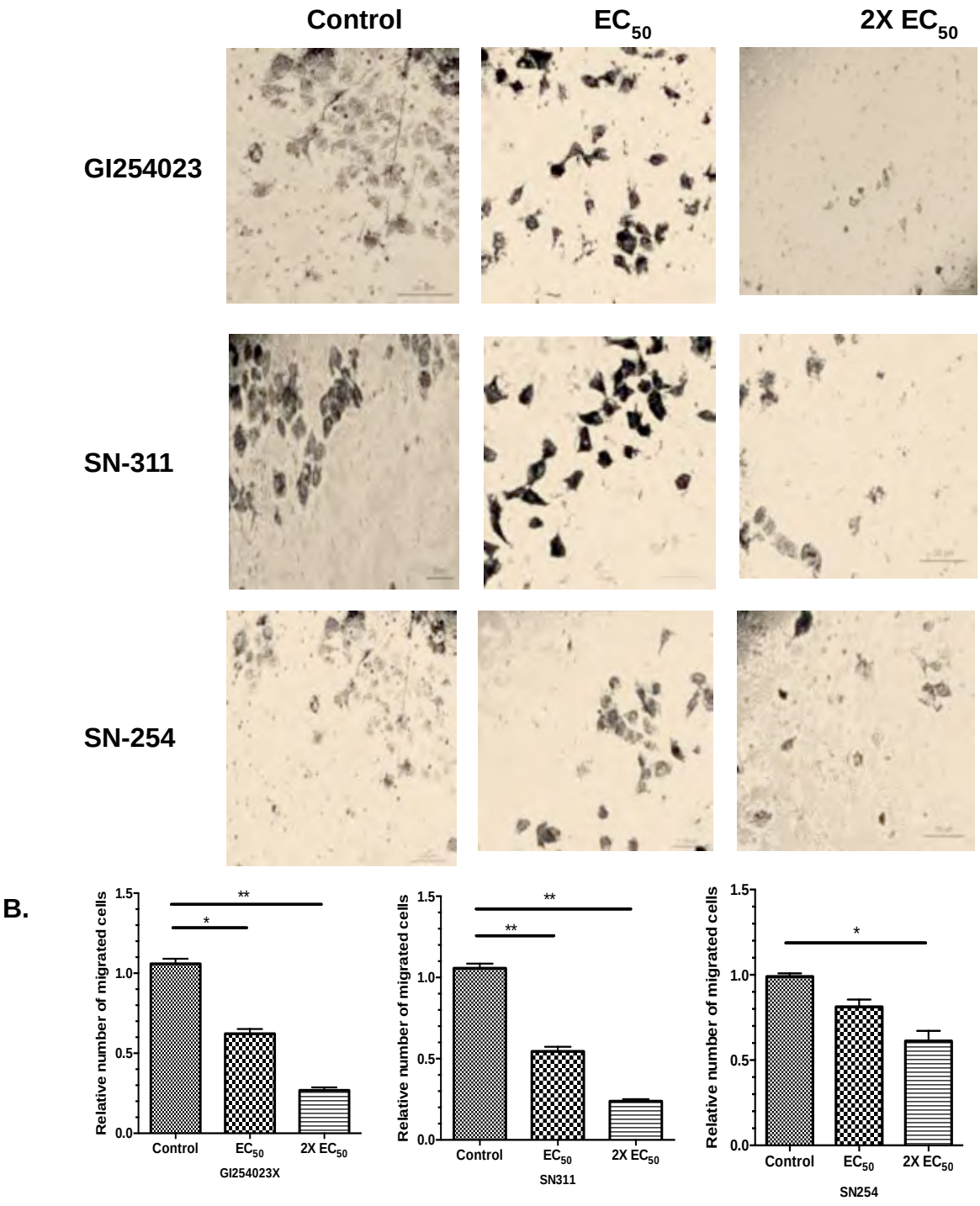

Figure 4.6: The effect of GI254023X, SN-311, and SN-254 on WHCO5 oesophageal cancer cell line migration. (A) Photographs of 8µM pore inserts after different treatment, taken with a phase contrast Zeiss microscope (X100 magnification). **(B)** Quantified densitometric analysis of relative number of cells migrated through the insert per treatment condition. Experiments were performed in quadruplicate and repeated at least two times. Results are presented as the mean ± standard error of mean (SEM). Data presented was normalized to the experiment control. Cells were expressed relative to total cell number, and the control variables where normalised to a value of 1. * $p<0.05$; ** $p<0.01$. Size bar represents 50 µM.

Our data clearly indicated a significant decrease in HeLa cell migration (Figure 4.5A and 4.5B) in response to treatment with GI254023X (50% decrease; $p<0.05$), SN-311 (25% decrease; $p<0.05$), and SN-254 (30% decrease; $p<0.05$) at the EC_{50} respectively. Similarly in WHCO5 cells, we observed a statistically significant ($p<0.05$) decrease in cell migration after treatment with GI254023X (40% decrease) and SN-311 (50% decrease) with the EC_{50} concentration (Figure 4.6A and B). However, SN-254 only caused a significant reduction (40%, $p<0.05$) in cell migration at 2X EC_{50} treatment (Figure 4.6B). These results suggests that inhibition of ADAM-10 activity in both HeLa and WHCO5 cells with the small molecule inhibitor GI254023X, is associated with a substantial reduction (50%; $p<0.05$) in cell migration. Treatment with SN-311 and SN-254 had a similar effect, although SN-254 seemed less effective than SN-311 and GI254023X.

4.2.4 The effect of GI254023X, SN-311, and SN-254 on cancer cell invasion

A hallmark of metastatic cells is its ability to both migrate and invade into other tissues, organs within the body (Friedl and Alexander, 2011), and although cancer is often described as a disease of uncontrolled cellular proliferation, at its most lethal form, it could be described as a disease of unregulated cellular invasion (Clark and Vignjevic, 2015). Since treatment of HeLa and WHCO5 cells with GI254023X, SN-311 and SN-254 resulted in significant inhibition of migration, we next investigated whether these compounds had any effect on the invasive properties in HeLa and WHCO5 cells.

HeLa and WHCO5 were cultured and pre-treated with GI254023X, SN-254 and SN-311, after which they were re-plated into 1% FCS-containing media in a matrigel-coated chamber (Corning Matrigel Invasion Assay kit, USA). Cells invading through the matrigel layer towards the 20% FCS in the lower chamber were fixed and stained 24 hours later. Cell numbers were quantified and normalised to controls as described in Material and Methods.

The results obtained showed a significant reduction in HeLa and WHCO5 invasion when treated with GI254023X, SN-311 and SN-254 (Figure 4.7A – B). Treatment with GI254023X resulted in a 30% and 50% decrease in HeLa and WHCO5 cells invasion ($p<0.05$) at 1X EC_{50} respectively. A smaller reduction (20 – 30%; $p<0.05$) in invasion was observed with treatment of

HeLa and WHCO5 cells with SN-311 at 1X EC_{50} respectively. SN-254 caused a significant (40%; $p<0.05$) decrease in HeLa cell invasion 1X EC_{50} treatment. Furthermore, SN-254 only caused a significant reduction (40%; $p<0.05$) in WHCO5 cell invasion at 2X EC_{50} treatment (Figure 4.7B).

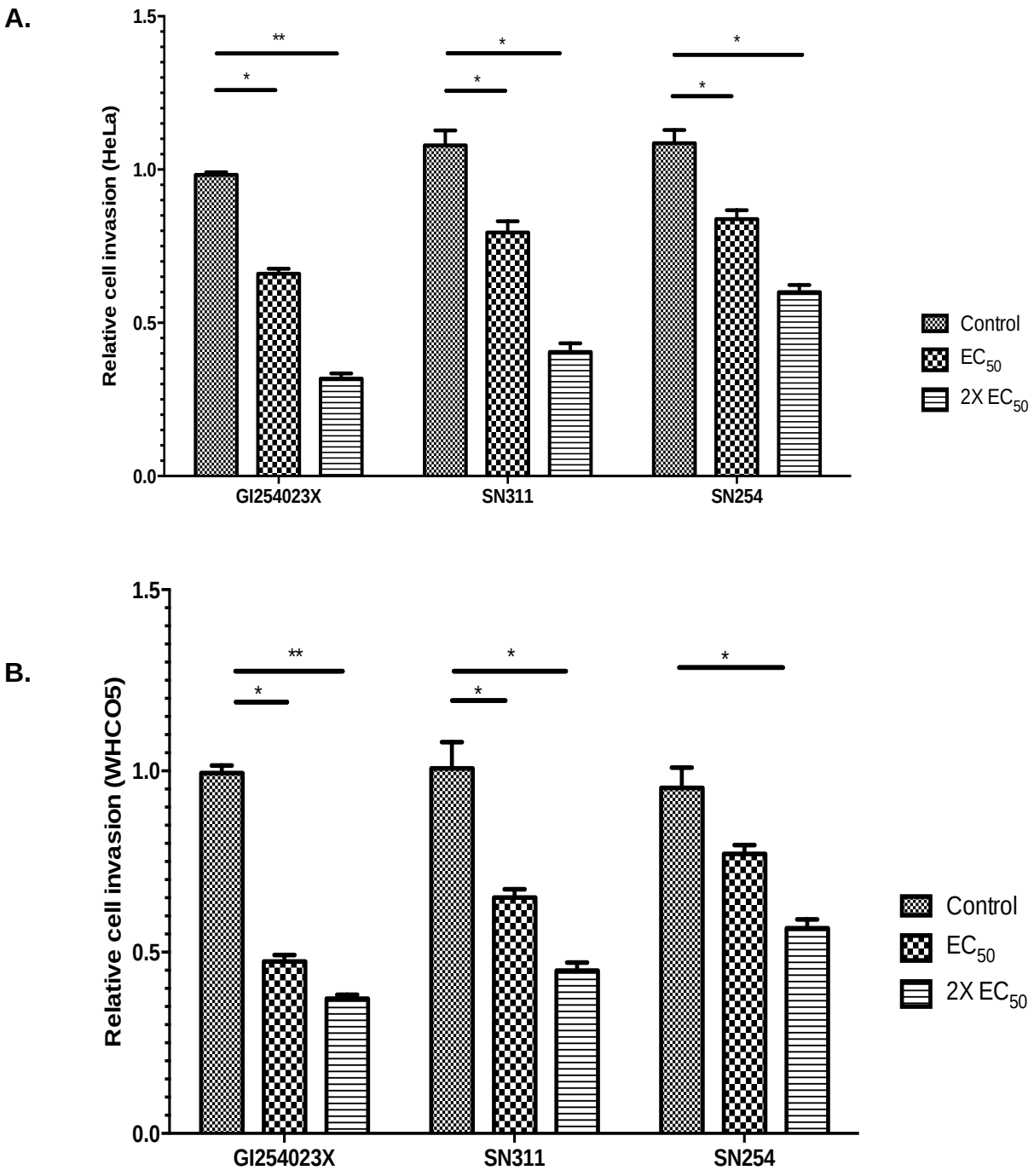

Figure 4.7: The effect of GI254023X, SN-311 and SN-254 on (A) HeLa, and (B) WHCO5 cancer cell invasion. HeLa and WHCO5 cancer cell lines were treated with EC_{50} and 2X EC_{50} equivalents of SN254, SN-311 and GI254023X; (DMSO only served as the control variable). Experiments were performed in triplicate and repeated at least two times. Results are presented as the mean ± standard error of mean (SEM). Data presented was normalized to the experiment control. Migrated cells were expressed relative to total cell number, and the control variables were normalised to a value of 1. * $p<0.05$; ** $p<0.01$.

4.2.5 The effect of GI254023X, SN-311, and SN-254 on cancer cell epithelial and mesenchymal phenotype markers: E-Cadherin, B-Catenin and Vimentin

Our data has shown significant increases in cell adhesion (non-coated and fibronectin-coated plastic surfaces) accompanied with a reduction in both migration and invasion activity, a decrease cellular proliferation as well as a decrease in F-actin expression levels in the presence of GI254023X, SN-311 and SN-254.

As described in chapter 1, tumour progression frequently involves an EMT with cells displaying altered morphology (Sethi, *et al.,* 2011), as well as a loss of epithelial cellular adhesive ligand marker such as E-Cadherin, B-Catenin (Sethi, *et al.,* 2011). This is accompanied by an increase in expression and acquisition of mesenchymal markers like vimentin (Sethi, *et al.,* 2011; Christiansen and Rajasekaran, 2006). EMT progression can be monitored by the detection of biomarkers including epithelial adhesion based markers, E-Cadherin and B-Catenin, or mesenchymal derived markers such as vimentin (Sethi, *et al.,* 2011).

Literature has identified ADAM-10 as a protein enzyme responsible for E-cadherin ectodomain shedding (Maretzky, *et al.,* 2005), hence ADAM-10 may be a useful target to reduce invasion and metastasis of cancers (Maretzky, *et al.,* 2005).

To assess whether inhibition of ADAM-10 could alter the epithelial / mesenchymal phenotypic balance in HeLa and WHCO5 cells, the expression levels of E-Cadherin, B-Catenin and Vimentin was detected by western blot analysis. Our results in HeLa cells showed an increase in E-Cadherin and B-Catenin levels after treatment with GI254023X, and SN-311 (Figure 4.8A, and 4.8B), whereas the effect of SN-254 on E-Cadherin and B-Catenin levels was barely noticeable (Figure 4.8C). Conversely, a decrease in Vimentin levels was observed after GI254023X and SN-311 (Figure 4.8A and B) treatment. No change in Vimentin levels was observed on SN-254 treatment (Figure 4.8C).

Similar results were obtained in WHCO5 cells. A substantial increase in E-Cadherin (observed as a double band in WHCO5 cells, this double band was noted in two other oesophageal cancer cell lines test in our laboratory, namely KYSE30 and WHCO6) and B-Catenin levels observed in WHCO5 cells treated with GI254023X and SN-311, whereas SN-254 increased E-Cadherin levels substantially, but only caused a small increase in B-Catenin levels (Figure 4.9A-C). A decrease in Vimentin levels was noted for each of the compounds in WHCO5 (Figure 4.9A-C). Together these results show that GI254023X, SN-311 and SN-254 causes an elevation in epithelial phenotype markers such as E-Cadherin and B-Catenin expression levels, whilst decreasing the levels of a mesenchymal phenotype marker, Vimentin suggesting that these small molecules could alter epithelial to mesenchymal cell phenotype transition in HeLa and WHCO5 cells.

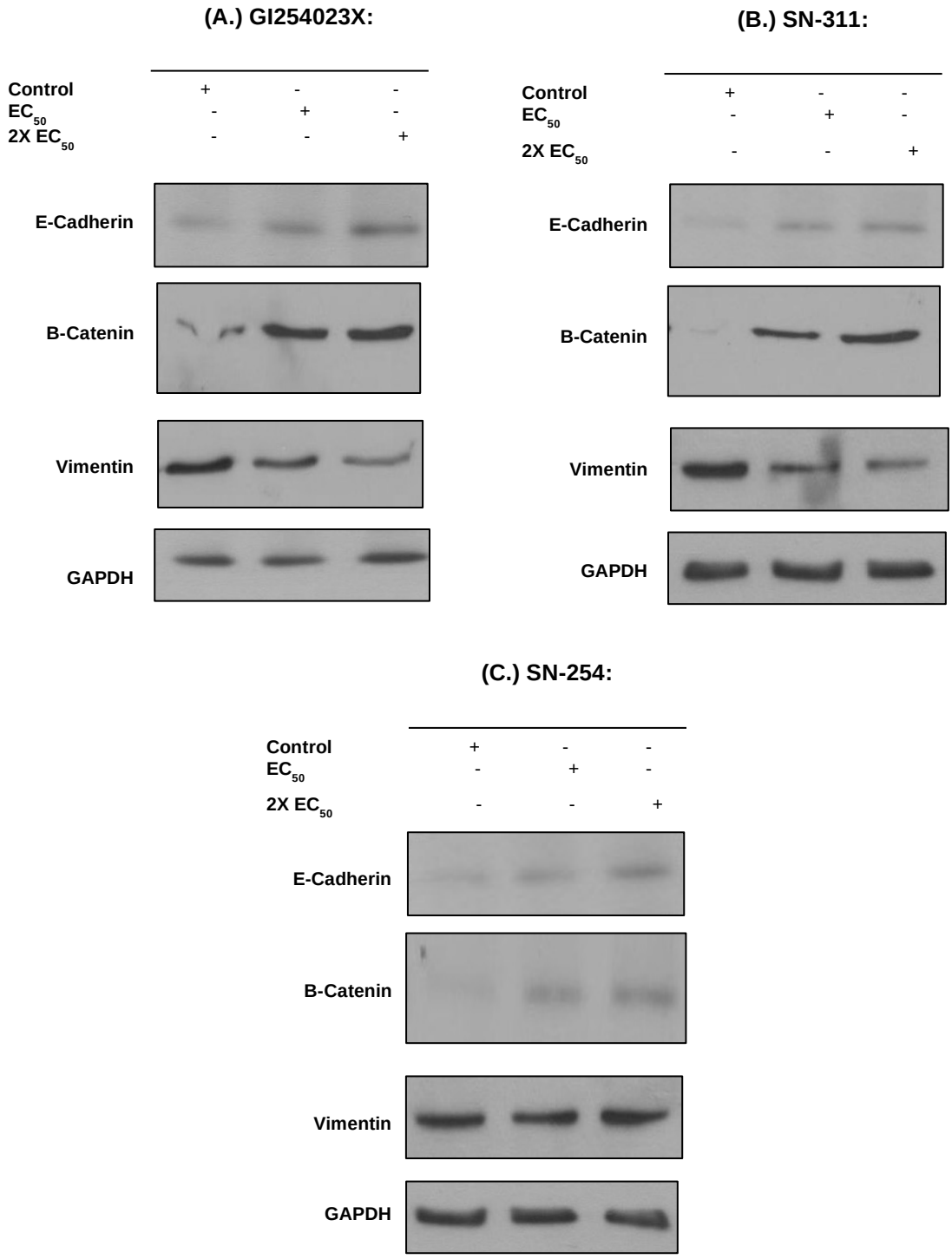

Figure 4.8: The effect of (A) GI254023X, (B) SN-311 and (C) SN-254 on HeLa cervical cancer cell epithelial and mesenchymal phenotype markers. E-Cadherin (120kDa), B-Catenin (92kDa) and Vimentin (57kDa) was detected in HeLa cells. GAPDH was used as a control for protein loading. Experiments were performed in quadruplicate and repeated at least three times.

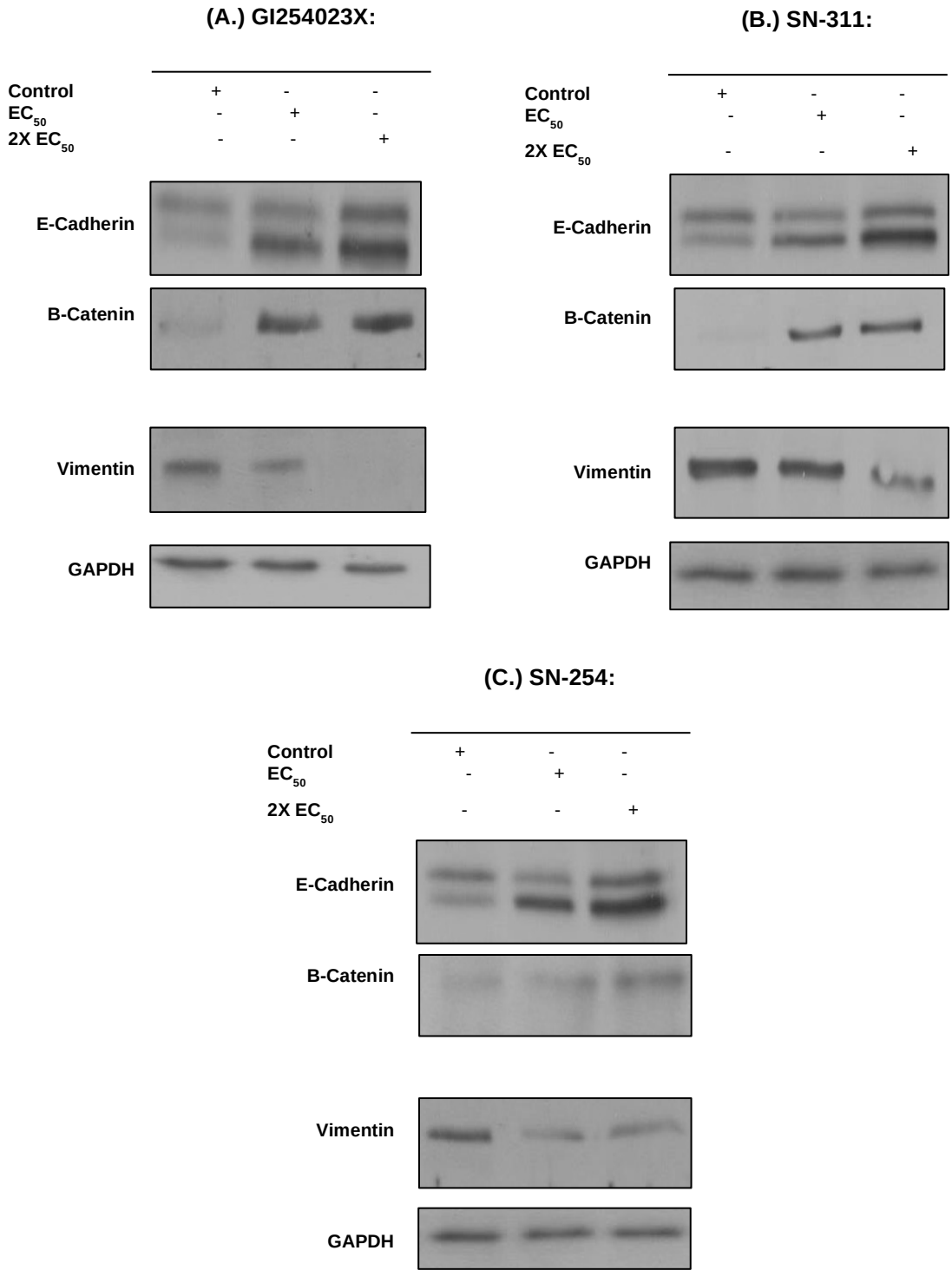

Figure 4.9: The effect of (A) GI254023X, (B) SN-311 and (C) SN-254 on WHCO5 oesophageal cancer cell epithelial and mesenchymal phenotype markers. E-Cadherin (120kDa), B-Catenin (92kDa) and Vimentin (57kDa) was detected in WHCO5 cells. GAPDH was used as a control for protein loading. Experiments were performed in quadruplicate and repeated at least three times.

4.2.6 The effect of GI254023X, SN-311, and SN-254 on VEGF expression levels

Having detected a decrease in migration, invasion and cellular proliferation, accompanied with changes in the levels of markers that associate with epithelial and mesenchymal transition in the presence of GI254023X, SN-311 and SN-254, we next set out to investigate whether these compounds affect angiogenic growth factors, which regulate the process of angiogenesis. Angiogenic factors, such as the vascular endothelial growth factor (VEGF), is instrumental in maintaining the vasculature status as well as further enhancing growth and development of tissues requiring new blood vessels (Verheul and Pinedo, 2000). A potent specific angiogenic factor, many studies have shown that VEGF induces angiogenesis, and contributes significantly to the regulation of vasculogenesis (Neufeld, *et al.,* 1999; Donners, *et al.,* 2010; Li *et al.,* 2015).

Previous studies have shown that inhibiting ADAM-10 via siRNA resulted in the decrease in expression and secretion of vascular endothelial growth factor A (VEGF-A) (Li, *et al.,* 2015; Isozaki, *et al.,* 2013; Dreymeuller, *et al.,* 2012). Based on this published work, we investigated whether GI254023X, SN-311 and SN-254 could similarly affect VEGF levels in oesophageal and cervical cancer cells.

The results obtained showed a reduction in VEGF levels when ADAM-10 was inhibited with GI254023X in HeLa and WHCO5 cells (Figure 4.10A and

4.11A). A similar effect was detected after HeLa and WHCO5 cells were treated with SN-311 (Figure 4.10B and 4.11B). Furthermore, treatment of HeLa and WHCO5 with SN-254, induced a decrease in VEGF expression, albeit not as strongly as with GI254023X and SN-311 (Figure 4.10C; Figure 4.11C). It must be highlighted that detecting for VEGF expression in SN-254 treated HeLa cells had consistently produced faint VEGF bands (Figure 4.10C). SN-254 treated WHCO5 cells, though produced a reduction in VEGF expression at EC_{50} concentration, no further decreases in expression was detected at 2X EC_{50} treatment (Figure 4.11C), which could be attributed to difficulty experienced in western blotting transfer step.

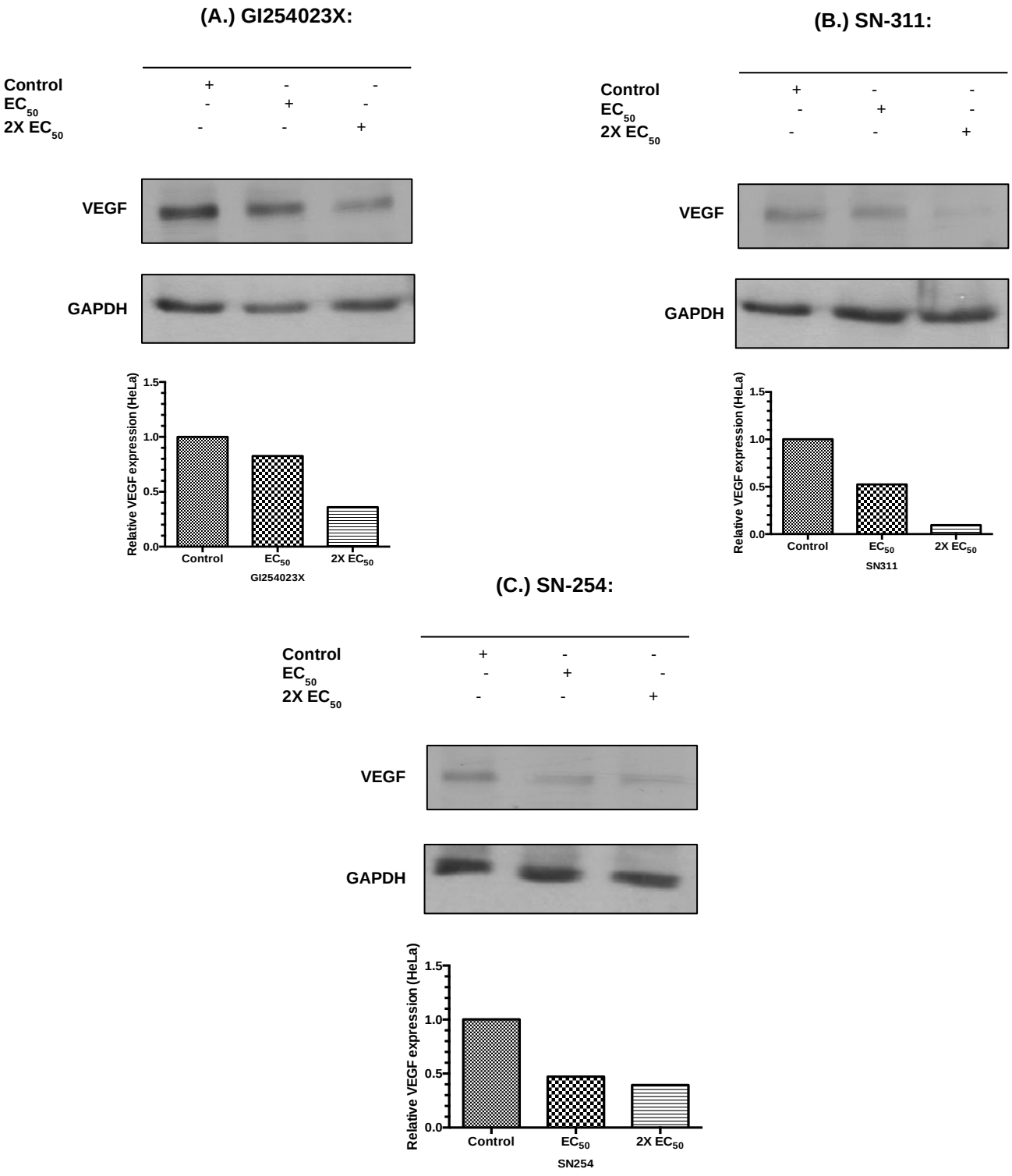

Figure 4.10: The effect of (A) GI254023X, (B) SN-311 and (C) SN-254 on VEGF expression in HeLa cervical cancer cells. VEGF (21kDa) was detected in HeLa cancer cells. GAPDH was used as a control for protein loading. Quantitation of VEGF expression (histogram below each compound treatment) relative to GAPDH determined by densitometry of western blot band intensity using ImageJ software. Results are representative of experiments performed at least two independent times.

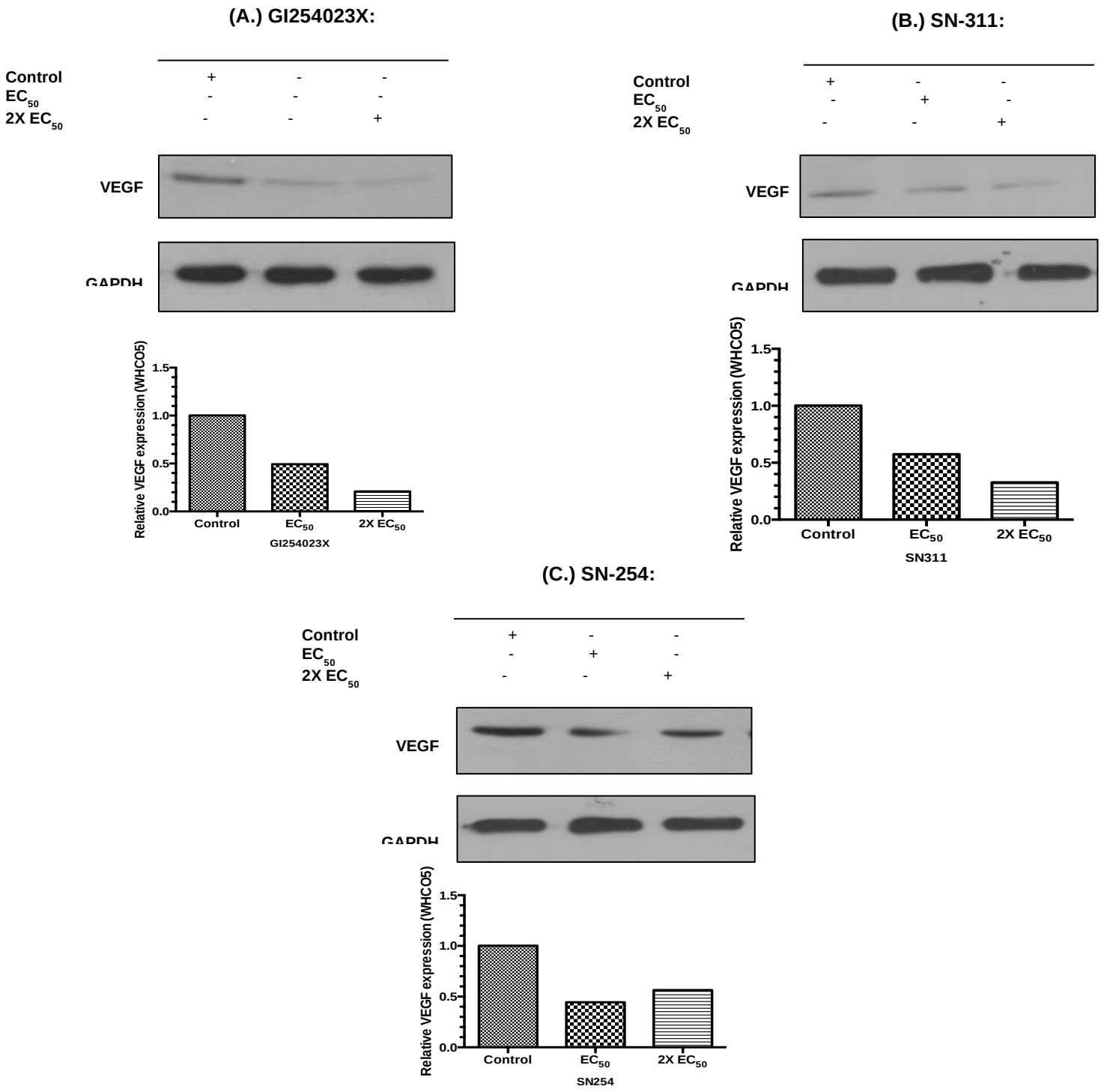

Figure 4.11: The effect of (A) GI254023X, (B) SN-311 and (C) SN-254 on VEGF expression in WHCO5 oesophageal cancer cells. VEGF (21kDa) was detected in WHCO5 cancer cells. GAPDH was used as a control for protein loading. Quantitation of VEGF expression (histogram below each compound treatment) relative to GAPDH determined by densitometry of western blot band intensity using ImageJ software. Results are representative of experiments performed at least two independent times.

4.3 Discussion

In this study, we reported that treatment with GI254023X, SN-254 and SN-311 in HeLa, and WHCO5 cell lines, induced an inhibitory effect on F-actin levels as well as on cell migration and invasive abilities. This was accompanied with an increase in both cell to cell and cell to surface adhesion properties. We also reported an increase in epithelial phenotypic markers, E-Cadherin and B-Catenin, with a simultaneous decrease in mesenchymal cell marker, Vimentin, and suppression of vascular endothelial growth factor (VEGF) after treatment with GI254023X, SN-254 and SN-311.

The data generated suggest that the inhibition of ADAM-10 with treatment of GI254023X in HeLa and WHCO5, leads to the observed increase of markers associated with the epithelial phenotype (increase in E-Cadherin, and B-Catenin), coupled with a decrease in expression of markers associated with mesenchymal phenotype (decrease in Vimentin). A similar trend was detect with treatment with SN-311, and to a lesser extent, SN-254. These results collectively show that these compounds are able to cause an elevation in markers associated with the epithelial phenotype, whilst simultaneously decreasing mesenchymal phenotype markers. It suggests that these small molecules are able to suppress epithelial to mesenchymal transition.

A recent study silencing ADAM-10 expression in gastric and leukaemia cells induced an up-regulation of the epithelial marker, E-Cadherin, and a suppression of the mesenchymal marker, Vimentin (You, *et al.,* 2015). The

results of You and colleagues (2015) therefore suggest that targeting ADAM-10 expression can effect cell phenotype. Our study similarly showed that inhibiting ADAM-10 activity with small molecules resulted in an increase in E-Cadherin and a decrease in Vimentin. High ADAM-10 has been reported to associate with transformation of cell morphology into structures that increase cellular motility, as well as a loss of epithelial cellular adhesive ligand marker such as E-Cadherin, B-Catenin, accompanied by the increase in expression and acquisition of mesenchymal markers like Vimentin (Sethi, *et al.,* 2011; Christiansen and Rajasekaran, 2006). Such changes noted within invading cells are characteristic of epithelial to mesenchymal transition (EMT). Furthermore, ADAM-10 has been identified to be responsible for activating E-Cadherin (Maretzky, *et al.,* 2005; Zhang, *et al.,* 2014; Li, *et al.,* 2016), as well as contributing to B-Catenin translocation (Maretzky, *et al.,* 2005).

ADAM-10 up-regulation has been associated with the growth and metastasis of many cancers, these include non-small lung cancer, oral cavity, stomach as well as ovarian cancers (Mullooly, *et al.,* 2016; Mullooly, *et al.,* 2015; Mochizuki and Okada, 2007). Structural features expressed within metastatic cells compared to normal cells include cytoskeletal organization rearrangement, unregulated growth, migration, and invasion. To assess for possible cytoskeletal changes in HeLa and WHCO5 cells, post ADAM-10 suppression with small molecule inhibitor GI254023X treatment, F-actin cytoskeletal protein suppression in expression levels were detected via a phalloidin staining. The filamentous actin (F-actin) cytoskeletal network was been well studied and shown to be a critical role- player in regulating

numerous biophysical and biochemical signals to control and process a variety of cell behaviours, such as cellular adhesion, migration, invasion as well as proliferation (Byron and Frame, 2016; Stricker, Falzone, and Gardel, 2010).

The association of ADAM-10 with the ectodomain cleavage of many adhesion related factors linked to cell-cell adhesiveness and the extracellular matrix (ECM) as well as cell ectodomain surface binding and shedding receptor targets such as E-Cadherin, and B-Catenin translocation has been well researched (Maretzky, *et al.,* 2005). Our results also indicated a similar trend in suppression of phalloidin staining with a corresponding increase in treatment by the novel compounds SN-311 and SN-254.

Filamentous (F) actin is linked with multiple biophysical cellular processes such as cellular adhesion (Byron and Frame, 2016; Stricker, Falzone, and Gardel, 2010), Previous work conducted in our laboratory had shown significant increases in cell adhesion in HeLa and WHCO5 when ADAM-10 was inhibited using shRNA ADAM-10 (Williams, 2013, unpublished data). Our data showing significant increases in cell adhesion after treatment with GI254023X is in accordance with previous reported studies (Maretzky, *et al.,* 2005). Our results also show that treatment with SN-311 and SN-254 can similarly increase cellular adhesion, suggesting that these compounds are able to perform functionally similar to GI254023X. This observation is consistent with the results obtained regarding the increase in E-Cadherin and B-Catenin expression.

Our results obtained in assessing the effect of GI254023X, SN-311 and SN-254 on cancer cell migration and adhesion, showed significant reduction in migratory and invasive HeLa and WHCO5 cancer cells, suggesting a functional role for ADAM-10 in cervical and oesophageal cancer cell migration and invasion. Our results align with other studies, which has shown that inhibition and suppression of ADAM-10 via shRNA, siRNA and small molecule GI254023X, results in decreases in migration and invasion of oral squamous cell carcinoma, hepatocellular carcinoma (HepG2 cells), bladder cancer cells, and nasopharyngeal cancer cells (Jones, *et al.,* 2013; Yuan, *et al.,* 2013; Fu, *et al.,* 2014; You, *et al.,* 2015; Liu, *et al.,* 2014; Mullooly*, et al.,* 2016; Maretzky, *et al.,* 2005). These results, collectively suggest that ADAM-10 may be an important contributing factor in cervical and oesophageal cancer progression. As tumour progression occurs, the cancer cells become more invasive and metastatic (Clark and Vignjevic, 2015; Yilmaz and Christofori, 2009; Sethi, *et al.,* 2011).

In summary, our current study indicates that ADAM-10 has the potential to be an oesophageal and cervical cancer therapeutic target, as inhibition of its expression via GI254023X suppressed cancer cell migration, invasion, induced an increase in adhesion activity, suppressed pro-invasive changes in cell phenotype, and decreased vascular endothelial growth factor expression. Furthermore, our results have shown that for most of the parameters tested, SN-311 and SN-254 seem to have the same qualitative effect as GI254023X, strongly suggesting that these two novel agents may be causing these effects observed through inhibiting ADAM-10. However, we cannot exclude that

these results observed with SN-311 and SN-254 may be due to impacts on other molecular targets, or due to impacts on other ADAM receptors, such as ADAM-17. To address this, future possible specificity and binding studies should be conducted with possible targets.

Chapter 5:

Conclusion

In an earlier study conducted in our laboratory, we identified a number of genes differentially expressed genes in a microarray analysis performed in cervical tissue compared to normal tissue (van der Watt, 2009). One of the cDNAs shown to be highly expressed in the cancer samples, was one encoding the ADAM-10 protein (Ward, 2011). An additional expression profiling analysis was conducted in our laboratory in patient material isolated from cervical and oesophageal cancer and normal tissue samples. This expression pattern too indicated a significant up-regulation of ADAM-10 expression in the cancer tissue material compared to that of the normal samples (Williams, 2013, MSc dissertation). This observation is consistent reports from other authors who performed similar expression profiling studies, demonstrating that ADAM-10 is overexpressed in a variety of tumours and contributes actively in cancer development and progression (Ma, *et al.,* 2015; Mullooly, *et al.,* 2016; Mullooly, *et al.,* 2015; You, *et al.,* 2015; Jones, *et al.,* 2013; Arribas, *et al.,* 2006; Zhao, *et al.,* 2014).

The potential for ADAM-10 to serve as a therapeutic target in cervical and oesophageal cancer was investigated using the established GI254023X and two newly synthesized small molecules, namely SN-311 and SN-254. The

results in this study demonstrated that in at least two independent cancer cell lines, HeLa cervical, and WHCO5 oesophageal, a decrease of ADAM-10 expression with GI254023X led to a decrease in markers of proliferation, a shift in the balance of phenotypic markers from mesenchymal to epithelial (based on the elevated levels of E-Cadherin and B-Catenin, and decrease in levels of Vimentin). The result obtained in GI254023X treatments was in accordance with literature, citing it as a small molecule able to decrease proliferation in a range of cancers, including breast, hepatocellular carcinoma and tongue squamous cell carcinoma (Duffy, *et al.,* 2012; Fu, *et al.,* 2014; Zhang, *et al.*, 2014; Shao, *et al.,* 2015).

Prior work conducted in our laboratory had shown significant increases in cell adhesion in HeLa and WHCO5 when ADAM-10 was inhibited using shRNA ADAM-10 (Williams, 2013, unpublished data). Our data showed increases in cell adhesion after treatment with GI254023X, consistent with the elevated epithelial phenotypic markers detected. This generated result is in accordance with other studies in the literature (Maretzky, *et al.,* 2005). Furthermore, our results showed significant reduction in migratory and invasive HeLa and WHCO5 cancer cells after treatment with GI254023X, suggesting a functional role that ADAM-10 has within cervical and oesophageal cancer cell migration and invasion properties. This finding correspond with other studies in different cell lines, which has shown that inhibition and suppression of ADAM-10 via shRNA, siRNA and GI254023X, had resulted in decreases in migration and invasion of oral squamous cell carcinoma, hepatocellular carcinoma (HepG2 cells), bladder cancer cells, and nasopharyngeal cancer cells (Jones, *et al.,*

2013; Yuan, *et al.,* 2013; Fu, *et al.,* 2014; You, *et al.,* 2015; Liu, *et al.,* 2014; Mullooly*, et al.,* 2016; Maretzky, *et al.,* 2005).

Having detected a decrease in proliferative cancer cell activity after treatment with GI254023X, we investigated potential mechanisms involved. Our results had shown significant increases in caspase 3/7 activity levels in treatment with GI254023X, furthermore we determined that poly (ADP-Ribose) polymerase (PARP), a known caspase cleaved substrate (Bock and Chang, 2016; Kotsopoulos, 2016) had increased in expression post treatment. This result suggests that apoptosis, is induced by GI254023X. Our findings with GI254023X treatment correspond with literature, whereby GI254023X was shown to not only block proliferation, but also induce apoptosis within acute T-lymphoblastic leukaemia Jurkat cells (Mullooly, *et al.,* 2016; Ma, *et al.,* 2015).

For all the markers examined in this study; inhibition of ADAM-10 with GI254023X in HeLa and WHCO5 cells is associated with the decrease in markers linked with tumorgenicity (proliferation, angiogenesis, migration and invasion), and in fact shown also to induce apoptosis. Of great significance, this study has shown that for most of the tumorgenicity parameters tested, the two novel compounds (SN-311 and SN-254) seem to have a similar qualitative effect as that of GI254023X seen in both HeLa and WHCO5 cells respectively. To assess whether the two novel small molecule compounds, would target ADAM-10, a human fractalkine CX_3CL1 immunoassay was performed. ADAM-10 is described as a candidate for constitutive cleavage of CX_3CL1, thus solubilizing this transmembrane bound protein via shedding

activity (Hundhausen, *et al.,* 2003). Prior research has also shown that GI254023X is able to reduce significantly the cleavage of human fractalkine by preferentially blocking ADAM-10 receptor (Hundhausen, *et al.,* 2003). Our results shown here in this functional ADAM-10 activity assay illustrated that both SN-311 and SN-254 were able to induce a decrease in cleaved soluble CX_3CL1 expression levels, strongly suggesting that the two novel agents may well be causing the effects observed in the tumorgenicity parameters through inhibiting ADAM-10, as SN-311 and SN-254 were both able to inactivate CX_3CL1 cleavage, a known ADAM-10 shedding function.

However, we cannot conclusively say that SN-311 and SN-254 may be causing its effects by targeting ADAM-10 directly. Further binding and specificity studies are needed to be conducted to determine whether these compounds are indeed directly targeting ADAM-10. By performing these specificity assays we will know whether the results obtained are due solely by directly interacting with ADAM-10, or through impacting of other ADAMs, this as literature cites the ability of different ADAMs family members able to perform compensatory roles for each other. ADAM-10 is described as structurally and functionally related to ADAM-17, where both are shown to be leading proteases in trans-membrane protein ectodomains (Mullooly, *et al.,* 2016; Bzowska*, et al.,* 2009). Furthermore, prior research has linked ADAM-10 and ADAM-17 as able to compensate functionally in the absence of the other (Bzowska*, et al.,* 2009).

5.1 Concluding statement

In summary, our study has established that the two newly generated small molecules en route to synthesizing GI254023X, namely SN-311 and SN-254 shares an EC_{50} concentration range in both oesophageal and cervical cancer cell lines; that SN-311 and SN-254 as able to target and inhibit the shedding of CX_3CL1, an ADAM-10 functional activity. Furthermore, SN-311 and SN-254 are able to suppress cellular proliferation, induce cell death by activating caspase 3/7 activity and increase cleavage of PARP, in a similar manner as GI254023X. This study also reports that ADAM-10 inhibition via GI254023X, inhibits cancer cell migration, invasion, and induces an increase in adhesion activity, suppresses pro-invasive changes in cell phenotype, and decreases vascular endothelial growth factor expression. Such findings were similarly detected in both novel compounds, SN-311 and SN-254. These results strongly suggest that ADAM-10 may play a critical role in maintaining the cancer phenotype in oesophageal cancer and cervical cancer, and that ADAM-10 may be a potential therapeutic target in these cancers.

Reference List

Acloque, H., Adams, M.S., Fishwick, K., Bronner- Fraser, M., and Nieto, M.A. (2009). Epithelial-mesenchymal transitions: the importance of changing cell state in development and disease. *The Journal of Clinical Investigation*; **119**: 1438–1449.

Adams, J.M., and Cory, S. (2007). The Bcl-2 apoptotic switch in cancer development and therapy. Oncogene, 26. pp. 1324–1337

Alizadeh, A. M., Shiri, S., and Farsinejad, S. (2014). Metastasis review: from bench to bedside. *Tumour Biol* **35**, 8483-8523

Arbyn, M., Castellsague, X., de Sanjose, S., Bruni, L., Saraiya, M., Bray, F., Ferlay, J. (2011). Worldwide burden of cervical cancer in 2008. Ann Oncol. 2011 Dec; 22(12):2675-86.

Arnold, M., Soerjomataram, I., Ferlay, J., and Forman, D. (2015). Global incidence of oesophageal cancer by histological subtype in 2012. *Gut* **64**, 381-387

Arribas, J., Bech-Serra, J.J., Santiago-Josefat, B., (2006). ADAMs, cell migration and cancer. Cancer Metastasis Rev. 25 (1), 57–68.

Berridge, M.V., Tan, A.S. (1993). Characterization of the cellular reduction of 3-(4,5- dimethylthiazol-2-yl)-2,5-diphenyltetrazolium bromide (MTT): subcellular localization, substrate dependence, and involvement of mitochondrial electron transport in MTT reduction. *Arch Biochem Biophys,* **303**(2):474–82. [PubMed: 8390225]

Bock, F. J., and Chang, P. (2016) New Directions in PARP Biology. *FEBS J*

Bruni L, Barrionuevo-Rosas L, Serrano B BM, Cosano R, Muñoz J, Bosch FX, et al. (2014). Institut Català d'Oncologia (ICO) Information Centre on HPV and Cancer (HPV Information Centre) Human Papillomavirus and Related Diseases in South Africa. Summary Report. [Internet]. March

17, 2014 [cited 26 March 2014]. URL: http://www.hpvcentre.net/statistics/reports/ZAF.pdf

Byron, A., and Frame, M. C. (2016) Adhesion protein networks reveal functions proximal and distal to cell-matrix contacts. *Curr Opin Cell Biol* **39**, 93-100

Bzowska, M., et al., (2009). Identification of ADAM10 as a major TNF sheddase in ADAM17-deficient fibroblasts. *Cytokine,* 46, pp.309-315.

Camodeca, C., Nuti, E., Tepshi, L., Boero, S., Tuccinardi, T., Stura, E. A., Poggi, A., Zocchi, M. R., and Rossello, A. (2016). Discovery of a new selective inhibitor of A Disintegrin And Metalloprotease 10 (ADAM-10) able to reduce the shedding of NKG2D ligands in Hodgkin's lymphoma cell models. *Eur J Med Chem* **111**, 193-201

Caolo, V., Swennen, G., Chalaris, A., Wagenaar, A., Verbruggen, S., Rose-John, S., Mollin, D. G. M., Vooijs, M., Post, M. J. (2015). ADAM10 and ADAM17 have opposite roles during sprouting angiogenesis. *Angiogenesis.* **18.** 13 – 22**.** Springer: DOI 10.1007/s10456-014-9443-4

Cavallo, F., De Giovanni, C., Nanni, P., Forni, G., and Lollini, P.-L. (2011). 2011: the immune hallmarks of cancer. *Cancer immunology, immunotherapy : CII*, *60*(3), 319-26.

Cervantes-Arias, A., Pang, L. Y., and Argyle, D. J. (2013). Epithelial-mesenchymal transition as a fundamental mechanism underlying the cancer phenotype. *Vet Comp Oncol* **11**, 169-184

Charlton, P., and Spicer, J. (2016). Targeted therapy in cancer. *Medicine* **44**, 34-38

Christiansen, J. J., Rajasekaran, A. K. (2006). Reassessing epithelial to mesenchymal transition as a prerequisite for carcinoma invasion and metastasis. *Cancer Res.* **66**, 8319–8326.

Clark, A. G., and Vignjevic, D. M. (2015). Modes of cancer cell invasion and the role of the microenvironment. *Curr Opin Cell Biol* **36**, 13-22

Denny L. (2009). Human Papillomavirus Infections: Epidemiology, Clinical Aspects and Vaccines. The Open Infectious Diseases Journal. 2009;3:135-42.

Donners, M. M., Wolfs, I. M., Olieslagers, S., Mohammadi-Motahhari, Z., Tchaikovski, V., Heeneman, S., van Buul, J. D., Caolo, V., Molin, D. G.,

Post, M. J., and Waltenberger, J. (2010). A disintegrin and metalloprotease 10 is a novel mediator of vascular endothelial growth factor-induced endothelial cell function in angiogenesis and is associated with atherosclerosis. *Arterioscler Thromb Vasc Biol* **30**, 2188-2195

Dreymueller, D., Pruessmeyer, J., Groth, E., and Ludwig, A. (2012). The role of ADAM-mediated shedding in vascular biology. *Eur J Cell Biol* **91**, 472-485

Druker, B.J., Talpaz, M., Resta, D.J., et al. (2001). Efficacy and safety of a specific inhibitor of the BCR-ABL tyrosine kinase in chronic myeloid leukemia. N Engl J Med 2001; 344: 1031e7.

Duffy, M. J., McKiernan, E., O'Donovan, N., and McGowan, P. M. (2009). The role of ADAMs in disease pathophysiology. *Clinica Chimica Acta* **403**, 31-36

Duffy, M. J., McKiernan, E., O'Donovan, N., and McGowan, P. M. (2009). Role of ADAMs in cancer formation and progression. *Clin Cancer Res* **15**, 1140-1144

Duffy, M. J., Mullooly, M., O'Donovan, N., Sukor, S., Crown, J., Pierce, A., and McGowan, P. M. (2011). The ADAMs family of proteases: new biomarkers and therapeutic targets for cancer? *Clin Proteomics* **8**, 9

Edwards, D. R., Handsley, M. M., and Pennington, C. J. (2008). The ADAM metalloproteinases. *Mol Aspects Med* **29**, 258-289

Elmore, S. (2007). Apoptosis: a review of programmed cell death. *Toxicol Pathol* **35**, 495-516

Endres, K., and Fahrenholz, F. (2010). Upregulation of the alpha-secretase ADAM10 – risk or reason for hope? *FEBS J* **277**: 1585-1596.

Ferlay, J., Shin, H. R., Bray, F., Forman, D., Mathers, C., and Parkin, D. M. (2010). Estimates of worldwide burden of cancer in 2008: GLOBOCAN 2008. *Int J Cancer* **127**, 2893-2917

Ferlay, J., Soerjomataram, I., Ervik, M. (2013). GLOBOCAN 2012 v1.0, Cancer Incidence and Mortality Worldwide: IARC Cancer Base No. 11. Lyon, France: International Agency for Research on Cancer.

Ferlay, J., Soerjomataram, I., Dikshit, R., Eser, S., Mathers, C., Rebelo, M., Parkin, D. M., Forman, D., and Bray, F. (2015). Cancer incidence and mortality worldwide: sources, methods and major patterns in GLOBOCAN 2012. *Int J Cancer* **136**, E359-386

Franken, N. A., Rodermond, H. M., Stap, J., Haveman, J., and van Bree, C. (2006). Clonogenic assay of cells in vitro. *Nat Protoc* **1**, 2315-2319

Friedl, P., Alexander, S. (2011). Cancer invasion and the microenvironment: plasticity and reciprocity. Cell 2011, 147:992-1009.

Friedl, P., and Gilmour, D. (2009) Collective cell migration in morphogenesis, regeneration and cancer. *Nat Rev Mol Cell Biol* **10**, 445-457

Fu, L., Liu, N., Han, Y., Xie, C., Li, Q., and Wang, E. (2014). ADAM10 regulates proliferation, invasion, and chemoresistance of bladder cancer cells. *Tumour Biol* **35**, 9263-9268

Gadagkar, S.R; and Call, G. B. (2015). Computational tools for fitting the Hill equation to dose-response curves. Journal of Pharmacological and Toxicological Methods. 71 (2015). 68-76.

Gaida, M.M., Haag, N., Gunther, F., Tschaharganeh, D.F., Schirmacher, P., Friess, H., et al. (2010). Expression of A disintegrin and metalloprotease 10 in pancreatic carcinoma. Int J Mol Med 2010;26:281-8.

Gatenby, P. A. C., and Preston, S. R. (2014). Oesophageal cancer. *Surgery (Oxford)* **32**, 588-593

GAVI. Millions of Girls in Developing Countries to be Protected Against Cervical Cancer Thanks to New HPV Vaccine Deals. gavi.org/library/news/press-releases/2013/ hpv-price-announcement/. Accessed September 12, 2014.

Giebeler, N., and Zigrino, P. (2016) A Disintegrin and Metalloprotease (ADAM): Historical Overview of Their Functions. *Toxins (Basel)* **8**

GLOBOCAN 2012 v1.0, Cancer Incidence and Mortality Worldwide: IARC CancerBase No. 11 [Internet]. Lyon, France: International Agency for Research on Cancer; 2013. Available from: http://globocan.iarc.fr, accessed on day/month/year.

Groves, M.D., Puduvalli, V.K., Conrad, C.A., Gilbert, M.R., Yung, W.K., Jaeckle, K., Liu, V., Hess, K.R., Aldape, K.D., Levin, V.A. (2006). Phase II trial of temozolomide plus marimastat for recurrent anaplastic gliomas: a relationship among efficacy, joint toxicity and anticonvulsant status. *J Neurooncol*; **80**:83–90.

Guzman, C., Bagga, M., Kaur, A., Westermarck, J., Abakwa, D. (2014). ColonyArea: An ImageJ Plugin to Automatically Quantify Colony Formation in Clonogenic Assays. PLOS ONE. Volume 9. Issue 3. E92444.

Hadju, S. I. (2011). A note from history: landmarks in history of cancer, part 1. *Cancer* **117**, 1097-1102

Hanahan, D., Weinberg, R. A. (2000). The Hallmarks of Cancer. *Cell* **100**, 57-70

Hanahan, D. (2014). Rethinking the war on cancer. *The Lancet* **383**, 558-563

Hanahan, D., and Weinberg, R. A. (2011). Hallmarks of cancer: the next generation. *Cell* **144**, 646-674

Harrington, K. J. (2016). The biology of cancer. *Medicine* **44**, 1-5

Hoelder, S., Clarke, P. A., and Workman, P. (2012). Discovery of small molecule cancer drugs: successes, challenges and opportunities. *Mol Oncol* **6**, 155-176

Hoettecke, N., Ludwig, A., Foro, S., and Schmidt, B. (2010). Improved synthesis of ADAM10 inhibitor GI254023X. *Neurodegener Dis* **7**, 232-23.

Hottiger, M.O., Hassa, P.O., Lubscher, B., Schubler, H., and Koch-Nolte, F. (2010). Toward a unified nomenclature for mammalian ADP-ribosyltransferases. Trends Biochem Sci 35, 208–219.

Hundhausen, C., Misztela, D., Berkhout, T.A., Broadway, N., Saftig, P., Reiss, K., Hartmann, D., Fahrenholz, F., Postina, R., Matthews, V., Kallen, K-J., Rose-John, S., Ludwig, A. (2003). The disintegrin- like metalloproteinase ADAM10 is involved in constitutive cleavage of CX3CL1 (fractalkine) and regulates CX3CL1-mediated cell- cell adhesion. *Blood*; **102**:1186–1195.

Imai, K., and Takaoka, A. (2006). Comparing antibody and small-molecule therapies for cancer. *Nat Rev Cancer* **6**, 714-727

Isozaki, T., Rabquer, B. J., Ruth, J. H., Haines, G. K., 3rd, and Koch, A. E. (2013). ADAM-10 is overexpressed in rheumatoid arthritis synovial tissue and mediates angiogenesis. *Arthritis Rheum* **65**, 98-108

Jemal, A., Bray, F., Center, M. M., Ferlay, J., Ward, E., and Forman, D. (2011). Global cancer statistics. *CA Cancer J Clin* **61**, 69-90

Jones, A.V., Lambert, D.W., Speight, P.M., Whawell, S.A. (2013). ADAM 10 is over expressed in oral squamous cell carcinoma and contributes to invasive behaviour through a functional association with avB6 integrin. FEBS Letters 587 (2013) 3529–3534

Kalluri, R., and Weinberg, R.A. (2009). The basics of epithelial-mesenchymal transition. *Journal of Clinical Investigation.* **119**, 1420-1428.

Kauffman, S.H., Desnoyers, S., Ottaviano, Y., Davidson, N.E., and Poirier, G.G. (1993). Specific Proteolytic Cleavage of poly (ADP-Ribose) Polymerase: An early Marker of Chemotherapy-induced Apoptosis. Cancer Res. 53, 3976-3985.

Khalil, A.A., Friedl, P. (2010). Determinants of leader cells in collective cell migration. Integr Biol 2010, 2:568-574.

Klymkowsky, M. W., and Savagner, P. (2009). Epithelial-mesenchymal transition: a cancer researcher's conceptual friend and foe. *Am J Pathol* **174**, 1588-1593

Kotsopoulos, I. C., Kucukmetin, A., Mukhopadhyay, A., Lunec, J., and Curtin, N. J. (2016). Poly(ADP-Ribose) Polymerase in Cervical Cancer Pathogenesis: Mechanism and Potential Role for PARP Inhibitors. *Int J Gynecol Cancer* **26**, 763-769

Kramer, N., Walzl, A., Unger, C., Rosner, M., Krupitza, G., Hengstschlager, M., Dolznig, H. (2013). Review: *In vitro* cell migration and invasion assays. Mutation Research/ Review in Mutation Research. Elsevier. http://dx.doi.org/10.1016/j.mrrev.2012.08.001. Pp.10-24.

Kwon, J., Jeong, S. M., Choi, I., and Kim, N. H. (2016). ADAM10 Is Involved in Cell Junction Assembly in Early Porcine Embryo Development. *PLoS One* **11**, e0152921

Lee, S.B., Schramme, A., Doberstein, K., *et al*. (2010). ADAM10 is upregulated in melanoma metastasis compared with primary melanoma. J Invest Dermatol 130: 763-773, 2010.

Lee, K., and Nelson, C. M. (2012). New insights into the regulation of epithelial-mesenchymal transition and tissue fibrosis. *Int Rev Cell Mol Biol* **294**, 171-221

Li, S., Qin, X., Chai, S., Qu, C., Wang, X., and Zhang, H. (2016). Modulation of E-cadherin expression promotes migration ability of esophageal cancer cells. *Sci Rep* **6**, 21713

Li, X., Gu, F., Niu, C., Wang, Y., Liu, Z., Li, N., Pan, B., He, D., Kong, J., Zhang, S., Wang, X., Yao, Y., Zheng, L. (2015). VEGF111b, a C-terminal splice variant of VEGF-A and induced by mitomycin C, inhibits ovarian cancer growth. Journal of Translational Medicine (2015) 13:164 DOI 10.1186/s12967-015-0522-0

Liao, S.Y., Brewer, C., Zavada, J., Pastorek, J., Pastorekova, S., Manetta, A., Berman, M.L., Disaia, P.J., and Stanbridge, E. (1994). Identification of the MN Antigen as a Diagnostic Biomarker of Cervical Intraepithelial Squamous and Glandular Neoplasia and Cervical Carcinomas. Am. J. Pathol. *145*, 598-609.

Liu, S., Zhang, W., Liu, K., Ji, B., and Wang, G. (2014). Silencing ADAM10 inhibits the in vitro and in vivo growth of hepatocellular carcinoma cancer cells. *Mol Med Rep* **11**, 597-602

Lu, X., Lu, D., Scully, M., Kakkar, V. (2008). ADAM Proteins- Therapeutic Potential in Cancer. *Current Cancer Drug Targets* **8**, 13

Ludwig, A., Hundhausen, C., Lambert, M. L., Broadway, N., Andrews, R. C., Bickett, D. M., Bickett, Leesnitzer, M. A., and Becherer, J. D. (2005). Metalloproteinase Inhibitors for the Disintegrin-Like Metalloproteinases ADAM10 and ADAM17 that Differentially Block Constitutive and Phorbol Ester-Inducible Shedding of Cell Surface Molecules. *COmbinational Chemistry & High Throughput Screening* **8**, 11

Ma, L., Teruya-Feldstein, J. & Weinberg, R.A., (2007). Tumour invasion and metastasis initiated by microRNA-10b in breast cancer. *Nature,* **449**(7163), pp.682-688.

Ma, S., Xu, J., Wang, X., Wu, Q.Y., Cao, J., Li, Z.Y., Zeng, L.Y., Chen, C., Xu, K.L. (2015). Effect of ADAM10 Inhibitor GI254023X on proliferation and

apoptosis of acute T- lymphoblastic leukemia Jurkat cells in vitro and its possible mechanisms. Zhongguo Shi Yan Xue Ye Xue Za Zhi. 2015;23:950-5. Chinese.

Man, S. M., and Kanneganti, T. D. (2016). Converging roles of caspases in inflammasome activation, cell death and innate immunity. *Nat Rev Immunol* **16**, 7-21

Maretzky, T. et al., (2005). ADAMI0 mediates E-cadherin shedding and regulates epithelial cell- cell adhesion, migration, and Beta-catenln translocation. *Proceedings* of *the National Academy of Science(PNASj,* 102(**26**), pp.9182-91B7.

Mochizuki, S., and Okada, Y. (2007). ADAMs in cancer cell proliferation and progression. *Cancer Sci* **98**, 621-628

Moss, M.L., White, J.M., Lambert, M.H., Andrews, R.C. (2001). TACE and other ADAM proteases as targets for drug discovery. Drug Discovery Today. Volume 6, Issue 8, Pages 417–426

Moss, M. L., Bomar, M., Liu, Q., Sage, H., Dempsey, P., Lenhart, P. M., Gillispie, P. A., Stoeck, A., Wildeboer, D., Bartsch, J. W., Palmisano, R., and Zhou, P. (2007). The ADAM10 prodomain is a specific inhibitor of ADAM10 proteolytic activity and inhibits cellular shedding events. *J Biol Chem* **282**, 35712-35721

Moss, M. L., Stoeck, A., Yan, W., Dempsey, P. J. (2008). ADAM10 as a target for anti-cancer therapy. *Curr. Pharm. Bitechnol.* **9.** 2 – 9.

Moustakas, A., Heldin, C.-H., (2005). Non-Smad TGF-b signals. *J. Cell Sci.* **118**, 3573–3584.

Mullooly, M., McGowan, P.M., Kennedy, S.A., Madden, S.F., Crown, J., O' Donovan, N., Duffy, M.J. (2015). ADAM10: a new player in breast cancer progression? Br J Cancer 2015;113:945-51.

Mullooly, M., McGowan, P., Crown, J., and Duffy, M. J. (2016). The ADAMs Family of Proteases as Targets for the Treatment of Cancer. *Cancer Biol Ther*, 0

Murphy, G. (2008). The ADAMs: signalling scissors in the tumour microenvironment. *Nat Rev Cancer* **8**, 929-941

Mqoqi, N., Kellet, P., Sitas, F., and Jula, M. (2004). Incidence of Histologically Diagnosed Cancer in South Africa, 1998 – 2004. Johannesburg,

National Cancer Registry of South Africa, National Health Laboratory Service.

Nanda, K., McCrory, D.C., Myers, E., Bastian, L.A., Hasselblad, V., Hickey, J.D., and Matchar, D.B. (2000). Accuracy of the Papanicolaou Test in Screening for and Follow-up of Cervical Cytologic Abnormalities: A Systematic Review. Ann. Intern. Med. *132*, 810- 819.

Neufeld, G., Cohen, T., Gengrinovitch, S., et al. (1999). Vascular endothelial growth factor (VEGF) and its receptors. *FASEB J* 1999; 13:9-22.

O'Shea, C., McKie, N., Buggy, Y., Duggan, C., Hill, A.D.K., McDermott, E., O'Higgins, N., Duffy, M., (2003). Expression of Adam-9 mRNA and protein in human breast cancer. Int. J. Cancer: 105, 754 –761

Portt, L., Norman, G., Clapp, C., Greenwood, M., and Greenwood, M. T. (2011). Anti-apoptosis and cell survival: a review. *Biochim Biophys Acta* **1813**, 238-259

Primakoff, P., Hyatt, H., Tredick-Kline, J. (1987). Identification and purification of a sperm surface protein with a potential role in sperm-egg membrane fusion. *J. Cell Biol.* **1987**, *104*, 141–149.

Proctor, R.A. (1987). Fibronectin: A Brief Overview of its Structure, FUnction, and Physiology. *Reviews of infectious diseases.* Vol. 9, Supp 4. 0162-0886/87/0904-0020$02.00. pp.S317-S321.

Reiss, K., Maretzky, T., Ludwig, A., Tousseyn, T., de Strooper, B., Hartmann, D., Saftig, P. (2005). ADAM10 cleavage of N-cadherin and regulation of cell-cell adhesion and beta- catenin nuclear signalling. EMBO J 2005;24:742-52. Erratum in: EMBO J. 2005;24:1762.

Reiss, K., Ludwig, A. and Saftig, P., (2006). Breaking up the tie: disintegrin-like metalloproteinases as regulators o f cell migration in Inflammation and invasion. *Pharmacology & therapeutics,* 111(3), pp.985-1006.

Robert, I., Karicheva, O., Reina San Martin, B. (2013). Functional aspects of PARylation in induced and programmed DNA repair processes: preserving genome integrity and modulating physiological events. Mol Aspects Med. 2013;34:1138Y1152.

Rocks, N., Paulissen, G., El Hour, M., Quesada, F., Crahay, C., Gueders, M., Foidart, J.M., Noel, A., Cataldo, D., (2008). Emerging roles of ADAM

and ADAMTS metalloproteinases in cancer. Biochimie 90 (2), 369–379.

Roghani, M., Becherer, J.D., Moss, M.L., Atherton, R.E., Erdju- ment-Bromage, H., Arribas, J., Blackburn, R.K., Weskamp, G., Tempst, P., and Blobel, C.P. (1999). Metalloprotease disintegrin MDC9: Intracellular maturation and catalytic activity. *J. Biol. Chem.* **274:** 3531–3540.

Rogers, S.J., Harrington, K.J., Rhys Evans, P., O-Charoenrat, P., Eccles, S. A. (2005). Biological significance of c-erbB family oncogenes in head and neck cancer. Cancer Metastasis Rev 2005; 24: 47e69.

Saftig, P., and Reiss, K. (2011) The "A Disintegrin And Metalloproteases" ADAM10 and ADAM17: novel drug targets with therapeutic potential? *Eur J Cell Biol* **90**, 527-535

Sahin, U., Weskamp, G., Kelly, K., Zhou, H.M., Higashiyama, S., Peschon, J., Hartmann, D., Saftig, P., Blobel, C.P. (2004). Distinct roles for ADAM10 and ADAM17 in ectodomain shedding of six EGFR ligands. J Cell Biol 2004;164:769-79.

Seals, D. F. and Courtneidge, S. A. (2003). The ADAMS family of metalloproteases: multidomain proteins with multiple functions. Review. *Genes & Development.* **17,** 7 – 30. Cold Spring Harbor Laboratory Press ISSN 0890-9369/03.

Sethi, S., Sarkar, F. H., Ahmed, Q., Bandyopadhyay, S., Nahleh, Z. A., Semaan, A., Sakr, W., Munkarah, A., and Ali-Fehmi, R. (2011). Molecular Markers of Epithelial-to-Mesenchymal Transition Are Associated with Tumor Aggressiveness in Breast Carcinoma. *Translational Oncology* **4**, 222-226

Shao, Y., Sha, X. Y., Bai, Y. X., Quan, F., and Wu, S. L. (2015). Effect of A disintegrin and metalloproteinase 10 gene silencing on the proliferation, invasion and migration of the human tongue squamous cell carcinoma cell line TCA8113. *Mol Med Rep* **11**, 212-218

Shook, D., Keller, R., (2003). Mechanisms, mechanics and function of epithelial-mesenchymal transitions in early development. Mech. Dev. 120, 1351–1383.

Somdyala, N.I.M., Bradshaw, D., Gelderblom, W.C.A., Parkin, D.M. (2010). Cancer incidence in rural population of South Africa, 1998 – 2002.

International Journal of Cancer: 127, pp2420–2429 (2010) VC 2010 UICC

Stricker, J., Falzone, T., and Gardel, M. L. (2010). Mechanics of the F-actin cytoskeleton. *J Biomech* **43**, 9-14

Swann, J. B., and Smyth, M. J. (2007). Immune surveillance of tumors. *J Clin Invest* **117**, 1137-1146

Tathiah, N., Moodley, I., Denny, L., Moodley, J., Jassat, W. (2013). Cervical cancer in South Africa: challenges and opportunities. Chapter 11. SAHR 2013/14. Pp 117 – 125.

Thiery, J.P. (2002). Epithelial-mesenchymal transitions in tumour progression. *Nature Reviews Cancer.* **2**, 442-454.

Thiery, J. P., (2003). Epithelial-mesenchymal transitions in development and pathologies. *Current Opinion in Cell Biology*; **15**: 740–746.

Thiery, J. P., Acloque, H., Huang, R. Y., and Nieto, M. A. (2009). Epithelial-mesenchymal transitions in development and disease. *Cell* **139**, 871-890

Torre, L. A., Bray, F., Siegel, R. L., Ferlay, J., Lortet-Tieulent, J., and Jemal, A. (2015). Global cancer statistics, 2012. *CA Cancer J Clin* **65**, 87-108

Tousseyn, T. et al., (2009). ADAM10 , the Rate-limiting Protease of Regulated Intramembrane Proteolysis of Notch and Other Proteins, Is Processed by ADAMS-9 , ADAMS-15 , and the V- Secretase. *The Journal* 0f *Biological Chemistry,* 284(17), pp.11738-11747.

Vaccarella, S,. Lortet-Tieulent, J., Plummer, M., Franceschi, S., Bray, F. (2013). Worldwide trends in cervical cancer incidence: impact of screening against changes in disease risk factors. Eur J Cancer. 2013;49:3262-3273.

Valkovskaya, N., Kayed, H., Felix, K., Hartmann, D., Giese, N.A., Osinsky, S.P., Friess, H., Kleef, J. (2007). ADAM8 expression is associated with increased invasiveness and reduced patient survival in pancreatic cancer. J. Cell. Mol. Med. Vol 11, No 5, 2007 pp. 1162-1174

van der Watt, P. J., Maske, C. P., Hendricks, D. T., Parker, M. I., Denny, L., Govender, D., Birrer, M. J., and Leaner, V. D. (2009). The Karyopherin proteins, Crm1 and Karyopherin beta1, are overexpressed in cervical

cancer and are critical for cancer cell survival and proliferation. *Int J Cancer* **124**, 1829-1840

Varmus, H., Kumar, H. S. (2013). Addressing the Growing International Challenge of Cancer: A Multinational Perspective. *Science Translational Medicine* **5**, 1 - 5

Veale, R.B., and Thornley, A.L. (1989). Increased single class low-affinity EGF receptors expressed by human oesophageal squamous carcinoma cell lines. S. Afr. J. Sci. *85*, 375-379.

Verheul, H. M. W., and Pinedo, H. M. (2000). The Role of Vascular Endothelial Growth Factor (VEGF) in Tumor Angiogenesis and Early Clinical Development of VEGFReceptor Kinase Inhibitors. *Clinical Breast Cancer* **1**, S80-S84

Voulgari, A., and Pintzas, A. (2009). Epithelial-mesenchymal transition in cancer metastasis: mechanisms, markers and strategies to overcome drug resistance in the clinic. *Biochim Biophys Acta* **1796**, 75-90

Wang, J., Wei, Q., Wang, X., Tang, S., Liu, H., Zhang, F., Mohammed, M. K., Huang, J., Guo, D., Lu, M., Liu, F., Liu, J., Ma, C., Hu, X., Haydon, R. C., He, T.-C., and Luu, H. H. (2016). Transition to resistance: An unexpected role of the EMT in cancer chemoresistance. *Genes & Diseases* **3**, 3-6

Wang, K., Seo, B. R., Fischbach, C., and Gourdon, D. (2016). Fibronectin Mechanobiology Regulates Tumorigenesis. *Cell Mol Bioeng* **9**, 1-11

Ward, M.C., (2011). lamina-associated polypeptide 2 (lAP2) expression patterns in transformed and cancer cells. *unpublished Masters Dissertotion.*

Wildeboer, D., Naus, S., Amy Sang, Q. X., Bartsch, J. W., Pagen- stecher, A. (2006). Metalloproteinase disintegrins ADAM8 and ADAM19 are highly regulated in human primary brain tumors and their expression levels and activities are associated with invasiveness. *J. Neuropathol. Exp. Neurol.*, ***65***, 516-527.

Williams, C. (2013). Characterization of ADAM10 in Cervical and Oesophageal Cancers. (Unpublished Master's thesis, University of Cape Town.

Wolf, K., Mazo, I., Leung, H., Engelke, K., von Andrian, U.H., Deryugina, E.I., Strongin, A.Y., Bro¨cker, E-B., Friedl, P. (2003). Compensation mechanism in tumor cell migration: mesenchymal–amoeboid transition after blocking of pericellular proteolysis. J Cell Biol 2003, 160:267-277.

Wolfsberg, T.G., Straight, P.D., Gerena, R.L., Huovila, A.P., Primakoff, P., Myles, D.G., White, J.M., (1995). ADAM, a widely distributed and developmentally regulated gene family encoding membrane proteins with a disintegrin and metalloprotease domain. Dev. Biol. 169 (1), 378–383.

World Health Organization, International Agency for Research on Cancer. GLOBOCAN 2012: Estimated Cancer Incidence, Prevalence and Mortality Worldwide in 2012. [Internet]. 2012 [cited 26 March 2014]. URL: http://globocan.iarc.fr/

Yilmaz, M., and Christofori, G. (2009). EMT, the cytoskeleton, and cancer cell invasion. *Cancer Metastasis Rev* **28**, 15-33

You, B., Shan, Y., Shi, S., Li, X., and You, Y. (2015). Effects of ADAM10 upregulation on progression, migration, and prognosis of nasopharyngeal carcinoma. *Cancer Sci* **106**, 1506-1514

Yuan, S., Lei, S., and Wu, S. (2013). ADAM10 is overexpressed in human hepatocellular carcinoma and contributes to the proliferation, invasion and migration of HepG2 cells. *Oncol Rep* **30**, 1715-1722

Zhang, W., Liu, S., Liu, K. (2014) A disintegrin and metalloprotease (ADAM)10 is highly expressed in hepatocellular carcinoma and is associated with tumour progression. *J Int Med Res.* **42**. 611-618.

Zhao, R., Ni, D., Tian, Y., Ni, B., Wang, A. (2014). Aberrant ADAM10 expression correlates with osteosarcoma progression. *European Journal of Medical Research*. **19**:9.8.

Appendix A:
Chemical Solutions Recipes

A.1 Tissue culture solutions

10X PBS (500ml)

40 g NaCl

1 g KCl

5.75 g $Na_2HPO_4.7H_2O$

1 g KH_2PO_4

Make up to 500ml with dH_2O

Autoclave this solution

Dilute to 1x PBS when needed

Heat Inactivated Foetal Calf Serum

Heat FCS at 56°C for 30 minutes

Store at -20°C until use

Complete DMEM medium

450 mL Dulbecco's Modified Eagle's Medium (DMEM)

50 mL FCS

5 mL Penicillin and streptomycin (P/S)

Trypsinisation (Trypsin –EDTA) Solution (1000ml)

0.5 g Trypsin

8 g NaCl

1.45 g $Na_2HPO4.2H_2O$

0.2 g KCl

0.2 g KH_2HPO_4

10 mM EDTA

Make up to 1000 mL with 1X PBS

Freezing Media (10ml)

9 mL Complete DMEM Media 1ml 99% DMSO

Hank's balanced salt solution

4.5 mM KCl

0.3 mM Na_2HPO_4

0.4 mM KH_2PO_4

1.3 mM $CaCl_2$

0.5 mM $MgCl_2$

0.6 mM $MgSO_4$

137 mM NaCl

5.6 mM D-glucose

Hoechst stain (0.5 µg/ml)

5 mg Hoechst No. 33258

1000 mL Hank's Balanced Salt Solution

Store at 4°C in foil

Fixing solution

1:3 glacial acetic acid-methanol

Mounting fluid

22.2 mL 0.1 M citric acid

27.8 mL 0.2 M $Na_2HPO_4.2H_2O$

50 mL glycerol

pH 5.5 Store at 2-8°C

A.2 Western blot solutions

RIPA buffer

3 mL 5M NaCL (150mM)

1 mL Triton X-100 (1%)

1 g Na Deoxycholate (1%)

1 mL 10% SDS (0.1%)

1 mL 1M Tris pH. 7.5 (10mM)

94 mL dH_2O

Complete RIPA

450 µl RIPA

50 µl 10X Protease Inhibitor (Sigma, USA) (104mM AEBSF. 80µM Aprotinin,

4 mM Bestatin, 1.4mM E- 46, 2mM Leupeptin, 1.5mM Pepstatin)

5 µl 0.1M Na_3VO_4

Store at 4°C

30% acrylamide solution

30 g acrylamide

0.8 g bisacrylamide

0.1 g SDS

Make up to 100 mL with dH_2O

Store at 4°C covered in foil

Buffer 5X (15ml stock solution)

SDS 10% (1,5gr)

Glycerol 50% (7,5ml)

beta-mercaptoethanol 25% (3,75ml)

Bromophenol blue 0,01%

Tris-HCl pH 6,8 1,5M (3,13ml)

4 X Laemmli Loading Dye

250 mM Tris-Cl, pH 6.8

6 % SDS

0.005 % Bromophenol Blue

40 % Glycerol

10 % β-mercaptoethanol

10 X Running Buffer

20 g Glycine

31.6 g Tris

50 mL 10 % SDS

Up to 500 mL with dH_2O

10 X Transfer Buffer

72 g Glycine

19 g Tris

Up to 500 ml with dH_2O

1X Transfer Buffer

Dilute 100 mL 10X Transfer Buffer with 700 mL dH_2O and add 200 mL methanol or Isopropanol.

10X TBS (1000 mL)

60.5 g Tris

87.6 g NaCl pH7.5

Make up to 1000 mL with dH_2O

1X TBST (1000 mL)

100 mL 10X TBS

900 mL dH_2O

1 mL Tween 20

A.3 Immunocytochemistry

4% Paraformaldehyde (PFA)

16 g PFA

80 mL dH_2O

Cover with foil and stir for 1 hour not letting temperature exceed 60°C

Add 10 M NaOH until clear

Filter-sterilise

Adjust to pH 7.0

Store in 2.5 mL aliquots at -2o°C

Add 7.5 mL 1X PBS to make 4% PFA

50mM NH_4Cl

0.265 g NH_4Cl

100 mL 1X PBS

Mowiol 4-88

2 g Mowiol 4-88

2 mL Glycerol

4 mL dH_2O

Leave at RT O/N

8 mL 0.2 M Tris (pH8.5)

Incubate at 50°C for 1 hour

Store in 2 mL aliquots at -20°C

Add 2.5% Anti-Fading Agent (N-propyl gallate) day before use

0.2% gelatin

100 mg gelatin in 10 mL 1X PBS

A.4 Proliferation and drug treatment assays

MTT Reagent (3-[4,5-dimethylthiazol-2-yl]-2,5-diphenyltetrazolium bromide)

5 mg/ml in PBS Weigh out 100 mg MTT in sterile 50 ml conical tube

Add 20 ml sterile 1X PBS

Vortex the mixture and incubate at 37°C for 15 minutes

Filter sterilize the solution through a 0.2 µM filter Store in the dark at 4°C

Use within 1 month

Solubilisation Reagent

10% Sodium Lauryl Sulphate (SLS) in 0.01 M HCl

Filter sterilized Dissolve 25 g of SLS in 250 mL dH_2O

Add 76.6 µl concentrated HCl

Appendix B:
Protein marker

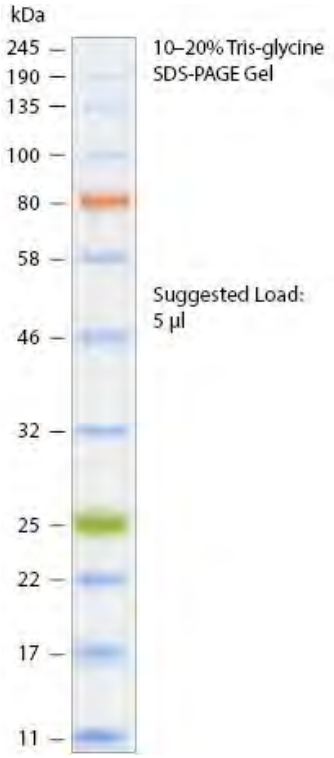

B.1: Protein molecular marker; Colour pre-stained Protein Standard, Broad range (11 – 245 kDa); 10 – 20% Tris-glycine SDS-Page. New England Biolabs (NEB), product number: #P7712.